



Foam Flotation Treatment of Industrial Wastewaters

Laboratory and Pilot Scale



RESEARCH REPORTING SERIES

Research reports of the Office of Research and Development, U.S. Environmental Protection Agency, have been grouped into nine series. These nine broad categories were established to facilitate further development and application of environmental technology. Elimination of traditional grouping was consciously planned to foster technology transfer and a maximum interface in related fields. The nine series are:

1. Environmental Health Effects Research
2. Environmental Protection Technology
3. Ecological Research
4. Environmental Monitoring
5. Socioeconomic Environmental Studies
6. Scientific and Technical Assessment Reports (STAR)
7. Interagency Energy-Environment Research and Development
8. "Special" Reports
9. Miscellaneous Reports

This report has been assigned to the ENVIRONMENTAL PROTECTION TECHNOLOGY series. This series describes research performed to develop and demonstrate instrumentation, equipment, and methodology to repair or prevent environmental degradation from point and non-point sources of pollution. This work provides the new or improved technology required for the control and treatment of pollution-sources to meet environmental quality standards.

EPA-600/2-80-138
June 1980

FOAM FLOTATION TREATMENT OF INDUSTRIAL WASTEWATERS:
LABORATORY AND PILOT SCALE

by

David J. Wilson and Edward L. Thackston
Vanderbilt University
Nashville, Tennessee 37235

Grant No. R-804438

Project Officers

Hugh B. Durham and Donald L. Wilson
Industrial Pollution Control Division
Industrial Environmental Research Laboratory
Cincinnati, Ohio 45268

INDUSTRIAL ENVIRONMENTAL RESEARCH LABORATORY
OFFICE OF RESEARCH AND DEVELOPMENT
U.S. ENVIRONMENTAL PROTECTION AGENCY
CINCINNATI, OHIO 45268

DISCLAIMER

This report has been reviewed by the Industrial Environmental Research Laboratory-Cincinnati, U. S. Environmental Protection Agency, and approved for publication. Approval does not signify that the contents necessarily reflect the views and policies of the U. S. Environmental Protection Agency, nor does mention of trade names or commercial products constitute endorsement or recommendation for use.

FOREWORD

When energy and material resources are extracted, processed, converted, and used, the related pollutional impacts on our environment and even on our health often require that new and increasingly more efficient pollution control methods be used. The Industrial Environmental Research Laboratory - Cincinnati (IERL-Ci) assists in developing and demonstrating new and improved methodologies that will meet these needs both efficiently and economically.

This report deals with bench and pilot plant scale studies of the removal of toxic inorganic compounds from aqueous systems by adsorbing colloid flotation. These results are relevant to the treatment of industrial wastewaters when a high degree of removal of toxic inorganics is necessary, and should be of use to the secondary lead smelting industry, brass mills, electroplating shops, copper and zinc smelters, and other sources of wastewaters containing toxic inorganics. The Industrial Pollution Control Division is to be contacted for further information on the subject.

David G. Stephan
Director
Industrial Environmental Research Laboratory
Cincinnati

ABSTRACT

A floc foam flotation pilot plant was shown to remove lead and zinc in dilute aqueous solution to quite low concentrations. The results suggest several design improvements. These include: (1) a larger mixer-flocculation tank to increase the detention time of the floc before flotation; (2) increased baffling of the stripping column section, to decrease channelling and foam overturn at high loadings; and (3) a decrease in the length of the foam drainage section of the column, to decrease the tendency of the foam to collapse before discharge. Axial dispersion studies indicate that a simple diffusion-type model is not accurate; the large scale of the turbulences precludes their modelling by diffusion. Hydraulic loading, column alignment, baffles, and influent dispersion head geometry affect axial dispersion.

The floc foam flotation of zinc is readily carried out with $\text{Al}(\text{OH})_3$ and sodium lauryl sulfate (NLS). $\text{Cr}(\text{OH})_3$ is floated with NLS, but adsorbing colloid flotation of $\text{Cr}(\text{III})$ with $\text{Fe}(\text{OH})_3$ or $\text{Al}(\text{OH})_3$ yielded better results. Cobalt and nickel levels are reduced to around 1 mg/l by flotation with $\text{Al}(\text{OH})_3$ and NLS. $\text{Mn}(\text{II})$ levels can be reduced to 1-2 mg/l by flotation with $\text{Fe}(\text{OH})_3$ and NLS. Floc foam flotation of copper was compatible with several precipitation pretreatments (soda ash, lime, $\text{Fe}(\text{OH})_3$ and $\text{Al}(\text{OH})_3$), although modifications were needed to prevent interference from excessive Ca or carbonate. Floc foam flotation can therefore be used as a polishing treatment. The flotation of mixtures of copper(II), lead(II) and zinc(II) was carried out using $\text{Fe}(\text{OH})_3$ and NLS. The flotation of simple and complexed cyanides and mixtures of metal cyanide complexes was also carried out with $\text{Fe}(\text{OH})_3$ and NLS; a pH of around 5 is optimum.

The flotation of $\text{Fe}(\text{OH})_3$ flocs with NLS is impeded by several polyvalent anions, some of which occur in industrial cleaners. These anions displace surfactant from the floc, rendering it unfloatable. This phenomenon, an interference in waste treatment, could be used to reclaim surfactant from flotation sludges.

A surface adsorption model for floc foam flotation was analyzed and found to account for the effects of surfactant concentration, ionic strength, specifically adsorbed ions, and surfactant hydrocarbon chain length.

This report was submitted in fulfilment of Grant No. R-804438 under the sponsorship of the U. S. Environmental Protection Agency. This report covers the period May 1, 1976 to November 1, 1978 and work was completed as of October, 1978.

CONTENTS

Foreword.....	iii
Abstract.....	iv
Figures.....	vi
Tables.....	viii
Acknowledgments.....	x
1. Introduction.....	1
2. Conclusions.....	5
3. Recommendations.....	7
4. Objectives of the Research Program.....	8
5. Pilot Plant Work (10-cm Dia Column).....	10
6. Pilot Plant Design and Construction (30-cm Dia Column).....	17
7. Pilot Plant Results (30-cm Dia Column).....	35
8. Continuous Flow Axial Mixing Studies.....	42
9. Batch Technique Laboratory Studies.....	62
Flotation of Zinc(II).....	62
Flotation of Nickel(II), Manganese(II), Chromium(III), and Cobalt(II).....	65
Compatibility of Floc Foam Flotation with Precipitation Pretreatments.....	71
Interferences with Floc Foam Flotation Resulting from Foreign Ions.....	75
Simultaneous Floc Foam Flotation of Cu(II), Pb(II), and Zn(II).....	76
Floc Foam Flotation of Cyanides.....	78
References.....	86
Appendices	
A. Data on Lead Removal from Wastes and Simulated Wastes with the 10-cm and 30-cm Columns.....	92
B. Absorption Isotherms.....	106
C. Theory of Surfactant Displacement of Salts.....	121

FIGURES

<u>Number</u>	<u>Page</u>
1 The 10-cm pilot plant.....	11
2 Schematic diagram of 30-cm pilot plant.....	18
3 Adsorbing colloid flotation pilot plant.....	19
4 Plan view of pilot plant.....	20
5 Mixing chamber components.....	22
6 Flotation column.....	23
7 Flow dispersion head.....	25
8 Typical baffle installation.....	26
9 Foam breaker.....	27
10 Clarifier.....	28
11 Support structure.....	31
12 The foam flotation apparatus used in the axial dispersion studies...	43
13 Dispersion head designs.....	44
14 High-speed foam breaker design.....	45
15 The setup for photography of the axial dispersion experiments.....	47
16 Axial dispersion data, run I.....	49
17 Axial dispersion data, run II.....	50
18 Axial dispersion data, run III.....	51
19 Axial dispersion data, run IV.....	52
20 Axial dispersion data, run V.....	53
21 Axial dispersion data, run VI.....	54
22 Axial dispersion data, run VII.....	55
23 Axial dispersion data, run VIII.....	56
24 Axial dispersion data, run IX.....	57
25 Center of mass motion for Figures 17-20.....	59
26 Pulse width versus time for Figures 17-20.....	61

FIGURES (Continued)

<u>Number</u>	<u>Page</u>
B-1 Model of floc-bubble attachment.....	107
B-2 Adsorption isotherms of surfactant on floc with condensation.....	115
B-3 Dependence of σ_{crit} on w	116
B-4 Dependence of σ_{crit} on ψ_0	118
B-5 Dependence of σ_{crit} on c_∞	119
C-1 Effect of competing salt concentration c_B' on the adsorption isotherm.....	127
C-2 Effect of c_B on surfactant condensation concentration.....	128
C-3 Effect of χ_B on the adsorption isotherm.....	129
C-4 Effect of w on the adsorption isotherm.....	130
C-5 Effect of χ_A on the adsorption isotherm.....	131
C-6 Effect of temperature on the adsorption isotherm.....	132

TABLES

<u>Number</u>		<u>Page</u>
1	Proposed Experimental Design for 10-cm Flotation Column.....	13
2	Effects of pH on Lead Removal.....	15
3	Effects of Increasing Ionic Strength on Lead Removal.....	15
4	Recommended Design Parameters for Further Studies.....	16
5	Flow Rates for Various Settings of Chemical Feed Pump 7016.....	29
6	Effects of pH on Lead Removal.....	36
7	Effects of Increasing Ionic Strength on Lead Removal.....	37
8	Optimum Operating Parameters, 30-cm Column.....	39
9	Parameters for Figure 16.....	48
10	The Effect of $\text{Fe}(\text{OH})_3$ on $\text{Zn}(\text{II})$ Removal.....	63
11	The Effect of pH on $\text{Zn}(\text{II})$ Removal with $\text{Fe}(\text{III})$ and NLS.....	63
12	The Effect of $\text{Al}(\text{III})$ on $\text{Zn}(\text{II})$ Removal.....	64
13	Floc Flotation of Zinc with $\text{Al}(\text{OH})_3$ and NLS. Effect of Ionic Strength.....	64
14	Floc Flotation of Zinc with $\text{Al}(\text{OH})_3$ and NLS. Effect of Electrolyte Identity.....	65
15	Effect of pH on Nickel(II) Floc Foam Flotation.....	65
16	Effect of Ionic Strength on Nickel(II) Floc Foam Flotation.....	66
17	$\text{Ni}(\text{II})$ Flotation at Decreased $\text{Ni}(\text{II})$ Concentration.....	66
18	Precipitate Flotation of Chromic Hydroxide.....	67
19	Effect of pH on Chromium(III) Floc Foam Flotation.....	68
20	Effect of Iron(III) Concentration on Chromium(III) Floc Foam Flotation.....	69
21	Effect of Inert Salt Concentration on Chromium(III) Floc Foam Flotation.....	69
22	Floc Foam Flotation of Cobalt(II) with $\text{Al}(\text{OH})_3$ or $\text{Re}(\text{OH})_3$ and NLS...	70
23	Effect of Ionic Strength on Flotation of $\text{Co}(\text{II})$ with $\text{Al}(\text{OH})_3$ and NLS.....	70
24	Effects of Settling and Foaming pH's on $\text{Cu}(\text{II})$ Removal after precipitation with Na_2CO_3	72

TABLES (Continued)

<u>Number</u>		<u>Page</u>
25	Effects of Air Sparging at Low pH on Cu(II) Removal after Precipitation with Na_2CO_3	73
26	Effect of Foaming pH on Cu(II) Removal after Precipitation with $\text{Ca}(\text{OH})_2$	74
27	Effect of Foaming pH on Cu(II) Removal after Coprecipitation with $\text{Al}(\text{OH})_3$ or $\text{Fe}(\text{OH})_3$	75
28	Effect of Various Added Salts and Glycerol on the Flotation of Ferric Hydroxide.....	77
29	Results of the Floc Foam Flotation of Cu(II), Pb(II), and Zn(II) with $\text{Fe}(\text{OH})_3$ and NLS.....	78
30	Stability Constants for Cyanide Complexes.....	79
31	Solubilities of Cyanide Compounds.....	79
32	Cyanide Precipitate Flotation Runs.....	81
33	Molarity and mg/l Conversions.....	81
34	Standard Operating Conditions: Determining Runs.....	82
35	Cyanide Ionic Strength Runs.....	83
36	Heavy Metal Runs: Average Residual Concentrations.....	85
37	Percent Residual Metals: Run Types A and D.....	85
A-1	Data on Lead Removal from Wastes and Simulated Wastes with the 10-cm and 30-cm Columns.....	93
A-2	Data on Lead Synthetic Waste Removal with the 30-cm Column.....	98
A-3	Data on Zinc Removal (Plating Waste) with 30-cm Column.....	103
B-1	Floc-Bubble Binding Energy as a Function of Contact Angle.....	110
B-2	Effect of Temperature on σ_{crit}	117

ACKNOWLEDGMENTS

The experimental work presented in this report was carried out by Joseph C. Barnes, Ann N. Clarke, Ben L. Currin, Jo S. Hanson, Douglas L. Miller, Jr., F. John Potter and Ronald P. Robertson. The theoretical work was done with the aid of Ben L. Currin. The advice of Hugh B. Durham and Donald L. Wilson (who served as the first EPA project officer) is gratefully acknowledged.

SECTION 1

INTRODUCTION

The removal of trace levels of toxic metals has become a problem of current interest in the area of advanced wastewater treatment. Toxic metals are not efficiently removed by biological treatment or by conventional drinking water treatment techniques. They not only interfere with the efficient operation of secondary (biological) treatment plants, but their presence in biological sludge interferes with the disposal of this material by some methods, especially land application. The extent of the problem is detailed in our previous report (1) and in other government publications (2,3,4, for example).

Any metal removal technique should be: (a) rapid; (b) cheap in terms of labor, energy, equipment, and chemicals; (c) capable of application in small, intermediate, and large scales; (d) productive of small volumes of liquids or solids highly concentrated in the contaminant(s); and (e) capable of producing effluents well within the standards established or anticipated. Data presented here and in our earlier report (1) indicate that adsorbing colloid foam flotation may well meet these criteria.

LITERATURE REVIEW

The brief literature review given here can be supplemented by a more comprehensive review given in our first report (1), and by a very comprehensive review of the recent literature (5). Lemlich's book (6) provides an excellent introduction to principles and applications. Somasundaran published extensive general reviews in 1972 (7) and 1975 (8). Grieves (9), Ahmed (10), Bahr and Hanse (11), Panou (12), Richmond (13) and Bakerzak (14) have also written recent general review articles on foam flotation. In 1977, at least three articles reviewed the use of foam flotation techniques in wastewater treatment (15-17).

An extensive collection of symposium papers covering most aspects of particulate flotation was edited by Somasundaran and Grieves (18).

The operation of foam stripping columns has been analyzed by a number of workers. The earlier work was reviewed by Goldberg and E. Rubin (19), who also referenced work on foam drainage, a matter of some importance in foam separations. Wang and his co-workers worked out a theory for continuous

bubble fractionation columns which requires local equilibrium between surface and bulk phases (20,21,22). Goldberg and Rubin have analyzed stripping columns without solute transfer in the countercurrent region (23). Cannon and Lemlich presented a detailed analysis which assumes linear isotherms (24), and Lee has given a somewhat similar treatment (25). Sastry and Fuerstenau analyzed the differential equations modeling a countercurrent froth flotation column, obtaining formulas for column efficiencies in some limiting cases (26). Wilson and his co-workers analyzed stripping column operation with axial diffusion, non-linear isotherms, and finite rate of solute transport between surface and bulk liquid phases (27); they solved the differential equations describing mass transport by iterative use of a quasi-linearization method. Grieves and his co-workers have developed an approach which permits the use of batch foam fractionation data from one system to predict the performance of other systems, both batch and continuous (28).

Next, we will address the attachment of particles to bubbles. Petrakova, et al. (29) examined the mechanism of interaction of gas bubbles with mineral particles, and Abramov (30) has also worked on the physico-chemical modeling of flotation systems. Reay and Ratcliff (31) provided a theoretical treatment of the benefits of using smaller bubbles or larger particle sizes in dispersed air flotation systems. When particles are large enough that they are unaffected by Brownian motion, flotation rate increases with increasing diameter.

Scheludka, et al. (32) has given an elegant analysis in terms of capillarity of the attachment of a spherical particle to a planar liquid surface after contact is made. The minimum particle size ($\sim 10^{-4}$ cm) for which flotation can occur is calculated as well as the maximum particle size which can remain attached. The maximum size depends on the contact angle. Particle detachment may be the result of gravity or the kinetic energy of collision with a bubble; the former yields the larger particle radius, so the latter determines the upper limit of flotability for a given system. The maximum radius calculated for a representative system is 2.7×10^{-2} to 5.5×10^{-2} cm for gravity detachment; the smaller size corresponds to those particles found in practice to be removed by flotation. Deryagin, et al. (33) also studied the criteria for bubble attachment using the theory of heterocoagulation. Bleier, et al. (34) also used heterocoagulation to examine adsorption and critical flotation conditions. They claim that surface tension data show a large surface charge density on the bubble during flotation. Heterocoagulation suggests that the oppositely-charged double layer of a system reacts to produce a large potential energy of attraction. These electrostatic forces lead to the rupture of the aqueous film around the particles, and then these electrostatic forces decrease. The ionic species in the gas-liquid interface then desorb. The relative hydrophobicity of the particle surface then determines whether the particle and bubble will stay attached (will heterocoalesce).

Lai and Fuerstenau (35) proposed a model for the surface charge distribution and its effect on flotation response. In water, an oxide surface exhibits, simultaneously, positive, negative, and electrically neutral sites, due to the interplay of H^+ and OH^- with the surface. The distributions of these sites were calculated as functions of pH, and the point of zero charge

determined. Various oxide minerals and collectors (surfactants) which absorbed either physically or chemically were studied. It was expected that flotation efficiency would depend on surface site distributions since flotation had been shown to correlate with adsorption phenomena. Also, one expects that, at low collector concentrations, a physically adsorbing cationic collector would adsorb at a negative site; an anionic collector, at a positive site. Flotation responses correlated well with the site distribution model predictions, allowing, in some instances, for concomitant ionization of neutral flotation collectors.

Floc foam flotation isotherms and local rate effects have been investigated by Wilson and his co-workers by means of a modified Gouy-Chapman model in which the binding force between particles and the air-water interface is due to coulombic attraction between the negatively (positively) charged air-water interface and the positively (negatively) charged particles. The charge on the air-water interface is assumed to be due to the formation of a hemimicelle layer of ionic surfactant on it, and the coulombic interaction is modified by the ionic atmospheres in the vicinities of the two charge densities (36,37,38). They have extended the statistical mechanical treatment of floc adsorption isotherms to include the effects of non-ideal flocs and salts (39), the electrical repulsions between floc particles (40), the occurrence of cooperative phenomena in the surfactant film (41), and the effects on surface potentials of the specific adsorption of ions by flocs (42).

More recently, this group has also examined a model used by Fuerstenau, Somasundaran, Healy, and others for some time in interpreting the results of ore flotation experiments (43,44,45,46,47,48,49,50, for example). In this model it is assumed that the particle surface is made hydrophobic by the absorption of the ionic heads of the surfactant ions in the primary adsorption layer of the particle, leaving the hydrocarbon tails presented to the water. Van der Waals interactions between the hydrocarbon tails permit the possibility of surface condensation; particles with surfaces densely covered with surfactant are hydrophobic, with non-zero air-water contact angles; this results in bubble attachment. Wilson's group investigated the statistical mechanics of this phase change (41); the effects of specific adsorption of foreign ions on displacement of surfactant from the floc (51); and the calculation of adsorption isotherms for this non-coulombic model for the attachment of floc particles to the air-water interface (52). They also examined the magnitude of the viscous drag forces tending to detach floc particles from the air-water interface (51,52).

We turn next to recent work on adsorbing colloid flotation. Our first report (1) presented data on the precipitate and adsorbing colloid flotation of lead, copper, cadmium, mercury, arsenic and fluoride; many of these data are published elsewhere (53-57). Zeitlin and his co-workers have published very extensively on adsorbing colloid flotation separations; they have used the technique for concentrating the following from sea water: zinc (58), copper (59), molybdenum (60,61), uranium (62,63), mercury (64), phosphate and arsenate (65), silver (66), and vanadium (67). They also carried out a study of the foam separation of six flocs suitable for adsorbing colloid flotation [$\text{Fe}(\text{OH})_3$, $\text{Al}(\text{OH})_3$, $\text{Th}(\text{OH})_4$, MnO_2 , HgS , and CdS] with nine different surfactants (68); this work should prove invaluable, particularly to those

developing techniques for concentrating trace quantities of material for analysis.

Zhorov, et al. (69) studied the flotation of copper, molybdenum, and uranium with $\text{Fe}(\text{OH})_3$ as the floc, stearic acid and indolebutyric acid as collectors and Stearox 6 as the foaming agent. An application of adsorbing colloid flotation is suggested by a study of the sorption of arsenite by ferrous sulfide carried out by Grigor'ev and his co-workers (70).

Grieves and Bhattacharyya, very active workers in foam separation techniques, have investigated a number of waste treatment applications, many of which are reviewed in our first report. Studies of the flotation of $\text{Cr}(\text{OH})_3$ (71), and of the precipitate coflotation of CaSO_3 and CaCO_3 (of interest in treating wet scrubber slurries formed during SO_2 removal from stack gases) (72) are of particular interest here.

A problem which arises in the scaling up of foam flotation separations is that of collapsing the foam. Our experience has been that the high-speed spinning disc technique described some years ago by E. Rubin and his co-workers (73,75) is very effective.

Although we are not concerned with ore flotation techniques as such, their principles are quite significant for precipitate flotation and adsorbing colloid flotation. M. C. Fuerstenau edited a recent extensive collection of papers on ore flotation, which contains a wealth of relevant information (75).

SECTION 2

CONCLUSIONS

Floc foam flotation methods were investigated on a pilot-plant scale and demonstrated to reduce lead and zinc from dilute aqueous solution to very low concentrations. The pilot-plant experience suggests several improvements in the design of the apparatus which should result in an effluent of higher quality and a column of increased hydraulic loading capacity. These modifications include: (1) a larger mixer-flocculation tank to increase the detention time of the floc before it is removed by flotation; (2) increased baffling of the stripping column section, to decrease channeling and foam overturn at high hydraulic loadings; and (3) a decrease in the length of the foam drainage section of the column, to decrease the tendency of the foam to collapse before it has been discharged from the column.

Studies indicate that a simple diffusion-type model is not very accurate when column performance becomes seriously limited by axial dispersion. The scale of the turbulences (channeling, overturn, and eddies) is too large to permit their accurate modeling by simple diffusion. Hydraulic loading and alignment of the column, baffles, and influent dispersion head are the most important factors affecting axial dispersion.

The floc foam flotation of zinc(II) is readily carried out with aluminum hydroxide as a carrier floc and sodium lauryl sulfate (NLS) as surfactant; ferric hydroxide is much less effective as a carrier floc. Chromic hydroxide is floated with NLS, but the residual Cr(III) concentration was generally greater than 5 mg/l; adsorbing colloid flotation with $\text{Fe}(\text{OH})_3$ and $\text{Al}(\text{OH})_3$ yielded much better results. Cobalt(II) and nickel(II) levels are reduced to around 1 mg/l by flotation with $\text{Al}(\text{OH})_3$ and NLS; $\text{Fe}(\text{OH})_3$ is not so effective with nickel.

Floc foam flotation of copper(II) was shown to be compatible with a number of precipitation pretreatments (soda ash, lime, ferric and aluminum hydroxides), although some modifications are needed to prevent interference from excessive calcium or carbonate ion concentration. This makes possible the use of floc foam flotation as a polishing treatment for relatively concentrated wastewaters which are not adequately treated by precipitation alone.

The flotation of ferric hydroxide flocs with NLS is profoundly affected by a number of polyvalent anions, some of which are commonly found in industrial cleaners (silicates, phosphates). These can cause serious interference with floc foam flotation unless they are disposed of by preliminary

treatment, such as lime precipitation. These anions apparently are able to displace surfactant from the floc, thereby rendering it hydrophilic and unfloatable. This phenomenon, at times a troublesome interference in wastewater treatment, can apparently be used to recover surfactant from floc foam flotation sludges for recycling.

The flotation of mixtures of copper(II), lead(II) and zinc(II) was successfully carried out using $\text{Fe}(\text{OH})_3$ as the floc and NLS as the collector surfactant. The flotation of simple and complexed cyanides and mixtures of metal cyanide complexes was also carried out with $\text{Fe}(\text{OH})_3$ and NLS; a pH of around 5 is optimum. Zinc cyanide complex is not as well removed as are those of copper, chromium, nickel and cobalt.

A surface adsorption model for floc foam flotation was examined by statistical mechanical techniques and found to account for the effects of surfactant concentration, ionic strength, specifically adsorbed ions, and surfactant hydrocarbon chain length. The model proved to be a helpful tool for the designing and trouble-shooting of floc foam flotation separations.

SECTION 3

RECOMMENDATIONS

The results of the adsorbing colloid flotation pilot plant studies reported here justify a recommendation that the following design modifications in the pilot plant be investigated.

(1) The size of the mixer-flocculator tank should be increased to allow sufficient time for optimum floc formation and adsorption of the dissolved ion onto the floc. This should result in improved effluent quality. Laboratory scale kinetic studies of the rates of coprecipitation and/or adsorption of copper, zinc, and lead with ferric hydroxide are needed to determine the detention time required.

(2) More baffling should be added to the stripping section of the column to decrease channeling and foam overturn at high hydraulic loadings.

(3) The length of the foam drainage section of the column should be decreased to lessen the tendency of the foam to collapse and drop sludge through the column before it has been discharged from the top of the column.

(4) The pilot plant clarifier assembly should be modified to permit the use of sodium carbonate (or other salts) to displace surfactant from the sludge in the collapsed foamate in order to recover this surfactant for recycling.

The bench scale work supports the following recommendations:

(1) The use of mixed flocs (aluminum hydroxide ferric hydroxide, for example) for the removal of mixtures of metal ions should be studied.

(2) Additional work on interferences resulting from the presence of polyvalent anions likely to be present in waste streams is needed to determine the extent of these interferences and to develop techniques to counteract them.

Additional field testing of the pilot plant is necessary to facilitate improvements in equipment design, flotation procedures, and trouble-shooting techniques.

SECTION 4

OBJECTIVES OF THE RESEARCH PROGRAM

The objectives of our work included both pilot-scale work and bench-scale studies to demonstrate the feasibility of adsorbing colloid flotation for industrial wastewater treatment and to extend the applicability of the technique to substances and combinations of substances not dealt with in our earlier report (1). These objectives can be listed as follows:

A. Pilot-scale work

1. Laboratory testing of a 10-cm continuous flow pilot plant removing lead from simulated wastewaters with ferric hydroxide and sodium lauryl sulfate (NLS) to estimate optimal design parameters for a 30-cm pilot plant to be constructed.
2. Construction of a mobile 30-cm continuous flow adsorbing colloid flotation pilot plant suitable for field testing.
3. Operation of the 30-cm pilot plant with simulated and actual wastewater samples to determine optimum ranges of operating conditions and to indicate needed modifications of the design.
4. Examination of column performance characteristics (particularly axial dispersion) and their dependence on the operating parameters of the 10-cm continuous flow column.

B. Bench-scale work

1. Development of feasible methods, if possible, for the adsorbing colloid flotation of chromium(III), manganese (MnO_2), cobalt(II), zinc(II), nickel(II), and cyanides. (Initially we included antimony and thallium on this list; we could obtain no wastewaters containing these, so we replaced them with cyanides.)
2. Investigation of the compatibility of various precipitation pretreatments [Na_2CO_3 , $\text{Ca}(\text{OH})_2$, Na_2S , etc.] with subsequent adsorbing colloid foam flotation of copper(II). Demonstration of such compatibility would establish the feasibility of using adsorbing colloid foam flotation as a polishing technique to upgrade the quality of fairly concentrated wastewaters after their pretreatment by precipitation methods.

3. Investigation of the adsorbing colloid foam flotation of mixtures of zinc(II), lead(II), and copper(II) to determine the feasibility of using the technique on mixed wastes.
4. Investigation of the recovery of surfactant from collapsed foamate and sludge separated from collapsed foamate. Surfactant recovery would markedly improve the economics of the process and also reduce the likelihood of contamination of surface and ground waters with surfactant if the sludge is deposited in a landfill.
5. Investigation of interferences with adsorbing colloid flotation [using $\text{Fe}(\text{OH})_3$ and NLS] from the presence of other ions such as phosphate, oxalate, EDTA, cyanide, etc.

In connection with these lab studies, we note that industrial wastes are usually complex mixtures of markedly varying composition, and therefore neither studies on simple solutions of a single contaminant nor studies on a single type of waste can be expected to give an accurate assessment of the capabilities and limitations of any waste treatment technique. A broad range of bench scale tests on samples of an equally broad range of known compositions should provide invaluable guidance in trouble-shooting field tests and industrial operations employing this or any other treatment technique.

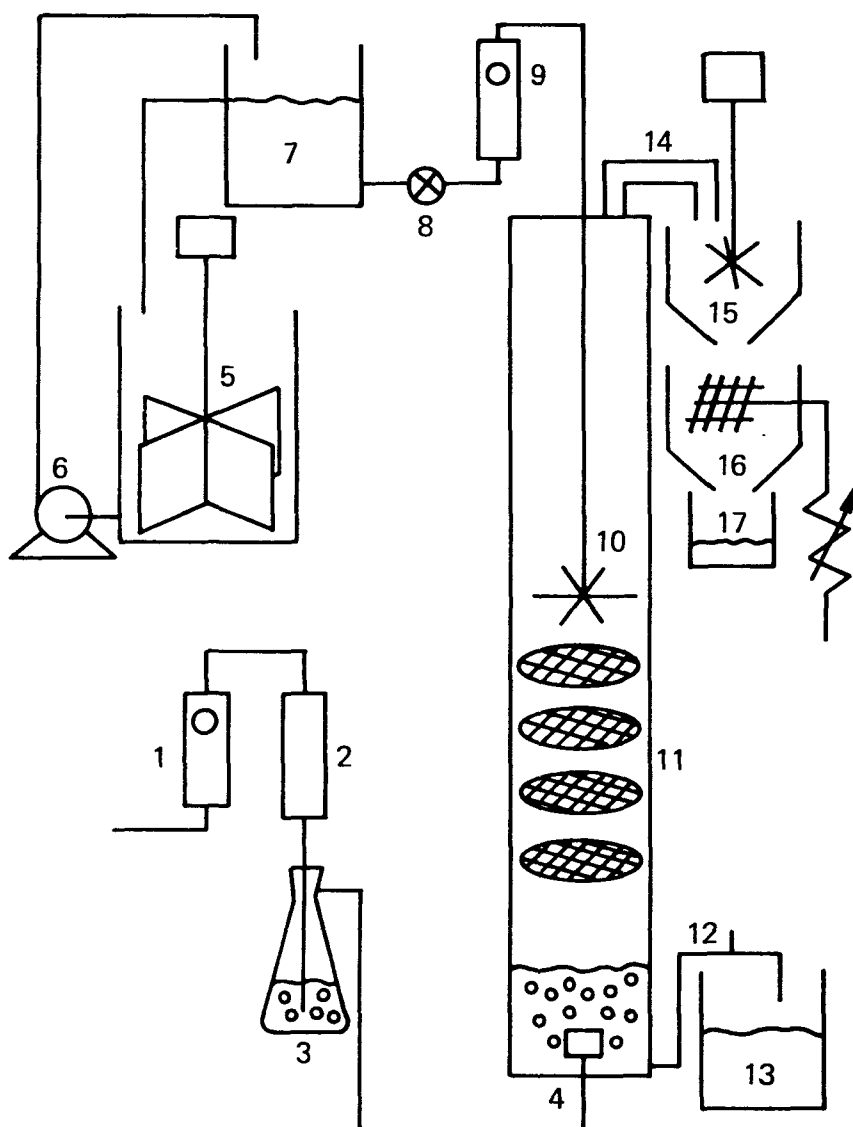
SECTION 5

PILOT PLANT WORK (10-cm DIAMETER COLUMN)

DESCRIPTION OF APPARATUS

Our first continuous-flow apparatus approaching pilot plant size was the flotation system diagrammed in Figure 1. The column was a lucite cylinder 10 cm in diameter and 186 cm in length. The influent was introduced through a tube passing through the top cover plate of the column, and was sprayed into the rising foam through a spider-like dispersion head mounted at the end of this tube about 90 cm below the top to the column. A foam discharge port was mounted in the top coverplate. Bubbles were generated by admitting air through a cylindrical bubbling stone (YWR Scientific Catalog No. 32568-007) mounted on the bottom coverplate. The air flow rate was measured with a variable area flow meter and the wastewater flow was determined by measuring the time required to discharge one liter. House air was humidified and passed through glass wool before being admitted to the column. The influent was prepared by adding the appropriate chemicals to approximately 50 l of water in a large plastic container. The solution was stirred continuously while the pH was adjusted to the desired value, and the solution was then pumped to a smaller constant head reservoir above the column, from which the influent flow to the dispersion head was controlled by a screw clamp. The effluent was discharged from the column through a plastic tube through the bottom coverplate, the vertical position of which could be adjusted to control the level of liquid in the bottom of the column. Four stainless steel wire mesh (0.05-cm mesh) baffles were mounted between 95 to 113 cm below the top of the column to aid in reducing turbulence and overturning in the foam. The foam was discharged to either a spinning screen foam breaker or a hot surface foam breaker, and collected in a glass beaker below the foam breaker.

Several designs of influent dispersion heads were tested before satisfactory results were obtained. Reduction of column cross-sectional area must be minimized, the distribution of influent over the column cross-section must be quite uniform, and the linear velocity of the liquid exiting the discharge ports must be small enough that the foam is not broken. If these conditions are not met, foam channelling and overturn occur at relatively low influent hydraulic loading. The design finally used was a spider made by bundling together seven 5-cm pieces of 1/16-in ID copper tubing and soldering these into the end of a 3.8-cm piece of 3.8-in ID copper tubing. The six outer tubes were bent at right angles to the axis of the distribution head and two 1/16-in holes were drilled into the top side of each tube. The ends of these tubes were pinched shut, and the center small tube was cut short



- | | |
|-----------------------------------|--------------------------------|
| 1. Air Flow Meter | 10. Influent Dispersion Head |
| 2. Glass Wool Column | 11. Foam Baffles |
| 3. Humidifier | 12. Effluent Drain |
| 4. Air Stone | 13. Effluent |
| 5. Influent Reservoir and Stirrer | 14. Foam Discharge Pipe |
| 6. Pump | 15. Spinning-wire Foam Breaker |
| 7. Constant Head Tank | 16. Hot-Wire Foam Breaker |
| 8. Influent Stopcock | 17. Collapsed Foamate |
| 9. Influent Dispersion Head | |

FIGURE 1. The 10-cm pilot plant.

and pinched shut. Wire struts to keep the distribution head centered radially in the column were soldered onto the bottoms of alternate tubes.

It is essential that the dispersion head and the baffles be carefully levelled and that the column be vertical. A 1° vertical misalignment of the column resulted in consistent channelling of the foam down the lower side. Slight tilting of the baffles or dispersion head also caused channelling.

The foam discharge port in the top of the column directed the foam to a spinning screen and wire spider foam breaker in an inverted gallon milk jug, the bottom of which had been cut out. This device was usually overwhelmed by foam, and a second inverted bottomless milk jug containing a hot wire gird was added below the first to catch the overflow. Neither of these foam breakers was really satisfactory; we have since used high speed, spinning disc foam breakers of the type described in Section 6. These are extremely effective.

PROCEDURES

Our objective was to investigate the removal of lead by adsorbing colloid flotation with ferric hydroxide and sodium lauryl sulfate (NLS). The procedures used were as follows.

Stock solutions of ferric chloride (FeIII, 10 g/l), lead nitrate (PbII, 10.0 g/l), NLS (10.0 gm/l), sodium hydroxide (5 molar) and sulfuric acid (1.25 molar) were prepared using tap water. Nitric acid (5 ml/l of concentrated acid) was added to the lead nitrate stock solution. Reagent grade lead nitrate, nitric acid, and sulfuric acid were used; NLS was laboratory grade; and ferric chloride and sodium hydroxide were technical grade. Ionic strength of the simulated waste was adjusted by the addition of the appropriate weight of solid reagent grade sodium nitrate to the waste reservoir.

To make up a wastewater sample, the desired volumes of lead nitrate and ferric chloride were added to roughly 10 l of tap water in the waste reservoir, sodium nitrate was added as needed, and the solution stirred until all solids were dissolved. We then added tap water until the desired volume was reached (25 or 50 l) and adjusted the pH by adding sodium hydroxide solution or sulfuric acid as needed. NLS solution was then added, the pH again adjusted, and the pump feeding the constant head reservoir turned on.

One liter of 200 mg/l NLS solution was poured into the column initially to permit rapid generation of foam. During this process an air flow rate of approximately 3 l/min was maintained. Influent was permitted to enter the column when the foam reached the dispersion head; at this point some channelling and overturn invariably occurred. The foam usually quickly stabilized, however, and the influent flow rate could then be increased somewhat and the air flow rate decreased.

The stirrer in the main waste reservoir and the two foam breakers were kept in operation during the entire run. Effluent samples were taken at approximately 5-minute intervals during the run.

Reagent grade lead nitrate and concentrated nitric acid (5 ml/l) in de-ionized water were used to make a stock solution and standards for analysis. Lead concentrations were determined on a Perkin-Elmer model 305B atomic absorption spectrophotometer operating at 217.0 nm.

RESULTS AND DISCUSSION

The objectives of this research were to investigate the feasibility of using adsorbing colloid flotation to treat lead-bearing wastes on a larger scale than the previous bench-scale experiments and to determine whether or not experimental results were consistent with the theoretical model presented in Section 1. Results of some work with a smaller (4.8-cm ID x 121 cm) continuous flow column (1), warranted a trial with a larger column. A larger column also seemed necessary to determine the effects of channeling and foam overturn which could not be estimated from the work with the 4.8-cm column.

In the work with the smaller column, Fe(III) concentration was usually set at 100 mg/l, NLS at 50 mg/l, and Pb(II) at 50 mg/l. At low ionic strength (Na_2SO_4 less than 4000 mg/l) optimum pH was in the range of 6.0-6.5. These conditions were used as a starting point for the experiments with the 10.2-cm column. Variables studied in this work were Fe(III) concentration, NLS concentration, pH, influent flow rate, air flow rate, and ionic strength. The influent Pb(II) concentration was 50 mg/l in all runs.

Table 1 shows the experimental design proposed for this work. The values for the variables were chosen to include what were thought to be the optimum operating conditions for the column. Air flow rate and influent flow rate were not specified in this proposed outline because they could be (and were) varied within each run.

As the work progressed, some of the proposed values were changed to agree with newly indicated optimum conditions. The values for parameters actually used in each run and the results from each run are listed in Appendix A.

TABLE 1. PROPOSED EXPERIMENTAL DESIGN FOR 10-cm FLOTATION COLUMN

Run Number ^a	pH	Fe(III) mg/l	NLS mg/l	NaNO ₃ Added moles/l	mg/l
1	6.0	150	40	-	-
2	5.5	150	40	-	-
3	5.0	150	40	-	-
4	6.5	150	40	-	-
5	7.0	150	40	-	-
6	6.0	150	35	-	-
7	6.0	150	30	-	-
8	6.0	100	40	-	-
9	6.0	200	40	-	-
10	6.0	150	40	.10	8500
11	6.0	150	40	.20	17000
12	6.0	150	40	.30	25500

^aAll runs made with initial Pb(II) concentration of 50 mg/l.

The aim of this study was not to reach the maximum hydraulic loading possible in the column, but to balance several variables to achieve a procedure which could produce consistently good effluent quality at low cost. Both influent flow rate and air flow rate could easily be adjusted during a run. Fe(III) concentration, NLS concentration, and ionic strength were held constant throughout any one run.

Constant pH monitoring and/or adjustment was impossible with this apparatus. Invariably the pH changed slightly during the course of a run. These changes were always small (less than 0.4 pH units) and seemed to be always toward a value around pH 5.5. When the initial pH was less than 5.5, the pH increased during the course of the run; if the initial pH was greater than 5.5, the pH decreased.

In very early runs (before the dispersion head problem was worked out) 100 mg/l Fe(III) seemed to be insufficient to achieve the lead removals expected. We therefore used a concentration of 150 mg/l Fe(III) in further preliminary runs.

It is desirable to use the smallest amounts of NLS and Fe(III) possible (while still maintaining good effluent quality) in order to keep chemical costs to a minimum. The wider the pH range in which good effluent quality can be maintained, the less accurate (and therefore less expensive) the pH control system on a full-scale operation can be. Increasing ionic strength has been shown (53,54,55,56,67) to seriously decrease the separation efficiency. Three runs were made in this work at higher ionic strengths. Influent and air flow rates were adjusted frequently during each run.

The effects of channelling and overturning in the foam proved to be the controlling factor in almost every run made. Effluent lead concentrations less than 0.15 mg/l could be attained within fairly wide ranges of pH and influent flow rates when foam overturning could be eliminated. When channelling and overturning occurred effluent concentrations in the range of 0.5 to 1.5 mg/l Pb(II) were common.

Influent flow rate seemed to affect the removal efficiency only when overturning produced excessive axial dispersion in the foam. In one run in which the foam was particularly stable, an influent flow rate of 0.95 l/min (15 gal/hr), producing a hydraulic loading rate of 2.9 gal/min-ft² or 171 m³/day m², was reached, and the effluent lead concentration was 0.05 mg/l. In most runs, serious overturning occurred above about 0.63 l/min (10 gal/hr), a hydraulic loading of 1.9 gal/min-ft² or 112 m³/day-m².

The air flow rate used in most runs was 2.0 l/min (1.24 m³/min-m²). At air flow rates below this value it was almost impossible to prevent overturning of the foam, even at the lowest influent flow rates. At air flow rates greater than 2 l/min, somewhat higher influent flow rates could be tolerated, but the foam coming out the top of the column was very wet. At an air flow rate of 2 l/min the volume of collapsed foamate was always 3% or less of the influent volume. At an air flow rate of 4 l/min (700 m³/day-m²), the collapsed foamate was as much as 9% of the influent volume. Since a smaller volume of more concentrated solution is easier to dispose of, the drier foam is

preferable, and the lower air flow rate was chosen.

Considerably lower concentrations of NLS than the 50 mg/ℓ used in the smaller column (1) were sufficient to produce a stable foam. The minimum concentration which could be relied upon to produce a consistently stable foam at influent flow rates above 0.50 ℓ/min (8 gal/hr), or 1.5 gal/min-ft² (88 m³/day-m²) was 35 mg/ℓ. Occasionally, 30 mg/ℓ NLS produced a sufficiently stable foam. Even at 30 mg/ℓ, there was some dissolved NLS being carried out with the effluent. This was evident from the foam which built up on the surface of the liquid in the effluent bucket.

A somewhat wider range of pH than the 6.0-6.5 recommended earlier (1) produced effluents of 0.1 mg/ℓ or less, as is shown in Table 2.

TABLE 2. EFFECTS OF pH ON LEAD REMOVAL

pH	Influent Flow Rate ^a		Residual Lead (mg/ℓ)
	(gal/hr)	(ℓ/min)	
5.0	12.5	.78	.10
5.5	5.5	.35	.08
6.0	8.0	.50	.10
6.4	8.0	.50	.10
7.1	8.5	.54	.84

Note: All runs were made with 50 mg/ℓ Pb(II), 150 mg/ℓ Fe(III) and 35 mg/ℓ NLS. Air flow rate was 2 ℓ/min.

^a10 gal/hr = 1.9 gal/min-ft², or 112 m³/day-m².

Optimum Fe(III) concentration in the larger column was 150 mg/ℓ. At 100 mg/ℓ Fe(III), the effluent concentration was somewhat higher (0.3 mg/ℓ at 10.5 gal/hr) than at 150 mg/ℓ Fe(III) (0.10 mg/ℓ at 12.5 gal/hr). The effluent lead concentration at 200 mg/ℓ Fe(III) was essentially the same (0.10 mg/ℓ at 10.5 gal/hr) as that at 150 mg/ℓ Fe(III). Therefore, 150 mg/ℓ seemed to be the optimum Fe(III) concentration in this study.

As expected, increasing ionic strength seriously reduced the removal efficiency of the column. Three runs were made at increasing ionic strengths (addition of NaNO₃) at otherwise optimum conditions. Some of the results are shown in Table 3.

TABLE 3. EFFECTS OF INCREASING IONIC STRENGTH ON LEAD REMOVAL

NaNO ₃ Added		Influent Flow Rate		Residual Lead mg/ℓ
moles/ℓ	mg/ℓ	gal/hr ^a	ℓ/min	
0.10	8500	7.0	.44	0.44
0.10	8500	10.5	.66	0.38
0.20	17000	7.0	.44	1.80
0.20	17000	8.5	.54	2.10
0.30	25500	6.5	.41	2.80
0.30	25500	8.5	.54	3.50

Note: All runs made with 50 mg/ℓ Pb(II), 150 mg/ℓ Fe(III), and 35 mg/ℓ NLS. pH was 5.7 to 5.8, air flow rate was 2 ℓ/min.

As mentioned in the description of the apparatus, having the screen baffles and dispersion head level was very important in preventing overturning in the foam. The slightest misalignment of either led to overturning of the foam, which would then not stabilize. When the baffles and dispersion head were level and overturning of the foam occurred, the foam would often recover in a few minutes and return to a stable rise pattern.

The reddish-brown color of the ferric hydroxide floc was very obvious in the foam at the high concentrations present from the dispersion head to the top of the column. Very seldom was there any discernible color below the two screens; overturning of the foam was most common below the lowest screen. On some runs, especially those at pH's greater than 6.5 and those at high ionic strength, the ferric hydroxide was quite obvious in the effluent as a yellow color even when there seemed to be no color breaking through below the screens.

The glass rods supporting the screen baffles must be kept well away from the walls of the column. Toward the conclusion of the work with this apparatus the screens had deteriorated enough to allow one of the three support rods to move toward the column wall. This caused serious channelling of the influent between the rod and the wall, which was disastrous to effluent quality. Removing the whole screen-support-rod assembly, taking the screens off the rods, and punching new holes for the rods at least 1/2 inch from the edge remedied the problem.

Bubble size was not measured quantitatively in this work, but at one point during the work the air stone which had been in use was replaced because it was clogged by oil present in the compressed air. The new stone, which looked identical to the old one, produced bubbles which were obviously larger than those produced by the original stone. The effluent from a run began with the second stone in place was very yellow and the run was not continued. When the original stone was replaced after backwashing with a commercially available detergent, the bubbles were smaller, and the effluent from the same batch of waste was colorless.

Channelling and foam overturning proved to be the major determinants of effluent quality in this work. Increasing ionic strength seriously decreases separation efficiency. Above an NLS concentration of 35 or 40 mg/l, increasing the surfactant concentration does not improve removal efficiency, and at higher concentrations, more NLS is lost with the effluent. pH values outside of the range 5.0-6.5 increase residual lead concentrations. Temperature effects were not considered here. Table 4 summarizes recommended design parameters.

TABLE 4. RECOMMENDED DESIGN PARAMETERS FOR FURTHER STUDIES

pH	5.5-6.5 ^a
Fe(III) concentration	150 mg/l
NLS concentration	35-40 mg/l
Hydraulic loading rate	2-3 gal/min-ft ² (118-176 m ³ /day-m ²)
Air supply	0.2-0.3 m ³ /min-m ²

^aFor high ionic strength wastes, a lower pH than 5.5 may be necessary.

SECTION 6

PILOT PLANT DESIGN AND CONSTRUCTION (30-cm DIAMETER COLUMN)

The principal objective of the present study was the design, construction and testing of a mobile adsorbing colloid foam/flotation facility suitable for both laboratory studies and field testing. Several major changes from the design used for the continuous flow apparatus described in Section V were necessary. These included (a) a high-capacity spinning disk foam breaker to deal with the very large volumes of foam generated; (b) a monitoring and control system to provide continuous adjustment of the pH; (c) a chemical feed system to meter the process chemicals into the waste stream at the proper locations; (d) a mixing and flocculation chamber; and (e) a small clarifier to separate sludge from the collapsed foamate.

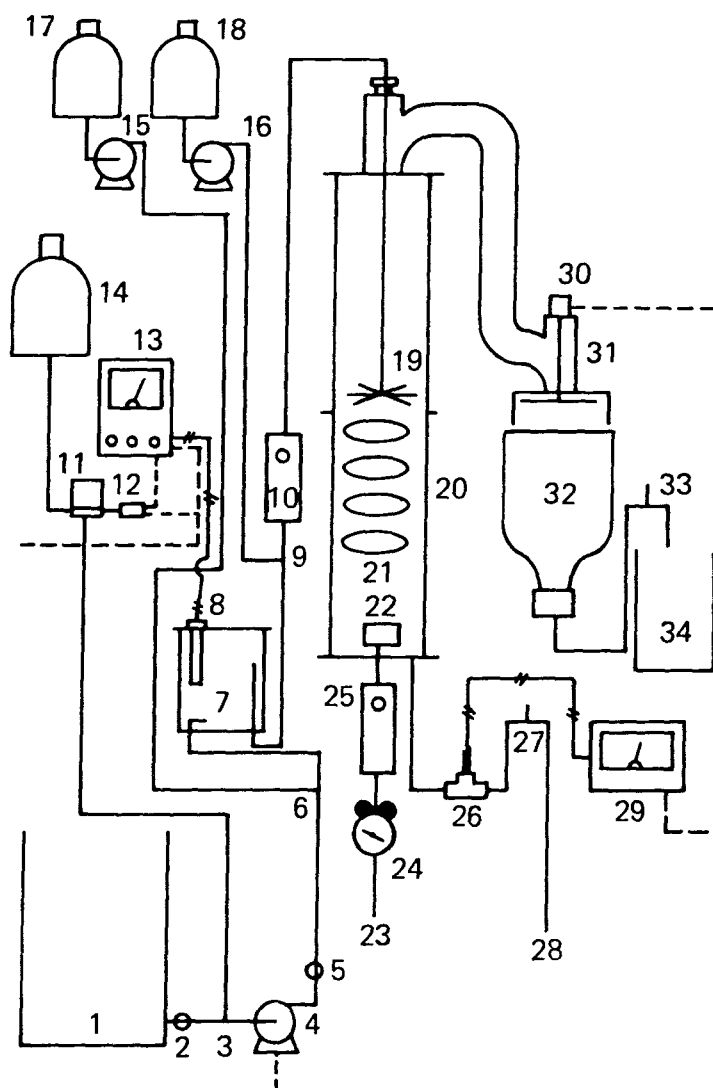
The foam flotation apparatus used in this study is shown in Figures 2 and 3. The system was built on a steel frame mounted on casters so that it would be portable. The equipment mounted on this support frame includes the pumping system, mixing and flocculation chamber, flotation column, foam breaker, foamate clarifier, chemical feed system, pH monitoring and control system, air and waste stream flowmeters, and electrical control panel. A separate waste storage tank was also used in the laboratory studies. All of these are described in detail below.

PUMPING SYSTEM AND RELATED PIPING

The pumping system and related piping are shown in Figures 2, 3 and 4. In order to achieve minimal friction losses at flow rates of 1 to 5 gal/min (.0631 to .315 l/sec), all flexible hose and rigid PVC piping is 3/4-inch. The influent line to the main pump is a PVC line with a tee which is adapted for NaOH injection. The other end of this line is fitted with an adapter for attaching the 3/4-inch influent hose. The pump is a Teel Model 1P 700 stainless steel centrifugal pump discharging 10 gal/min at 15 ft head. The pump discharge passes through a 3/4-inch butterfly valve used to control the liquid flow through the system. On the other side of this valve is a second tee used for injection of ferric chloride. The PVC pipe leading from this tee goes to the influent nozzle of the mixing chamber.

The discharge from the mixing chamber leads to a tee at which surfactant (generally sodium lauryl sulfate, NLS) is injected. From this tee, a PVC pipe leads to a flowmeter (Dwyer Ratemaster Flowmeter No. RMC-SSV-145) used to monitor the flow. A section of PVC pipe leading from the flowmeter connects to a flexible hose leading to the inlet at the top of the flotation column.

A section of PVC pipe is connected from the outlet at the bottom of the



- | | |
|-----------------------------------|------------------------------------|
| 1. Waste Tank | 18. NLS Tank |
| 2. Waste Tank Valve | 19. Flow Dispersion Head |
| 3. Sodium Hydroxide Injection Tee | 20. Column |
| 4. Main Pump | 21. Baffle |
| 5. Flow Control Valve | 22. Air Diffuser |
| 6. Ferric Chloride Injection Tee | 23. Air Supply Line |
| 7. Mixing Chamber | 24. Air Pressure Regulator |
| 8. Control pH Electrode | 25. Air Flow Rotometer |
| 9. NLS Injection Tee | 26. Monitoring pH Electrode |
| 10. Waste Flow Rotometer | 27. Column Liquid Level Control |
| 11. NaOH Solenoid Valve | 28. Effluent Line |
| 12. Electrical Junction Box | 29. Monitoring pH Meter |
| 13. Control pH Meter | 30. Foam Breaker Motor |
| 14. NaOH Tank | 31. Foam Breaker |
| 15. Ferric Chloride Fee; Pump | 32. Clarifier |
| 16. NLS Feed Pump | 33. Clarifier Liquid Level Control |
| 17. Ferric Chloride Tank | 34. Broke Foam Container |

FIGURE 2 - SCHEMATIC DIAGRAM OF 30 - CM PILOT PLANT

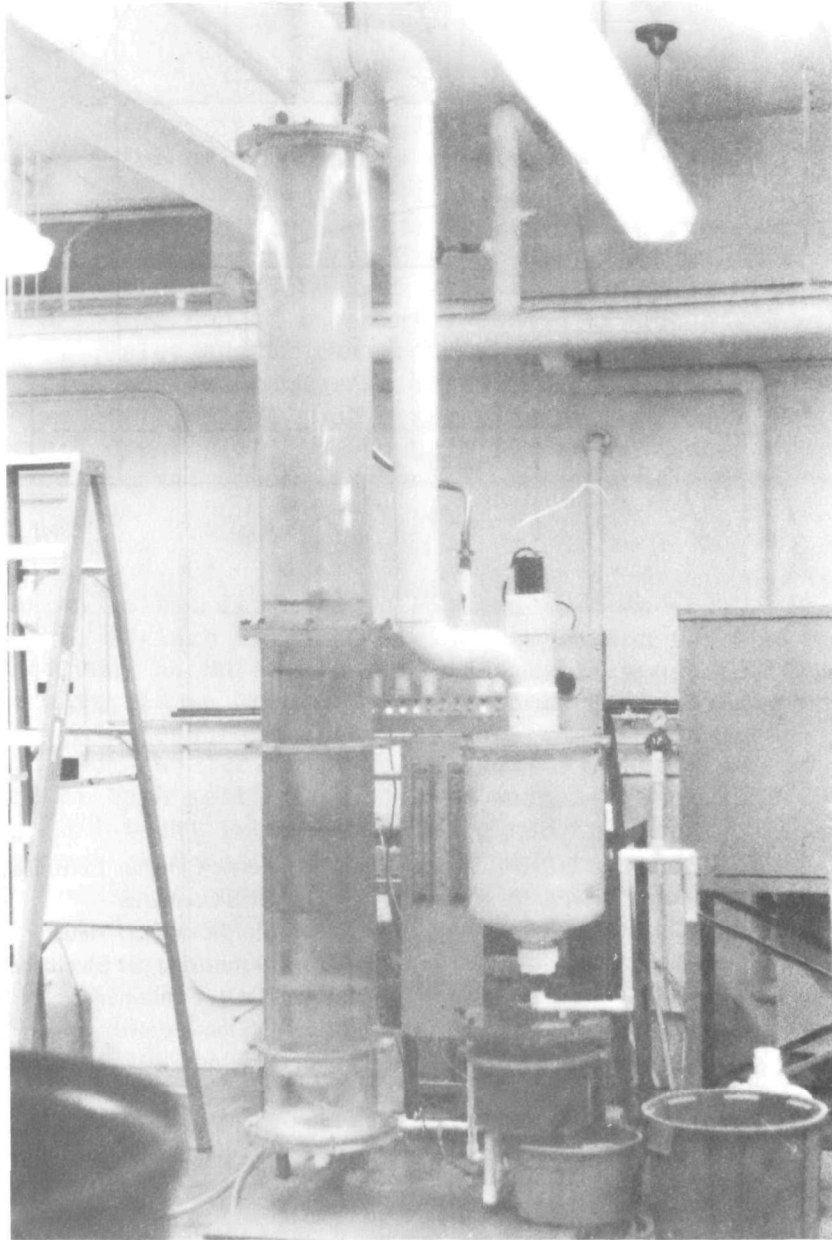
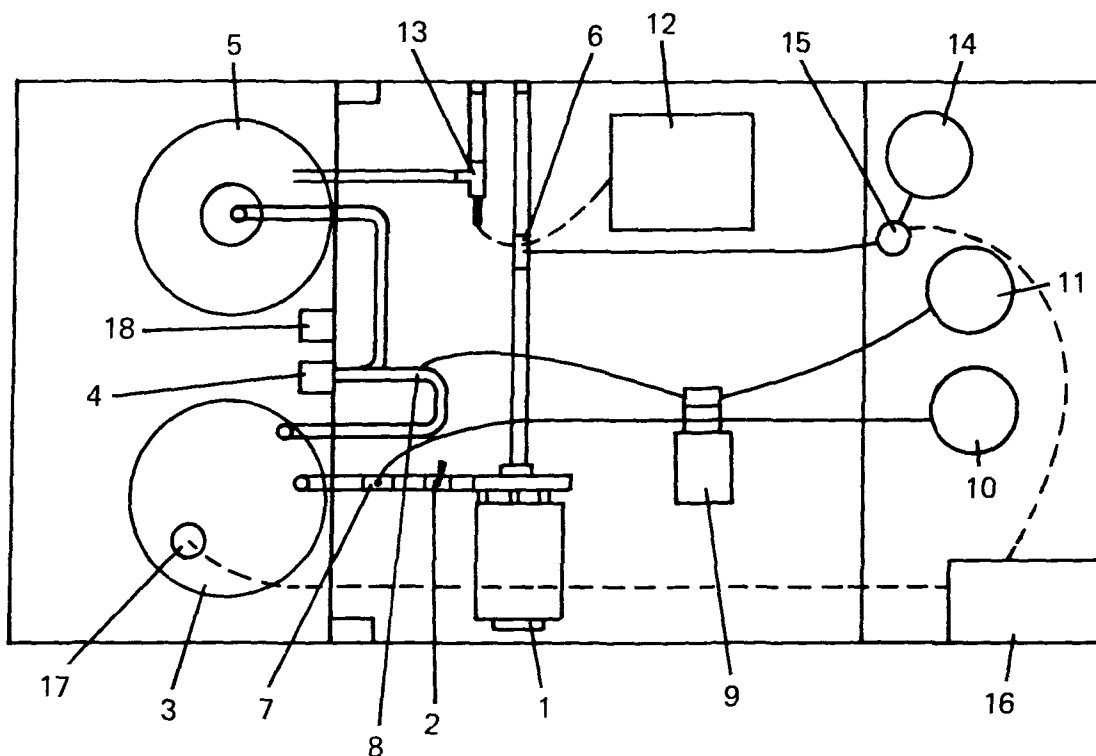


FIGURE 3 - ADSORBING COLLOID FLOTATION PILOT PLANT



COMPONENT LIST

- | | |
|----------------------------------|-------------------------------|
| 1. Waste Pump | 10. Ferric Chloride Container |
| 2. Flow Control Valve | 11. NLS Container |
| 3. Mixing Chamber | 12. Monitoring pH Meter |
| 4. Liquid Flowmeter | 13. Monitoring pH Electrode |
| 5. Flotation Column | 14. NaOH Container |
| 6. NaOH Injection Tee | 15. Solenoid Valve |
| 7. Ferric Chloride Injection Tee | 16. pH Control Meter |
| 8. NLS Injection Tee | 17. Control pH Electrode |
| 9. Chemical Feed Pump | 18. Air Flowmeter |

FIGURE 4 - PLAN VIEW OF PILOT PLANT, SHOWING
PUMPING, CHEMICAL FEED, AND pH CONTROL
AND MONITORING SYSTEMS.

flotation column to a tee which houses an electrode for pH monitoring. The other end of the tee attaches to a flexible hose drain line. This drain line contains a tee open to the atmosphere; this prevents siphoning from occurring when this section of the drain line is raised or lowered to control the level of the liquid pool in the bottom of the column.

MIXING CHAMBER

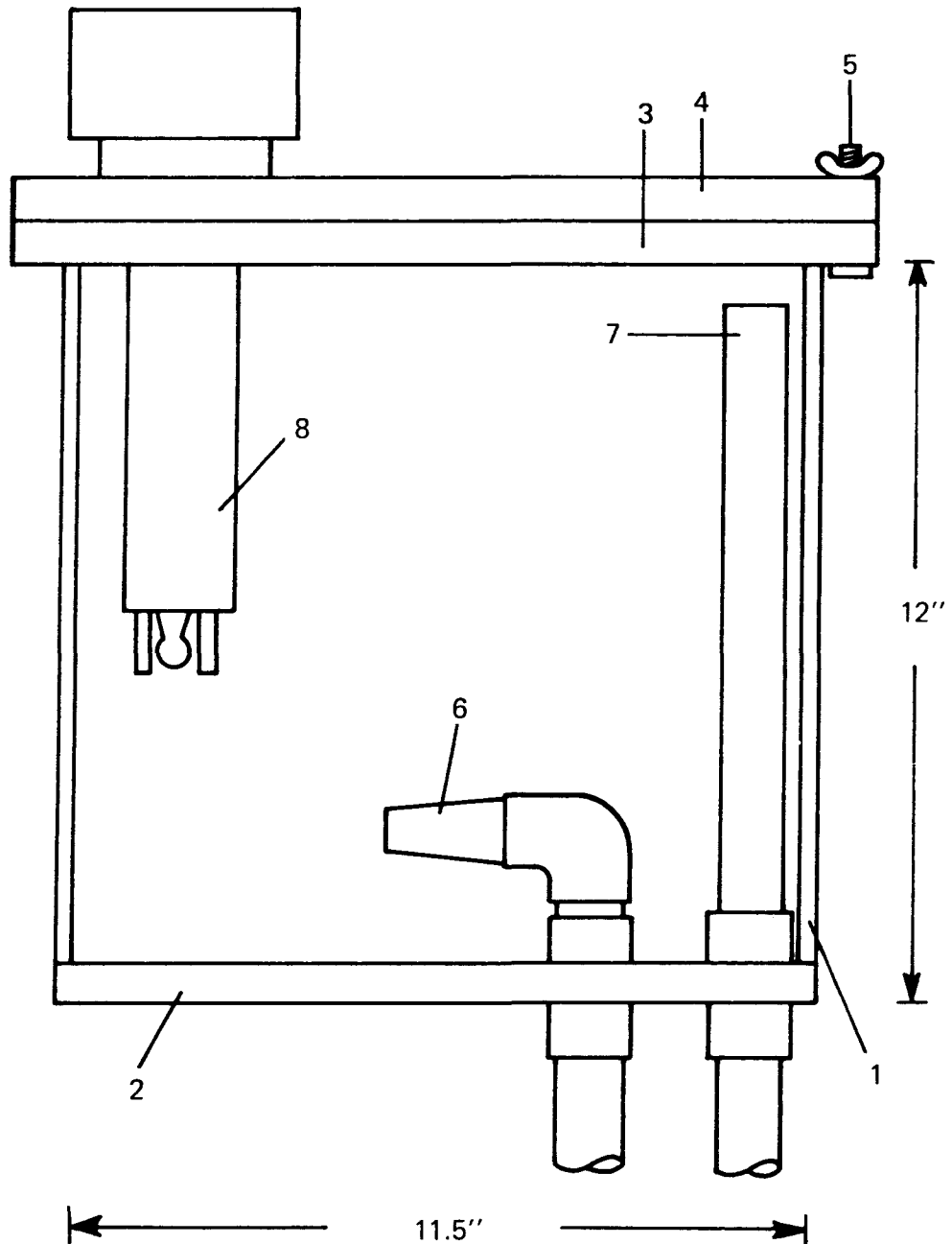
The mixing chamber, shown in Figures 2 and 5, is constructed from a 30.5-cm x 29.2-cm ID (12 x 11.5-inch) section of clear lucite pipe. The total volume of the mixing chamber is 20.4ℓ (0.72 ft³). This gives a detention time of about 1 minute when the pilot plant is operated at a flow rate of 0.32 ℓ/sec (5 gal/min). The bottom of the chamber is a 1.90-cm (3/4-inch) solid piece of lucite which is cemented in place. The top of the chamber is fitted with a 3.8-cm (1 1/2-inch) flange made from 3/4-inch lucite and glued in place. A 3/4-inch solid top is bolted to this flange and sealed with an O-ring. A pH probe is mounted in the top of the mixing chamber for control of the pH in the flotation column. Inlet and discharge ports are mounted in the bottom of the chamber. The inlet to the chamber is connected to a PVC elbow inside the chamber, which mounts a nozzle made by drawing a piece of 3/4 inch PVC pipe down to a 1/4-inch opening at one end. This constriction increases the discharge velocity into the chamber, enhancing the mixing action.

FLOTATION COLUMN

The flotation column is shown in Figures 2, 3 and 6. A 29.2-cm (11.5-inch) ID (30.5-cm, 12-inch OD) lucite pipe was chosen for the construction of the flotation column, because this size was small enough to result in a reasonably mobile unit, large enough to indicate the feasibility of possible full-scale future systems, and this size was readily available. The column was constructed from two 122-cm (4-ft) x 29.2-cm ID sections of clear lucite pipe. Each end of both sections is fitted with a 3.8-cm (1 1/2-inch) flange made of 1.9-cm (3/4-inch) lucite which is glued in place. The two sections are bolted together by 8 bolts through the flanges, and are sealed with an O-ring. The two remaining ends of the joined sections have solid 3/4-inch lucite covers bolted and sealed in the same way.

The bottom cover plate of the flotation column is fitted with an effluent discharge line and an air inlet line, which leads to an air diffuser for generating the foam. House air is used for the column. This air passed through a pressure regulator and then through a 0.64-cm (1/4-inch) tube to an air flowmeter (Dwyer Ratemaster Flowmeter No. RMC-SSV-102) mounted on the support frame of the apparatus. The discharge line from the flowmeter is a 3/4-inch PVC pipe which leads to the bottom cover plate of the flotation column. The air diffuser is a 12.7-cm (5-inch) fritted glass disc (modified fine fritted Büchner funnel).

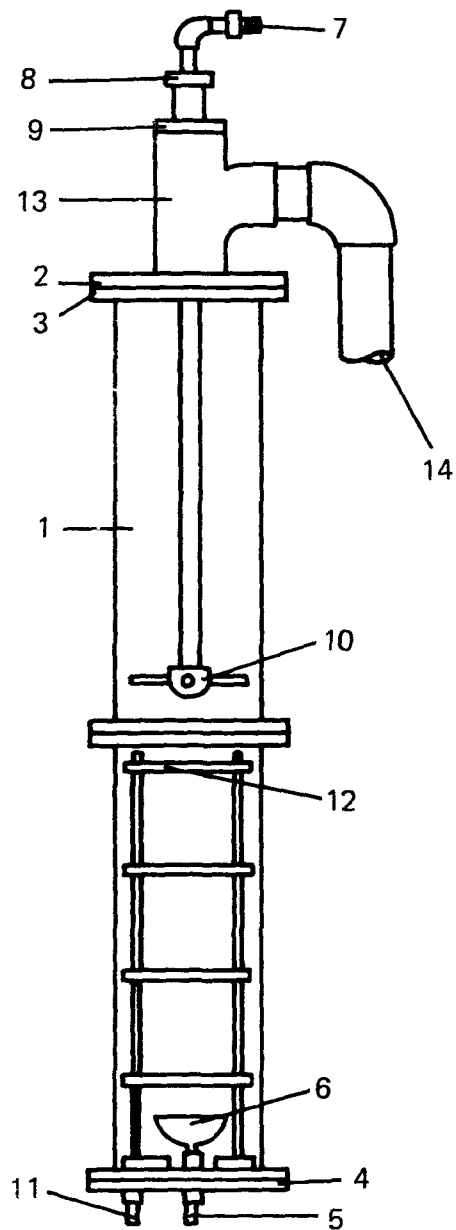
The top cover of the flotation column is fitted with a 10-cm (4-inch) PVC wye, which is the discharge point for the foam generated in the column. A 3/4 inch PVC pipe is run down through the center of this wye by use of adapters and a compression fitting. (See Figure 6) The top end of this pipe is connected by a hose adapter to the flexible hose bringing the wastewater from the



MIXING CHAMBER COMPONENTS

- | | |
|---------------------------------------|------------------------------------|
| 1. 12-In. x 11½-In. ID Lucite Section | 5. Typical Mounting Bolt (8 Total) |
| 2. ¾-In. Lucite Bottom | 6. Mixing Chamber Inlet |
| 3. ¾-In. Lucite Flange | 7. Mixing Chamber Effluent |
| 4. ¾-In. Lucite Cover | 8. Control pH Electrode |

FIGURE 5 - MIXING CHAMBER



FLOTATION COLUMN COMPONENTS

1. Flotation Column Section
2. Top Cover Plate
3. Flange
4. Bottom Cover Plate
5. Air Inlet
6. Air Diffuser
7. Waste Inlet
8. Compression Fitting
9. Adapter
10. Flow Dispersion Head
11. Effluent Line
12. Baffle Structure
13. 4-Inch PVC Wye
14. Foam Discharge Pipe

FIGURE 6 - FLOTATION COLUMN

influent flowmeter. The pipe extends down the axis of the column for about 80-120 cm (31-47 inches), and the influent dispersion head is mounted on its lower end.

The dispersion head was designed to have a linear discharge velocity of 40 cm/sec (1.3 ft/sec) at its orifices at a flow rate of 7.6 l/min (2 gal/min); the total orifice area required is 3.16 cm². The optimum number and size of the openings were found by trial and error; the best design (which was used in the work reported here) is shown in Figure 7. Each of the eight radial arms contains nine holes 0.238 cm (3/32 in.) in diameter.

A system of baffles was constructed and mounted in the lower (stripping) section of the column to reduce foam overturn and channelization. The baffles were cut out of 1.27-cm (1/2-in.) plastic "egg carton" - a decorative grating for lighting fixtures. The assembly consists of seven baffles 27.9 cm (11 in) in diameter mounted 15.2 cm (6 in.) apart on three 0.64-cm (1/4-in.) threaded nylon rods. Nylon nuts and washers were used to secure the baffles to the rods. See Figure 8.

FOAM BREAKER

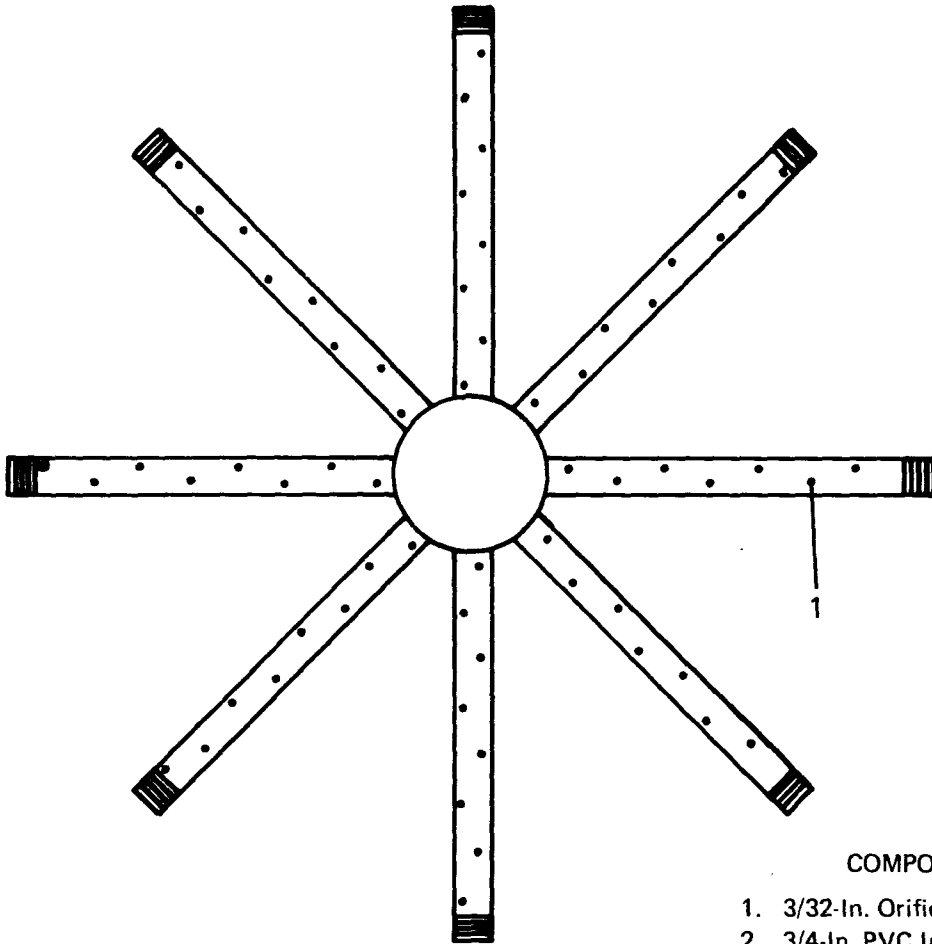
The foam breaker, shown in Figure 9, operates by allowing the foam to impinge on a disc spinning at 2-3000 rpm. The shearing action at the contact destroys the foam very effectively. The housing for the foam breaker was constructed from a 15.2-cm (6-in.) x 29.2-cm ID (11.5-in.) clear lucite pipe fitted with a 1.9-cm (3/4-in.) thick lucite cover. A 4-in. wye is mounted on the top of the cover and connected by a 4-in. PVC pipe to the wye on the top of the flotation column. A 1/8-HP, 3000-rpm permanent split capacitor motor mounted on top of the wye drives the disc. A 1.6-cm (5/8-in.) aluminum shaft with bearings is connected to the motor shaft; the other end extends into the foam breaker housing where it drives a 0.32-cm (1/8-in.) x 27.9-cm (11-in.) diameter nylon disc. Clearance between the disc and the top of the housing is 1.3 cm (1/2 in.).

CLARIFIER

The clarifier (see Figure 10) receives the collapsed foamate from the foam breaker and separates the (floating) solids from the liquid. The clarifier was made by cutting the bottom from a 49-l (13-gal) polyethylene carboy and mounting a level control and drain line (1.9-cm, 3/4-in. PVC) in the screw on cap of the inverted carboy.

CHEMICAL FEED SYSTEM

The chemical feed system is shown in Figures 2 and 3. Ferric chloride and sodium lauryl sulfate (NLS) solutions are stored in two 7.6-l (2-gal) polyethylene jugs on the shelves of the pilot plant support frame. The jugs are connected by 0.32-cm (1/8-in.) plastic tubing to two pump heads (Cole Parmer Instrument Co. Nos. 7016 and 7016-20) driven by a Masterflex Variable Speed Pump Drive (Cole Parmer No. 7545-10). The discharges from the pump heads are injected into tees in the influent line to the column as mentioned earlier. Table 5 shows the feed rates of the 7016 at various pump speed settings.



COMPONENTS

1. 3/32-In. Orifice
2. 3/4-In. PVC Inlet
3. 5-In. x 1/4-In. PVC Pipe Nipple
4. 1-1/2-In. PVC Cap
5. Nylon Plug
6. 1-1/2-In. x 3/4-In. Adapter

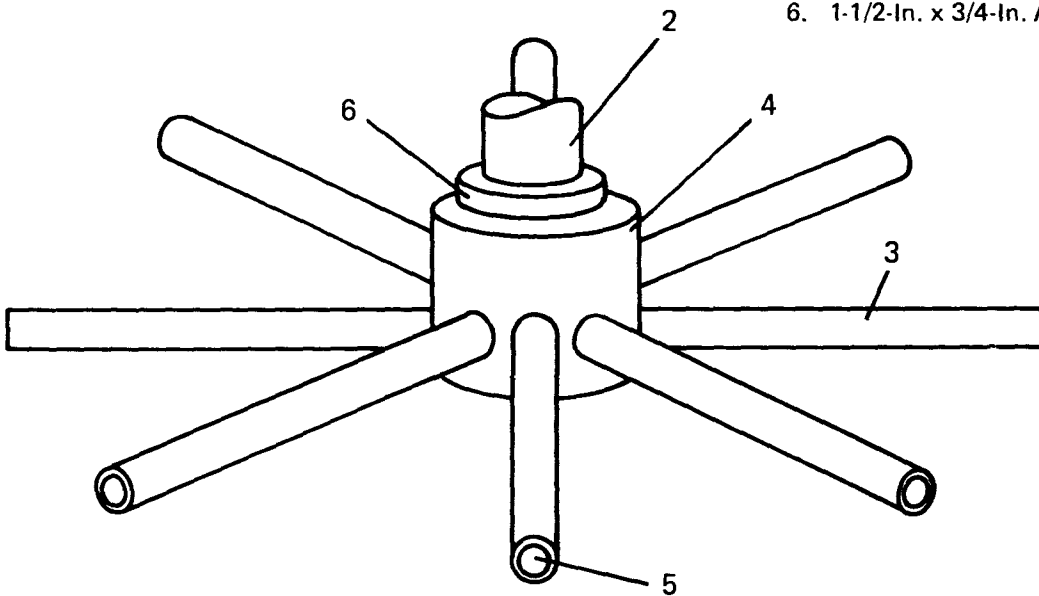
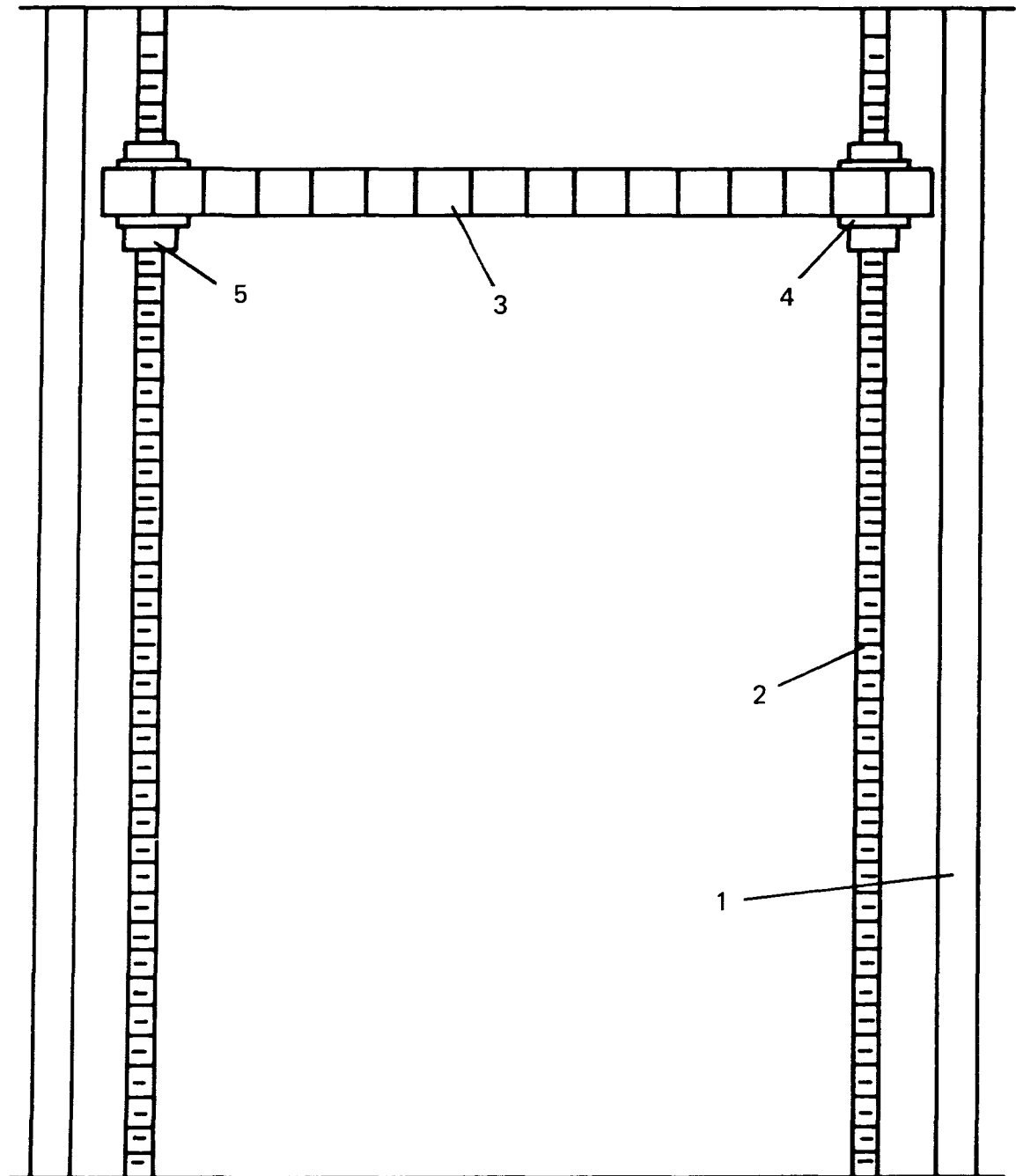


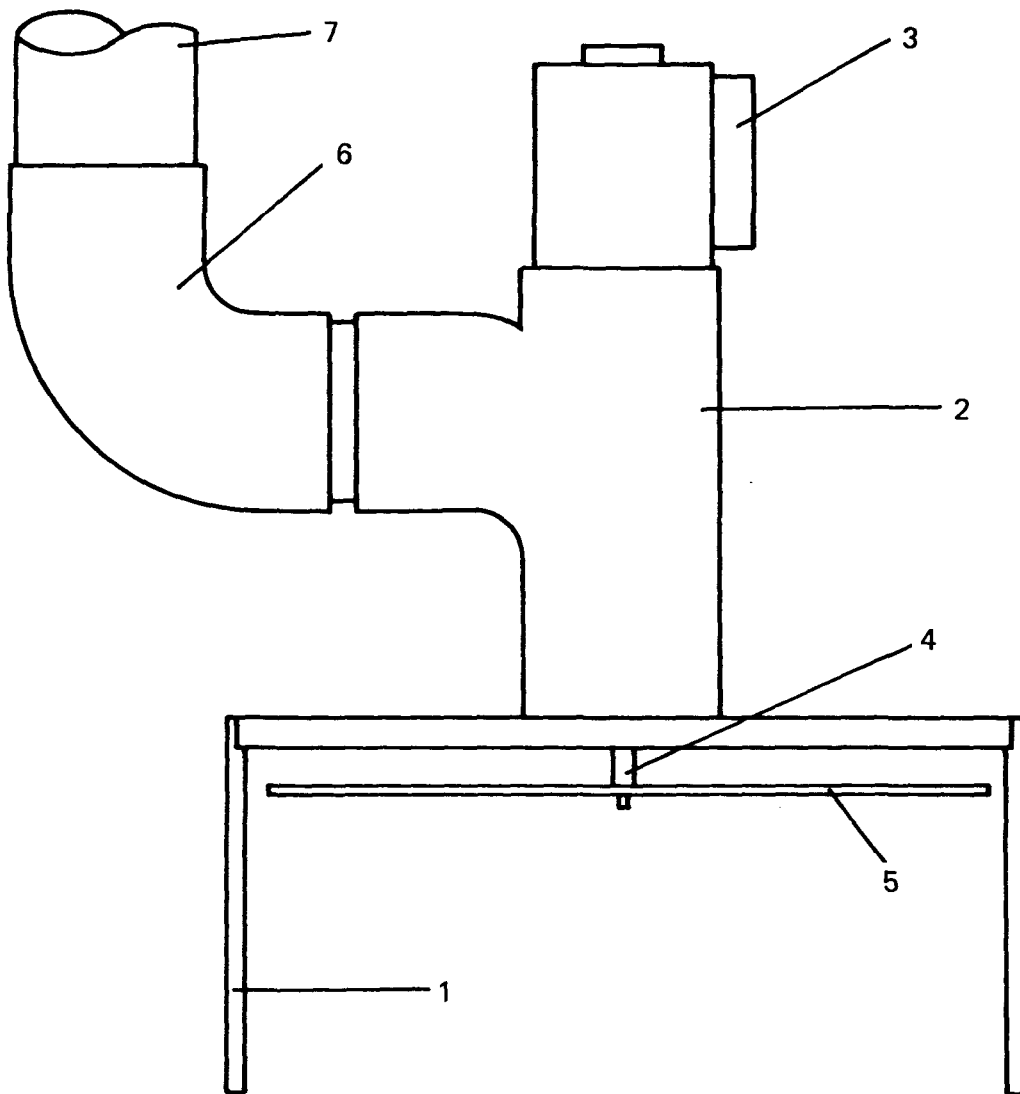
FIGURE 7 - FLOW DISPERSION HEAD



COMPONENTS

1. Flotation Column Wall
2. Nylon Support Rod
3. Plastic Baffle
4. Nylon Washer
5. Nylon Nut

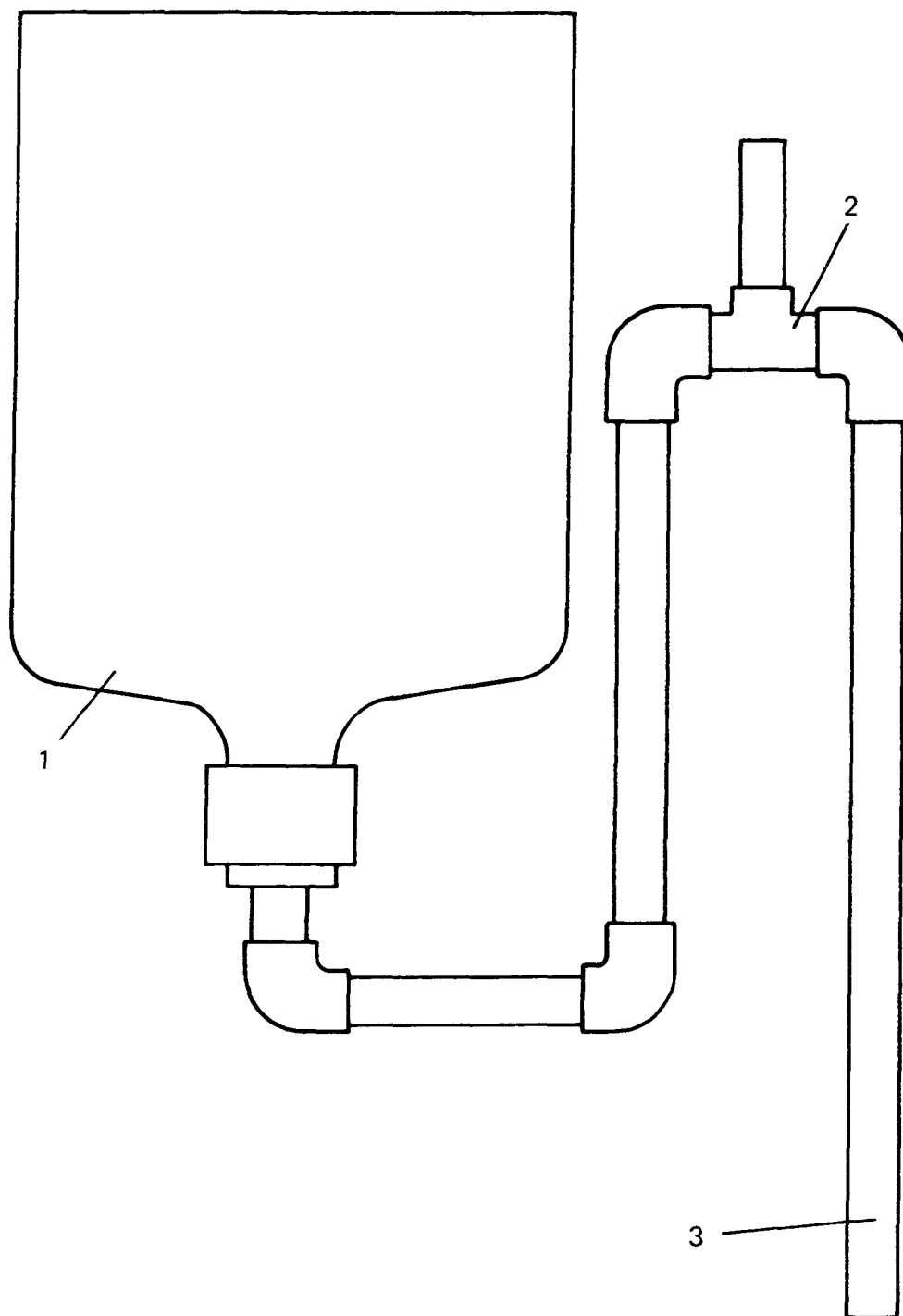
FIGURE 8 - TYPICAL BAFFLE INSTALLATION



COMPONENTS

1. Foam Breaker Housing
2. 4-In. PVC Wye
3. Foam Breaker Drive Motor
4. 5/8-In. Aluminum Drive Shaft
5. 11-In. Nylon Disc
6. 4-In. PVC Elbow
7. 4-In. PVC Foam Inlet

FIGURE 9 - FOAM BREAKER



COMPONENTS

1. Clarifier
2. Level Control
3. Clarifier Discharge Line

FIGURE 10 - CLARIFIER

TABLE 5. FLOW RATES FOR VARIOUS SETTINGS OF
CHEMICAL FEED PUMP 7016

Pump Speed Setting	Feed Rate (ml/min)
10	100
9	84
8	75
7	61
6	54
5	52
4	16

pH CONTROL AND MONITORING SYSTEM

The pH systems are shown in Figures 2 and 4. The pH electrode (Kruger and Eckels No. 80278) mounted in the mixing chamber is connected to a pH meter controller (Horizon Model 5650) mounted on a support frame shelf. This pH controller operates a solenoid valve (Peter Paul No. 22R9DCV-12060) which provides on-off control of the flow of sodium hydroxide into one of the tees mounted in the influent line before the mixing chamber and the main pump. A 7.6-l (2-gal) plastic jug is connected to the solenoid valve by a 0.32-cm (1/8 in.) plastic tube. The jug is mounted on the top support frame shelf, which allows the sodium hydroxide to flow by gravity into the influent line.

The pH of the flotation column effluent is monitored by a glass electrode mounted in a tee in the column effluent line. This electrode is connected to a monitoring pH meter (Sargent-Welch Model LSX) mounted on a support frame shelf.

ELECTRICAL CONTROL PANEL

The electrical control panel is shown in Figure 3. All the power cords to the electrical units of the pilot plant are connected to this panel. The panel has a toggle switch, indicator light, and fuse for each electrical unit. Other electrical controls, such as those for the pH meters and the chemical feed pump control, are located on the individual units. The entire system (and the support frame) is grounded, since otherwise the electrical hazard could be quite serious.

SUPPORT STRUCTURE

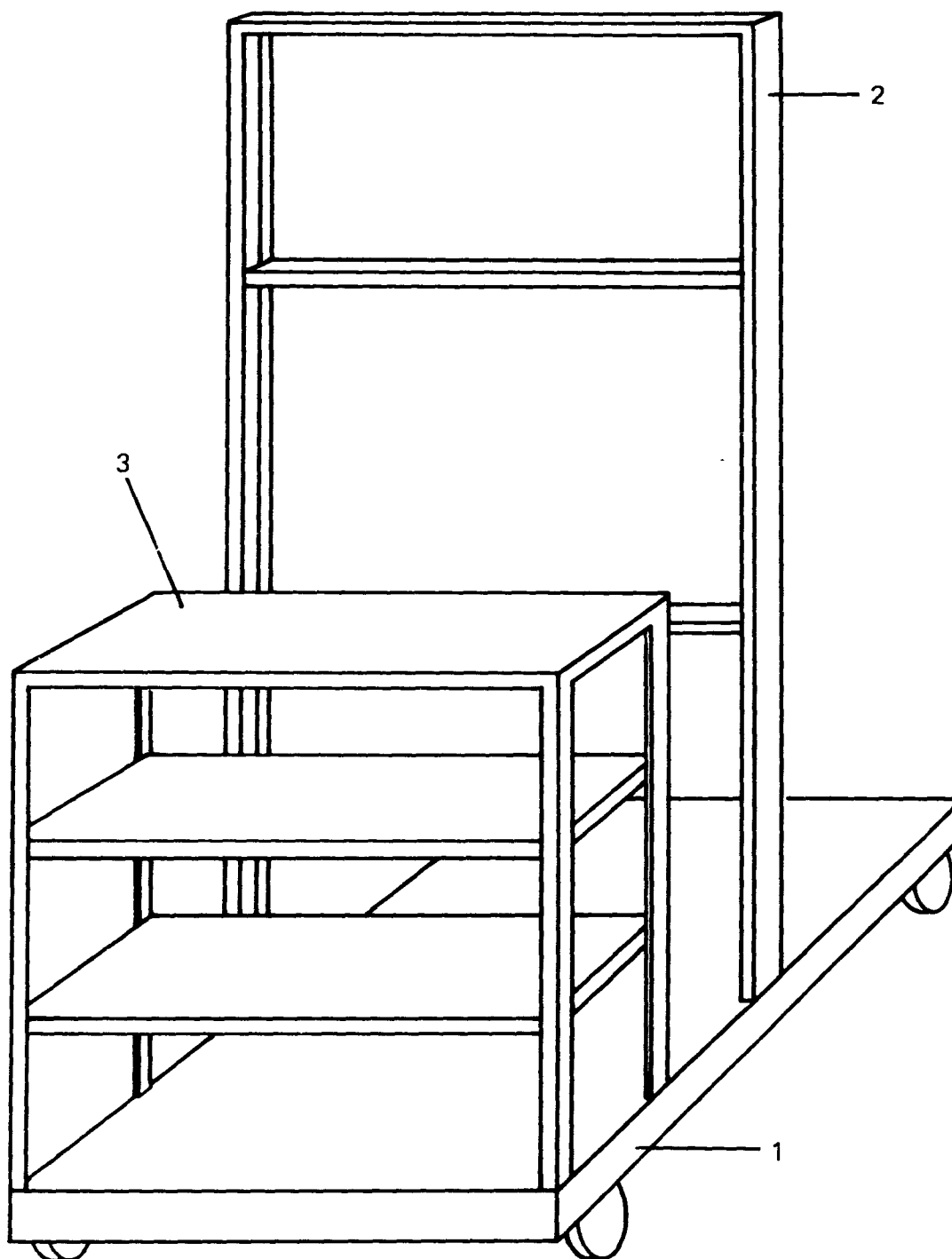
The pilot plant support structure is shown in Figure 11. The frame consists basically of a 91-cm x 152-cm (3-ft x 5-ft) vertical rectangular steel frame mounted on a 91 x 152-cm (3 x 5-ft) steel base frame covered with 3/4-in. plywood. There are also two 91 x 46-cm (3 x 1 1/2-ft) shelves mounted on a 91-cm (3-ft) frame; this frame is also mounted on the base. The support structure is mounted on casters.

WASTE PRETREATMENT AND STORAGE TANK

A 1136-l (300-gal) cylindrical polyethylene tank fitted with a 1.9-cm (3/4-in.) gate valve at the base was used for mixing of simulated wastes and pretreatment and storage of industrial wastewaters. The valve at the base of the tank is connected to the inlet hose of the pilot plant.

WORK ON SIMULATED LEAD-BEARING WASTES PROCEDURES

Chemical feed solution and the simulated waste were prepared for each run. The simulated waste was made by dissolving the required weight of reagent grade lead nitrate in about 4l of tap water acidified with roughly 5 ml of nitric acid. This solution was then mixed in the required volume of tap water in the waste storage tank. In all runs the waste solution was prepared to contain approximately 20 mg/l of lead. When sodium chloride was used to increase the ionic strength, the appropriate amount of commercial rock salt was



COMPONENTS

1. 3-ft x 5-ft Base
2. 3-ft x 5-ft Support Frame
3. Equipment Shelves

FIGURE 11 - SUPPORT STRUCTURE

weighed out and added to the storage tank with sufficient water to dissolve it. After it was dissolved with stirring, water and lead nitrate solution were added to make up the desired final volume.

The chemical feed solutions of technical grade ferric chloride and laboratory grade ferric chloride and laboratory grade NLS were made in 7-l quantities in the containers, from which they were fed to the influent line. The concentrations of the solutions were dependent on the waste flow rate, chemical feed rate, and the concentrations of reagents desired in the waste. A sample calculation for determining these solution concentrations is shown below.

Given: Waste Flow - 2 gal/min (7.57 l/min)
Chemical Feed Pump Setting - 6 (54 ml/min)

Desire: NLS Concentration - 50 mg/l
FeCl₃ Concentration - 100 mg/l
7 liters of each of the above solutions.

NLS Calculation:

$$\frac{\text{Waste Flow (l/min)} \times \text{Desired Conc. (mg/l)} \times \text{Volume Solution Desired (l)} \times 1000 \text{ ml/l}}{\text{Chemical Feed Pump Rate (ml/min)} \times 1000 \text{ mg/g}} = \text{Solute Weight (g)}$$

$$\frac{7.57 \text{ l/min} \times 50 \text{ mg/l} \times 7 \text{ l} \times 1000 \text{ ml/l}}{54 \text{ ml/min} \times 1000 \text{ mg/g}} = 49.06 \text{ g}$$

FeCl₃ Calculation:

$$\frac{\text{Waste Flow (l/min)} \times \text{Desired Conc. (mg/l)} \times \text{Volume Solution Desired (l)} \times 1000 \text{ ml/l}}{\text{Chemical Feed Pump Rate (ml/min)} \times 1000 \text{ mg/g} \times 0.3443} = \text{Solute weight (g)}$$

$$\frac{7.57 \text{ l/min} \times 100 \text{ mg/l} \times 7 \text{ l} \times 1000 \text{ ml/l}}{54 \text{ ml/min} \times 1000 \text{ mg/g} \times 0.3443} = 285.01 \text{ g}$$

From results of these calculations, it is seen that, if the waste flow rate is 2 gal/min and the chemical feed pump feed rate is 54 ml/min, it would require 49.06 g of NLS dissolved in 7 liters of water to give a concentration of NLS in the waste of 50 mg/l. It would also require 285.01 g of FeCl₃ dissolved in 7 liters of water to give a concentration of 100 mg/l Fe(III) in the waste.

Seven liters of 0.25-molar (M) sodium hydroxide solution for pH control were also prepared for each run. From preliminary experimentation this was found to be the optimum concentration for pH control in the apparatus. Technical grade flake sodium hydroxide was used.

After all the solutions were prepared, the pH meters were calibrated against two or three standard buffer solutions. The pH electrodes required occasional cleaning with HCl followed by soaking in KCl solution to remove ferric hydroxide deposits which gradually decreased the rate of response of the pH meters as it built up.

The first step in actually making a run with the column was to turn on the chemical feed pump, check its flow rates, and make any adjustment necessary to obtain the desired reagent solution flow rates. After this check, the chemical feed pump, air supply, main pump, and sodium hydroxide solenoid valve were turned on, and the pH meters were turned from standby to pH. The waste flow control valve was then adjusted to maintain the correct flow and the air flow rate was set to the desired level. After the main pump had run for about two minutes, the liquid level in the column was set by adjusting the level of the outlet hose. The pH controller was checked and set to maintain the desired pH range. The foam breaker was turned on when the column was filled with foam.

Throughout each run, all of the parameters were frequently checked and control settings adjusted to maintain the desired values. Influent flow rate, liquid level in the column, and column pH required frequent adjustment; pH control needed closest attention.

In a properly functioning run, the liquid in the bottom of the column would quickly become clear, and the ferric hydroxide would be carried upward in the foam immediately after leaving the dispersion head.

Samples of column effluent were taken at various times during the course of the run; samples of the influent were taken at the beginning and end of each run. All samples were stored in polyethylene bottles and were acidified with nitric acid before analysis. Lead analyses were carried out on a Perkin-Elmer Model 305 B atomic absorption spectrophotometer at 217 nm. Stock solutions and standards were prepared from reagent grade lead nitrate and nitric acid (5 ml concentrated acid per liter of solution) in deionized water.

Out objectives in this phase of the work were to continue previous continuous flow system studies of lead removal by adsorbing colloid flotation with ferric hydroxide and NLS and to determine the feasibility of developing this treatment method on a larger scale than that of Hanson's 10.2-cm ID x 186-cm continuous flow column described in Section 5. Her work involved adjusting the pH and adding the process chemicals to a container of lead-bearing waste; this was then pumped to the column. We felt that automatic pH control and a continuous chemical feed system should be developed and demonstrated to show the feasibility of practical large-scale systems.

Hanson suggested a set of optimum operating parameters determined from her work on the smaller continuous flow column; these are shown in Section 5 and we used them as a starting point with the 30-cm column. Some preliminary runs were made with lead-free influent, but most runs were made with simulated waste containing approximately 20 mg/l of lead added as lead nitrate.

SECTION 7

PILOT PLANT RESULTS (30-cm DIAMETER COLUMN)

SYNTHETIC LEAD-CONTAINING WASTES

In this study we wished to achieve an optimum balance between the various parameters which would yield good quality effluent under economical operating conditions. Influent flow rate, air flow rate, and pH were easily adjusted during the course of individual runs; NLS concentration, ferric iron concentration, and ionic strength were also varied during the course of individual runs, but these parameters are not as flexible as the first three. The parameter values used in each run and the results from each run are listed in Appendix B. We next discuss the individual parameters and the results of varying them.

The pH was monitored and controlled at the mixing chamber, which was located on the influent line just downstream of the point at which sodium hydroxide was injected for pH control. pH was also monitored in the column effluent. In our apparatus, 0.25 molar was the optimum concentration of the sodium hydroxide solution used for pH control. If a more concentrated solution were used, the pH control system over-compensated and the pH oscillated excessively. At much lower concentrations, the sodium hydroxide solution had to be replenished too frequently. A time lag between the two pH displays was observed. This lag was due to the time required for liquid to flow through the apparatus. There was also a roughly constant difference of about one pH unit between the two displays, due to the introduction of NLS downstream from the monitor-controller electrode. The alkaline NLS caused the pH of the column effluent to be higher than that of the influent in the mixing chamber. We adjusted the pH monitor-controller to a lower pH setting to yield the desired pH in the effluent.

The response time of the monitor-controller was observed to increase after several runs had been made, resulting in excessive oscillation of the pH. This resulted from the gradual formation of a deposit of ferric hydroxide on the glass electrode. We reconditioned the electrodes by cleaning them in hydrochloric acid (1 part concentrated acid to 3 parts deionized water) and then soaking them in concentrated KCl solution overnight. With a freshly prepared electrode, the pH control system could maintain the pH within a range of 0.4 pH units for several hours.

The operating pH was varied over a wide range in the pilot plant runs. In order to obtain the best separation and good foaming conditions, the pH should be in the range 6.0 to 7.0. (This range is somewhat higher than that recommended by Hanson, 5.5-6.5.) The dependence of effluent lead

concentration on pH is shown in Table 6. At pH's much above 7.2, the flotation of the ferric hydroxide floc is poor.

TABLE 6. EFFECTS OF pH ON LEAD REMOVAL

pH	Residual Lead (mg/l)
5.6	7.0
6.4	1.5
6.6	0.9
6.7	0.5
6.9	0.6
7.0	0.8
7.2	0.9

The maximum feasible hydraulic loading rate was determined by the geometries of the column and the influent dispersion head, and by the characteristics of the foam itself. The linear velocity of flow from the dispersion head could not be too great or it would break the foam and cause overturning. The influent also had to be spread evenly across the column without being directed against the column sides. With our best influent dispersion head, an influent flow rate of 7.57 l/min (2.0 gal/min) was the maximum which consistently did not produce overturning and/or channelling. This corresponds to a hydraulic loading rate of 163 m³/day-m² (2.77 gal/ft² min). Several different configurations and sizes of holes in the radial arms of the dispersion head were used over a range of flow rates. With all of these, the maximum hydraulic loading rates which could be tolerated fell in the range 120-180 ml/min-m² min (2-3 gal/ft² min).

The quality of effluent was very strongly affected by hydraulic loading rate. Lead concentrations increased dramatically at hydraulic loading rates at which channeling and overturning occurred.

We found that inclusion of a baffle system in the lower (stripping) section of the column improved column performance at high hydraulic loadings. In preliminary runs (without lead) it was visually apparent that the baffle system was effective to a limited extent in controlling foam overturn and in reducing the size of the eddies when overturn did occur. Near the baffles the foam appeared to move in a plug flow pattern even when overturning was taking place in the regions between the baffles. Plug flow could probably be further stabilized by the inclusion of more baffles. We also observed that the baffles and their support rods tended to cause channelling down the wall of the column if they were allowed to touch the wall.

The depth of liquid in the bottom of the column was varied in the preliminary runs. When the surface of the liquid was more than 2-3 cm (1 in) above the air diffuser, foam production was reduced (bubble size was increased), and the larger bubbles and turbulent motion of the liquid surface had a detrimental effect on the plug flow pattern of the foam upward through the column.

We destroyed the first air diffuser by permitting the air pressure to become excessive as the diffuser fouled with oil from dirty compressed air. A filter and pressure regulator were installed, and the air pressure was kept below 10 psi (0.7 kg/cm²). In the preliminary runs, an air flow rate of 1.1 m³/hr (40 SCFH) was used; this was satisfactory in some runs, but was not sufficient to push the foam up more than 3/4 of the length of the column in others. Usually, when the foam collapsed at this point ferric hydroxide deposited thickly on the wall, building up until eventually heavy clots of ferric hydroxide-rich dry foam broke loose from the wall, fell down through the rising, less dense foam, and contaminated the effluent pool at the bottom of the column.

We found that an air flow rate of 1.7-2.0 m³/h (60-70 SCFH), corresponding to 0.4-0.5 m³/min-m², markedly improved column performance. We note that Hanson's recommended range of 0.2-0.3 m³/min-m² was significantly lower, and believe that the air flow required by the present column could be reduced if the upper section of the column were shortened. We originally thought that this length was necessary for adequate drainage of the foam, but observation of the operating column leads us to believe that there was very little benefit from draining in the upper one-fourth, roughly, of the column.

Increasing ionic strength (dissolved salts concentration, essentially) has been shown experimentally (56,57) to markedly decrease lead removal efficiency, as is predicted theoretically (39,40). Therefore, a number of runs were made with all variables except ionic strength held constant. (Some unavoidable minor variations in pH also occurred.) Some of the results of these runs, shown in Table 7, show the detrimental effects of elevated ionic strength. Commercial rock salt was used to vary the ionic strength.

TABLE 7. EFFECTS OF INCREASING IONIC STRENGTH ON LEAD REMOVAL

NaCl Added		pH	Residual Level (mg/l)
(moles/l)	(mg/l)		
0.01	690	6.6	0.86
0.01	690	6.4	1.57
0.05	3450	6.5	2.29
0.05	3450	6.3	1.86
0.05	3450	6.4	2.43
0.07	4830	6.5	2.57
0.07	4830	6.7	3.14
0.07	4830	6.7	3.29

Note: All runs made with 20 mg/l Pb(II), 100 mg/l Fe(III), and 50 mg/l NLS. Air flow rate was 40 SCFH and liquid flow was 2.0-2.5 gal/min.

We could not consistently produce stable foams at an influent air flow rate of 7.6 l/min (2 gal/min) if concentrations of NLS less than 40 mg/l were used. Hanson (Section 5) had recommended an NLS concentration of 35-40 mg/l, and the results of this work are consistent with that figure. Some dissolved NLS was carried out in the effluent, as indicated by the formation of a light, relatively non-persistent foam on shaking an effluent sample.

The problem, mentioned earlier, of foam collapsing halfway up the drainage section of the column was thought to possibly be due to decreased temperature of the influent and column during the winter months. Use of simulated wastewater at a temperature of 27°C (80°F) yielded marginal benefits, if any.

The optimum Fe(III) (ferric iron) concentration was found to be in the range of 100-150 mg/l. At Fe(II) concentrations less than 100 mg/l, lead removal was markedly less complete, and, at concentrations greater than 150 mg/l, at times not all the ferric hydroxide (containing lead) was removed. These results are in agreement with Hanson's recommended Fe(III) concentration of 150 mg/l.

The spinning disc foam breaker, built on the principles of one described by E. Rubin (73,74), easily handled the maximum flow of foam that the column would deliver. The disc must be carefully balanced to avoid excessive vibration and wear on the bearings. After the foam was broken, the collapsed foamate drained down the inside of the disc housing and dripped into the clarifier unit. The ferric hydroxide, lead, and much of the NLS formed a scum and floated on top of the liquid in the clarifier. The clear liquid drained from the clarifier contained somewhat less than half of the NLS in the influent; the bulk of the rest was in the floating ferric hydroxide-lead sludge, from which it could be displaced by sodium carbonate. This complicates surfactant recycling, but does not make it impossible. The adsorption of surfactant on flocs, and its displacement by salts, is discussed in much more detail in Section 9 and Appendix D.

We were disappointed somewhat to note that the levels of lead removal attained with this pilot plant were not as favorable as those obtained in lab scale batch equipment, a lab scale continuous flow apparatus, and the 10-cm continuous flow pilot plant described in Section 5. Our earlier work had fairly routinely achieved residual lead levels of 0.1 mg/l or less if the ionic strength of the solution was not too great; in this study we were not able to reduce lead levels below 0.5 mg/l. It was some time before we realized the cause of this discrepancy. In all of the laboratory scale work and in the 10-cm pilot plant the simulated waste was mixed with ferric chloride and the pH adjusted to the desired level at least 5 to 10 min before entering the column itself. In the present (30-cm) apparatus, the time interval between the formation of the ferric hydroxide floc and the entrance of the influent into the column was of the order of only 1 min. Preliminary lab scale studies on the adsorption and/or coprecipitation of lead with ferric hydroxide indicate that 1 min is not long enough to permit adsorption to reach equilibrium. We are currently modifying the apparatus to increase the time interval during which flocculation and adsorption can take place. We believe that this should improve the performance of the apparatus substantially.

In summary, the study of simulated lead-bearing wastes in the 30-cm pilot plant leads us to the following conclusions:

1. Channeling and foam overturn are the determining factors of effluent quality at high hydraulic loadings. They can be controlled somewhat by a dispersion head which spreads the feed

uniformly at low linear velocity over the cross-sectional area of the column without excessively reducing the cross-sectional area of the column at that point. Baffles and dispersion head must be level, and the column must be precisely vertical.

2. Increasing ionic strength above about 0.05 molar (about 3000 mg/l of NaCl) decreases lead removal.
3. NLS concentrations in excess of 40 mg/l are not necessary; concentrations much below this level often did not produce sufficiently stable foams.
4. The optimum pH range is about 6.0-7.0; substantial variations outside of this range result in severe deterioration of the separation.
5. The most efficient Fe(III) concentration is from 100 to 150 mg/l.
6. Hydraulic loading rates up to 150-180 m³/day-m² are feasible, and air flow rates of 0.4-0.5 m³/min-m² seem to be optimal.
7. Design of the apparatus could be improved by increasing the size of the mixing chamber to permit a detention time of at least 5 min, by decreasing the length of the foam drainage section of the column to about 50 cm, and probably by the inclusion of more baffles in the stripping section.

The optimum operating parameters for this apparatus are summarized in Table 8.

TABLE 8. OPTIMUM OPERATING PARAMETERS

pH	6.0-7.0 ^a
Fe(III) concentration	100-150 mg/l
NLS concentration	35-40 mg/l
Hydraulic Loading Rate	150-180 m ³ /day-m ² (2.4-3.0 gal/min-ft ²)
Air Flow	0.4-0.5 m ³ /min-m ² (1.3-1.6 ft ³ /min-ft ²)

^aFor high ionic strength wastes, a lower pH than 6.0 may be necessary.

FIELD TESTS ON A ZINC AND COPPER-CONTAINING WASTEWATER

Arrangements were made to carry out field tests at a plant manufacturing water heater components. The plant conducts an automated copper descaling and zinc plating operation, with cleaning and pickling steps and countercurrent rinses. A zinc chloride bath is used for the plating and a hydrochloric acid pickling step is employed. Two commercial cleaners are used; these contain salts of polyvalent anions which undergo extensive hydrolysis, and a variety

of anionic and nonionic surfactants. Their exact compositions are proprietary. Spent pickle and spent plating solution are discharged from time to time to a holding tank, from which a small flow of acidic concentrated waste is continuously blended in a mixing tank with the alkaline overflow from the counter-current rinsing operations. After mixing and adjustment of the pH to approximately 8.5, the wastewater is sent to an upflow clarifier, where zinc hydroxide floc is removed. The clarifier effluent is then discharged to the city sewer mains. The waste in the mixing tank was used for our field tests. It showed considerable fluctuation in composition, ranging in Zn(II) concentration from roughly 30 to roughly 400 mg/l. The concentration of Cu(II) was substantially lower, generally around 1 mg/l. Total solids were 1-2 mg/l.

Waste was pumped from the mixing tank to our pretreatment and storage tank, from which it was then pumped through the foam flotation pilot plant as described in Section VI. Our original plan was to treat this wastewater by the same procedure used for the simulated lead wastes - to add 100-150 mg/l of Fe(III), adjust the pH to 6.0-6.5, add 30-35 mg/l of NLS, and run the waste through the column. This proved a failure. The presence of polyvalent hydrolyzable anions from the cleaners (phosphates and silicates) in the wastewater resulted in a change in sign of the zeta potential of the floc (normally positive, in these wastes the floc zeta potential was usually negative). These ions sorb very strongly on the $\text{Fe}(\text{OH})_3$ floc and prevent attachment of the floc to the air-water interface. (The theory of this competition is discussed in Appendix D.)

An alternative approach was therefore developed in which the interfering anions were precipitated with lime (approximately 5 g of lime per liter of waste) and the supernatant waste, containing 8-20 mg/l of Zn(II) and 0.1-0.2 mg/l of Cu(II) was then foamed with 50 mg/l of Fe(III) and the polyethoxy-ethanol surfactant present as a contaminant in the wastewater. No NaOH was added. The pH's were around 11. Effluent levels of Zn(II) in the range 0.7-11 mg/l were achieved; Cu(II) was removed to below our limit of detectability (<0.05 mg/l). Insufficient surfactant remained in the effluent to maintain a stable foam on shaking. The data are presented in Appendix B.

We found that the upper (foam draining) section of the column was somewhat too long for the concentrations of surfactant which occurred in this wastewater; the accumulation of heavy, sludge-bearing material in the long upper section of the column was occasionally too great to be supported by the surfactant-lean foam, resulting in lumps of this heavier material occasionally falling through the foam and contaminating the effluent. The collapsed foamate readily separates into a floating sludge and a clarified surfactant-rich bottom layer, which could advantageously be recycled into the influent, so there is no reason to strive for an extremely well-drained foam. A foam drainage section of the column of 50-60 cm length should be ample, and should prevent the occasional accumulation of sludge which occurred in the top 30-40 cm of the column with this waste. (The present length of this section is 120 cm).

A small amount of work was carried out with wastewater obtained from the electroplating line of an automobile bumper recycling operation. The combined wastewater contained 350-1900 mg/l total solids; had a conductivity of

365-1300 micromhos/cm; contained $\text{CrO}_4^{=}$ (10-120 mg/l), Cu(II) (from a cyanide bath, 18-230 mg/l), Ni(II) (7-110 mg/l) and cleaners. Two runs were made with hauled waste (space restrictions precluded setting up the apparatus at the plant), with rather erratic results. Pretreatment with sodium metabisulfite was necessary to convert Cr(VI) to Cr(III). Lime precipitation was necessary to remove polyvalent anions in the cleaners. Separation in both instances were erratic at pH 6.5-7.0, 150 mg Fe(III), 40 mg/l NLS. The best results obtained were Cr(III) of 0.5 mg/l, Cu(II) < 0.5 mg/l, and Ni(II) of 0.7 mg/l. These were not achieved with reliability, and the $\text{Fe}(\text{OH})_3$ frequently washed through the column and contaminated the effluent. We believe that the difficulty was caused by the rather high ionic strength of this waste after pretreatment with 300 mg/l of sodium metabisulfite and 1000 mg/l of lime. Preliminary batch tests indicated that smaller concentrations of the pretreatment chemicals were not adequate to convert Cr(VI) to Cr(III) and to precipitate interfering polyvalent anions from the cleaners. Our first report demonstrated the inability of flotation with NLS to deal with synthetic mixtures of high ionic strength, and we believe that our difficulties here reflect this fact.

SECTION 8

CONTINUOUS FLOW AXIAL MIXING STUDIES

In our first report we described a mathematical model, analyzed in more detail elsewhere (27), of foam flotation stripping column operation. One of the terms included in that model was an empirical correction term to take axial dispersion into account. The dispersion constant which appears in this term is not easily assessed on theoretical grounds. Our experimental work on continuous flow stripping columns indicated that axial dispersion is an important factor in column performance, especially at high hydraulic loadings, at which channeling and foam overturn occur. We here describe experimental work carried out on a 10-cm continuous flow stripping column to give more detailed insight into the factors affecting axial dispersion.

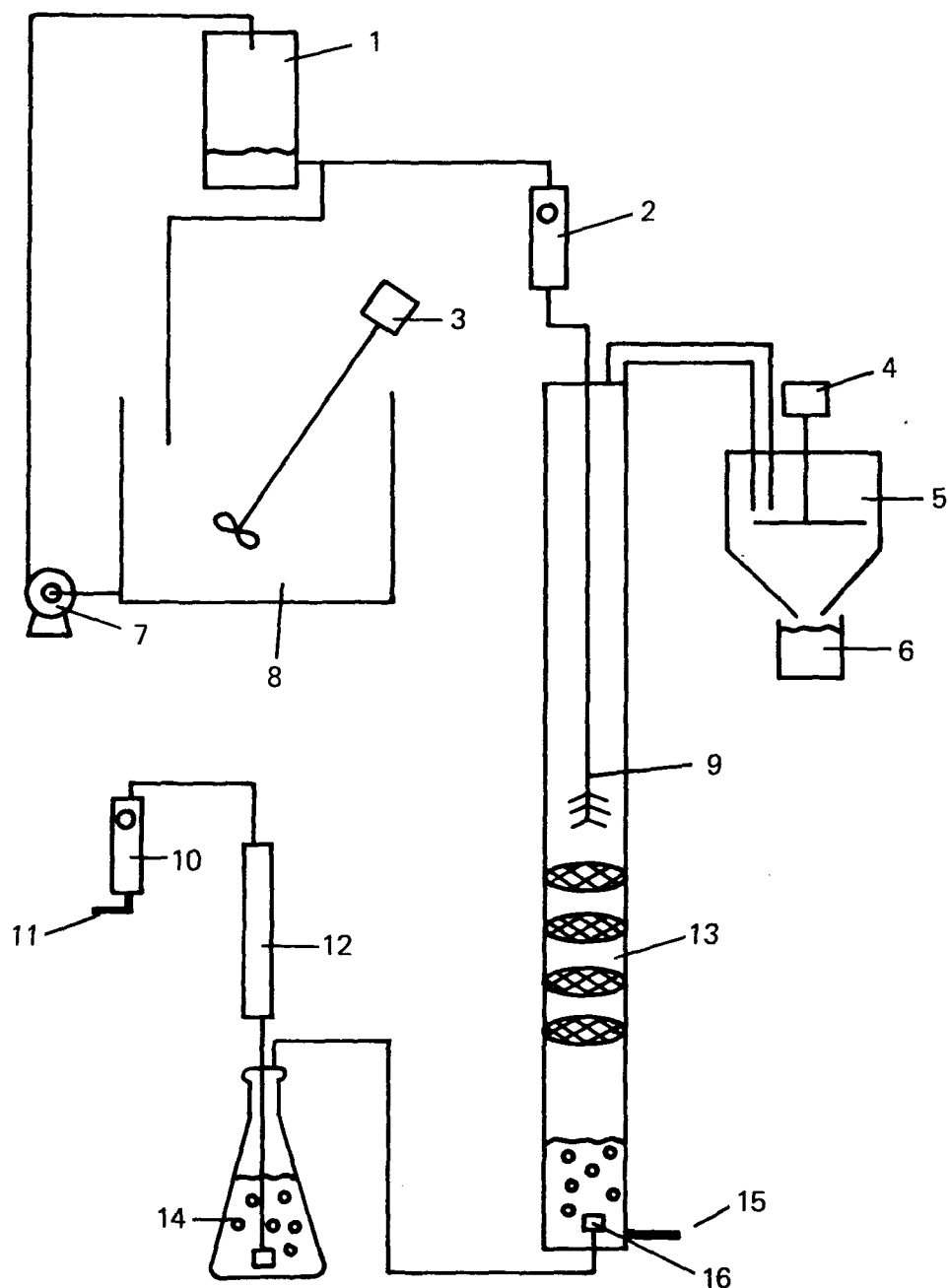
APPARATUS AND METHODS

Figure 12 diagrams the flotation system used in these studies. The column, 10.2 cm ID x 183 cm, was made of lucite. Influent was introduced at or slightly above the midpoint of the column through a 0.64-cm tube, entering through the top coverplate of the column and exiting through the dispersion head detailed in Figure 13. The most important aspect of the dispersion head design seemed to be that one must avoid spraying the influent onto the wall of the column, which results in channeling. A 1.90-cm I.D. lucite pipe mounted in the top coverplate of the column permitted discharge of the foam to the foam breaker, diagrammed in Figure 14.

Foam was generated by passing filtered, humidified air through a porous cylindrical air stone mounted on the bottom coverplate. The air flow rate was measured and controlled by a flowmeter. An exit port 1.5 cm above the bottom of the column allowed discharge of effluent through a rubber tube and screw clamp. Inside the column, three or four baffles made of 1/8-in. mesh galvanized hardware cloth were used to control foam overturn. These were held in place by metal washers made from large hose clamps.

A 190-l polyethylene cylindrical tank was used to mix and store the water to be treated. A stirring motor provided mixing adequate to keep the ferric hydroxide floc in suspension, and a small centrifugal pump supplied a constant head tank 180 cm above the dispersion head. Liquid flow rates to the column were measured and controlled with a flowmeter.

The following method was used to examine axial dispersion. The column was back-lighted by a 4-ft fluorescent lamp mounted vertically as close as possible behind the column. Stray light was blocked by aluminum foil taped



COMPONENTS

- | | |
|----------------------------|-----------------------|
| 1. Constant Head Tank | 9. Dispersion Head |
| 2. Influent Flowmeter | 10. Air Flowmeter |
| 3. Stirrer | 11. Air Inlet |
| 4. 3000 rpm Motor | 12. Glass Wool Filter |
| 5. High Speed Foam Breaker | 13. Baffles |
| 6. Foamate | 14. Humidifier |
| 7. Pump | 15. Effluent Drain |
| 8. Liquid Reservoir | 16. Air Stone |

FIGURE 12 - THE FOAM FLOTATION APPARATUS USED
IN THE AXIAL DISPERSION STUDIES

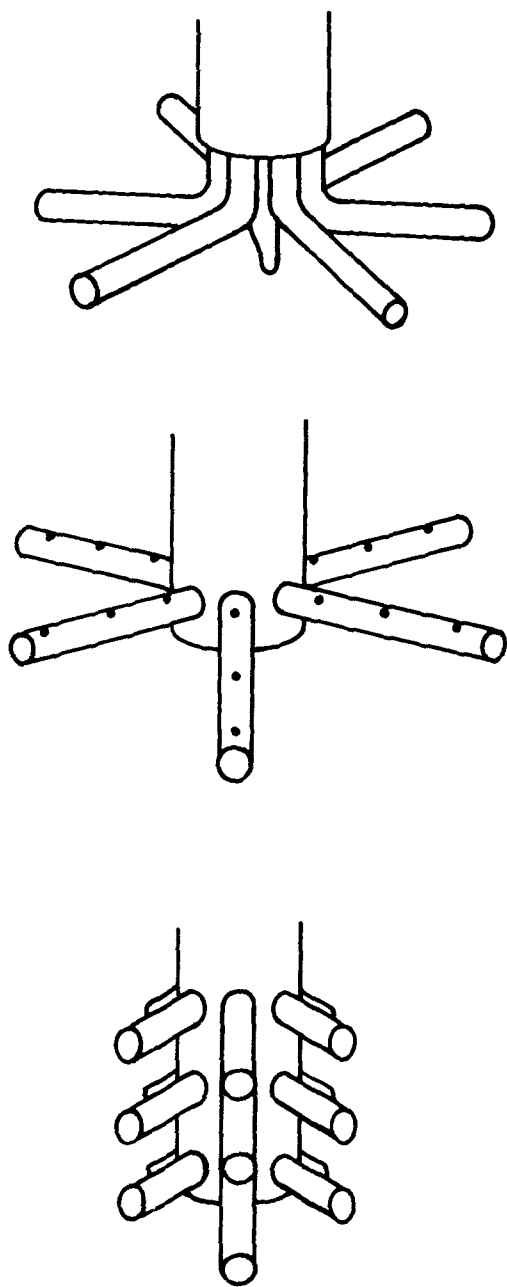
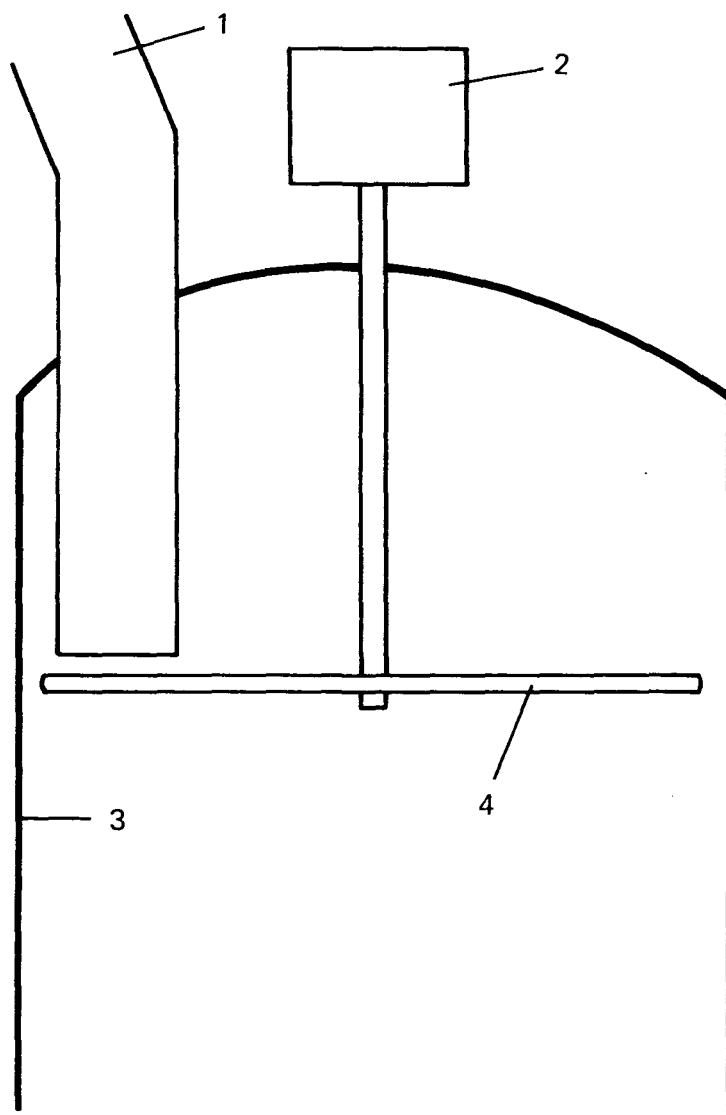


FIGURE 13 - DISPERSION HEAD DESIGNS .



COMPONENTS

1. Foam Inlet Tube
2. 3000 rpm Motor
3. Housing
4. Polyethylene Disc

FIGURE 14 - HIGH SPEED FOAM BREAKER DESIGN.

from the lamp fixture to the column. The lucite walls of the column refracted light around the column, obscuring events within; we therefore cut a slot from top to bottom on each side of the lucite tube and filled these with an opaque epoxy cement. This almost completely eliminated scattered light. Figure 15 shows the photographic setup.

Photographs of event sequences were taken on 35-mm film (Kodak TRI-X ASA 400, with a yellow filter). The developed negatives were scanned on a densitometer capable of measuring up to three absorbance units (A.U.) with a precision of ± 0.01 A.U. These absorbance values were plotted by a strip chart recorder. A "time zero" photograph was taken at the beginning of each run before the injection of ferric hydroxide was made; subsequent shots were compared to this, and the difference between the initial absorbances and the absorbances at time t plotted as functions of vertical position in the column for various values of t .

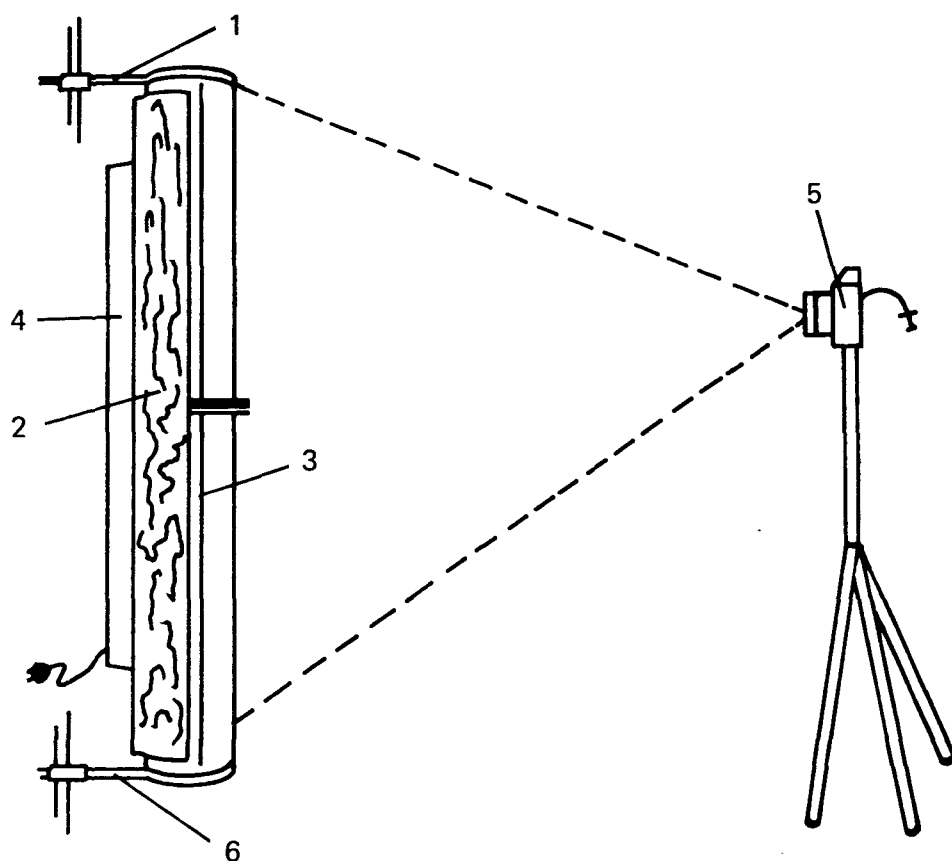
NLS was used as the surfactant in all runs, and ferric hydroxide was the floc which was removed by flotation. Ionic strength was adjusted with reagent grade sodium nitrate, and the pH was adjusted with sodium hydroxide and nitric acid, reagent grade. All chemicals were added to the water in the 190- ℓ storage tank; NLS was added after the precipitation of ferric hydroxide. The parameters for the runs reported here are given in Table 9.

Two types of runs were made: (1) "pulse" type runs, in which 2 ml of ferric hydroxide suspension containing 1000 mg/ ℓ of Fe (III) was suddenly injected into the feed line, and (2) "step change" type runs, in which ferric hydroxide was present in the feed at all times and an abrupt change in influent hydraulic loading or ionic strength was made at some point during the course of the run. Pulse type runs were more informative about axial dispersion of floc in the foam, while the step change type runs more closely approximated actual operating conditions for foam flotation columns. Before a photographic sequence was initiated for either type of run, the column was brought to a steady state with a feed containing surfactant and sodium nitrate.

EXPERIMENTAL RESULTS AND DISCUSSION

The experimental results for the runs described in Table are shown in Figures 16 through 24. A number of other pulse runs made at higher hydraulic loadings showed extremely rapid axial mixing by channelling and foam overturn. When all conditions are nearly optimal, a pulse of ferric hydroxide is removed very quickly, as seen in Figures 17 through 19. In Figures 17 through 20 the ionic strength (0.062/molar) was near its maximum feasible value, and the foam tended to be quite dry, enabling it to support a relatively high specific air flow rate of 0.84 m³/min-m². At an ionic strength of 0.031 molar, however, the foam was quite a bit wetter, especially at the higher hydraulic loading rates, and the maximum feasible specific air flow rate dropped to 0.66 m³/min-m².

Figure 16 shows the results of an NLS concentration which is too high to effect a good separation. At 200 mg/ ℓ NLS, the ferric hydroxide floc is



COMPONENTS

- | | |
|--|---------------------|
| 1. Clamp | 4. Fluorescent Lamp |
| 2. Aluminum Foil Reflector | 5. Camera |
| 3. Opaque epoxy-filled slot
in column | 6. Clamp |

FIGURE 15 - THE SETUP FOR PHOTOGRAPHY OF THE AXIAL DISPERSION EXPERIMENTS.

TABLE 9. PARAMETERS FOR FIGURES 16 - 24.

Figure Number	Fe ⁺⁺⁺ (mg/l)	pH	NaNO ₃ (mol/l)	NLS (mg/l)	Air Flow (l/m ² ·min) (cm/sec)		Water Flow (l/m ² ·min) (cm/sec)	
16	pulse*	5.5	.062	200	172	.15	140	.12
17	pulse*	5.5	.062	50	215	.19	140	.12
18	pulse*	5.5	.062	50	237	.21	108	.09
19	pulse*	5.5	.062	50	333	.29	129	.12
20	pulse*	5.5	.062	50	441	.38	127	.11
21	50	5.5	.031	50	215	.19	14→83	.01→.06
22	50	5.5	.031	50	215	.19	83→142	.06→.12
23	35	4.0	0→0.09	200→50	215	.19	73	.06
24	50	5.6	0→0.12	200→50	333	.29	140	.12

* Each pulse was a 2-ml suspension of ferric hydroxide at a concentration of 1000 mg/l.

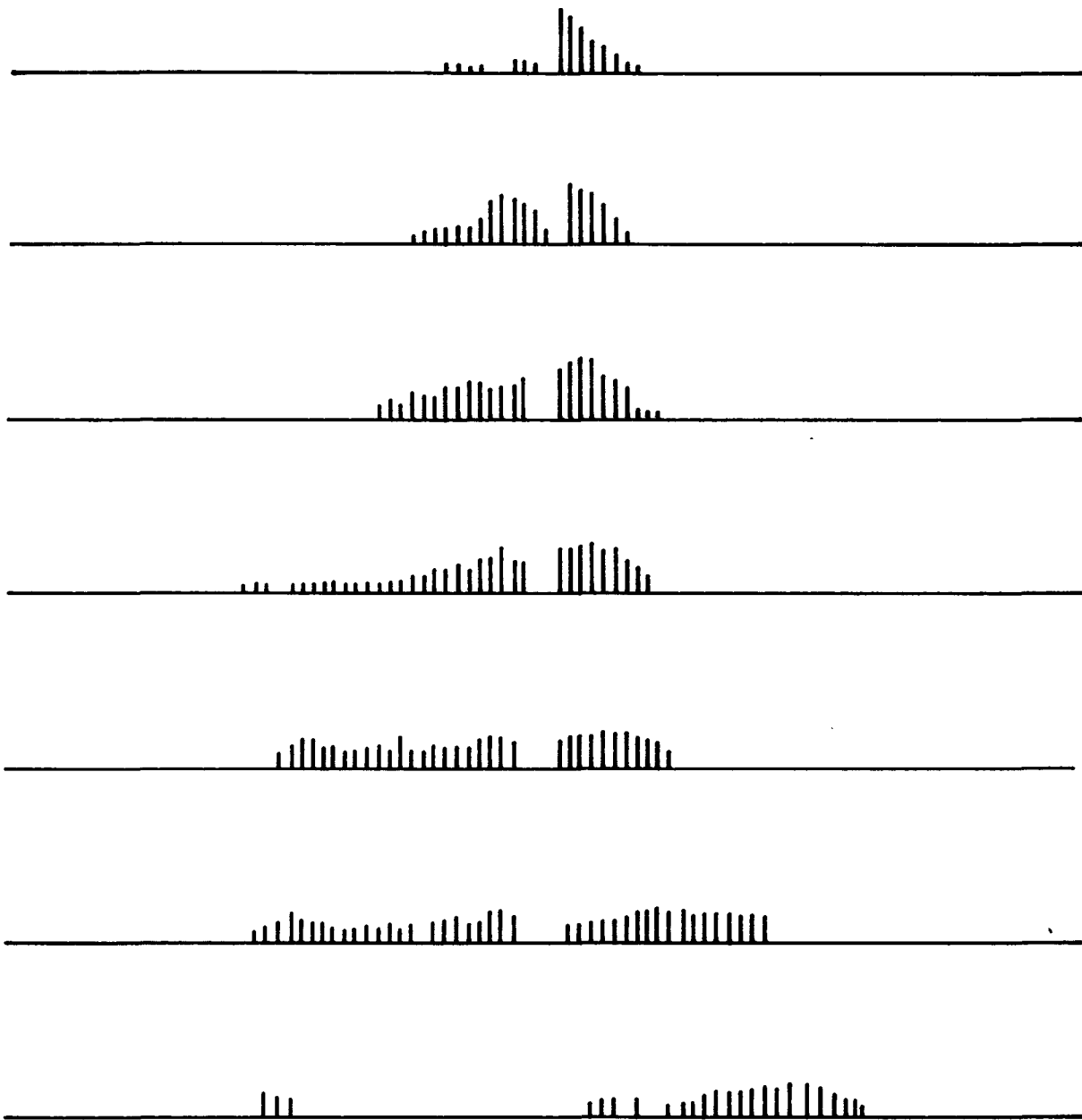


FIGURE 16 - AXIAL DISPERSION DATA. See Table 9 for run parameters.
Run I

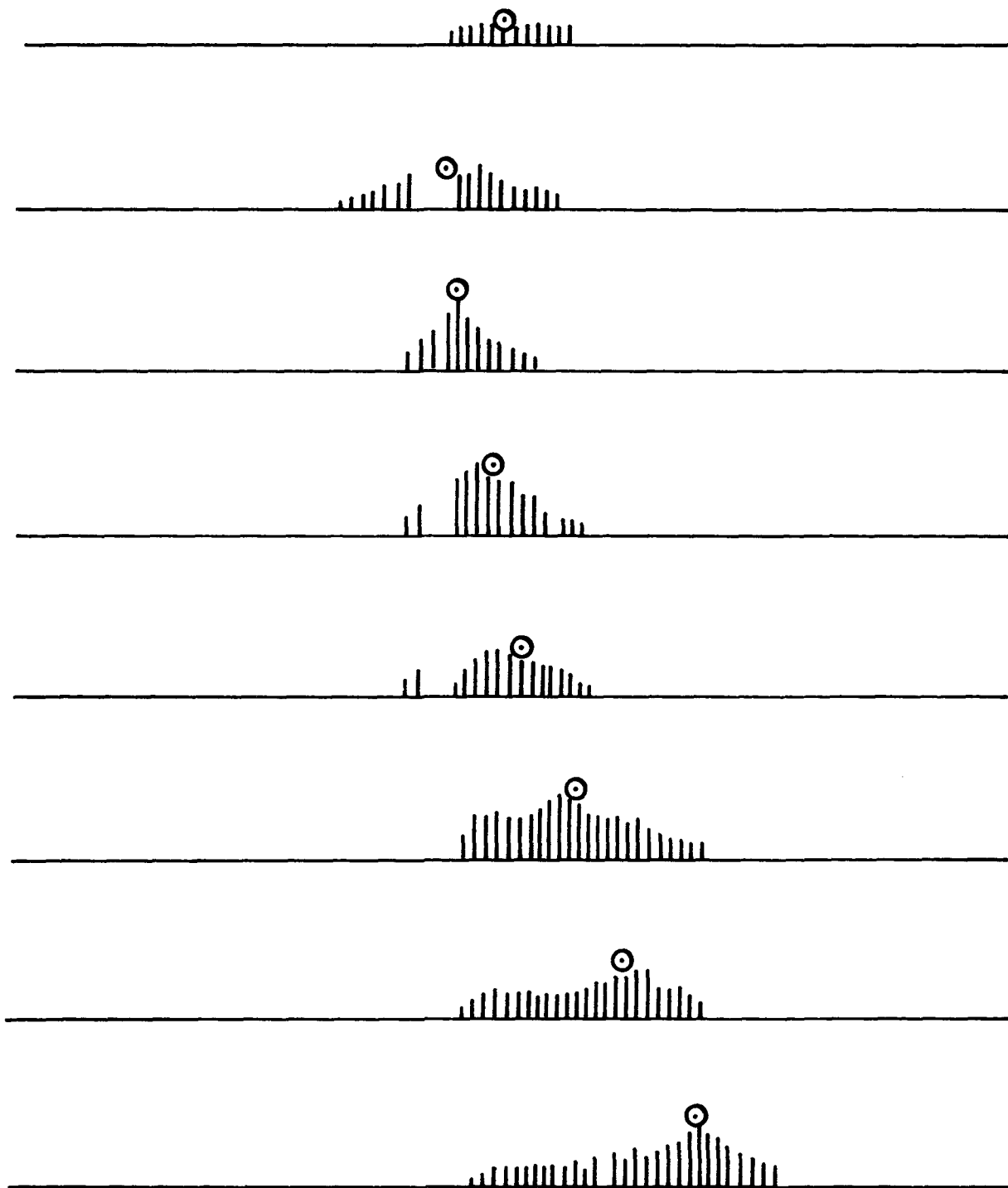


FIGURE 17 - AXIAL DISPERSION DATA. See Table 9.
Run II

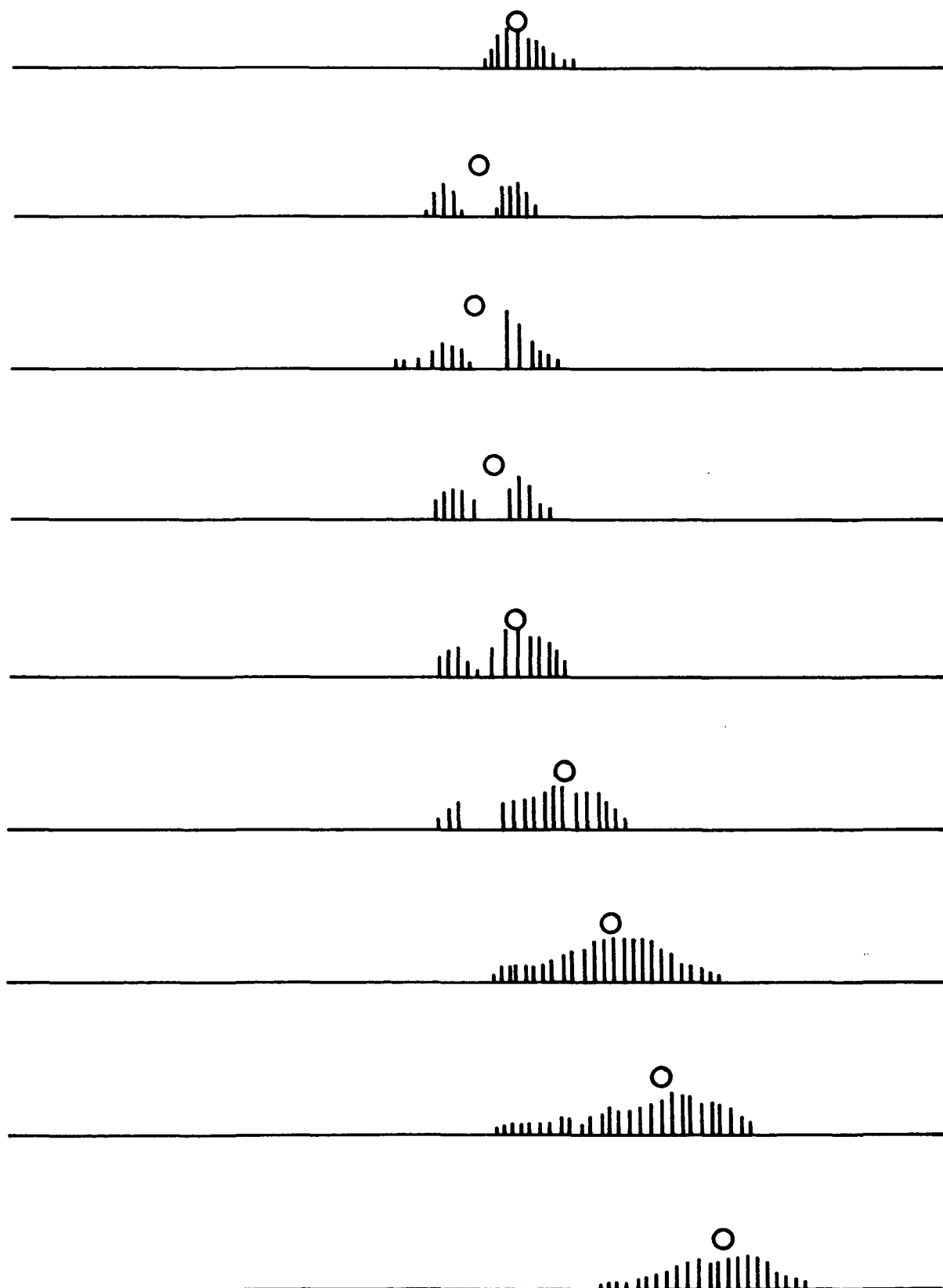


FIGURE 18 - AXIAL DISPERSION DATA. See Table 9.
Run III

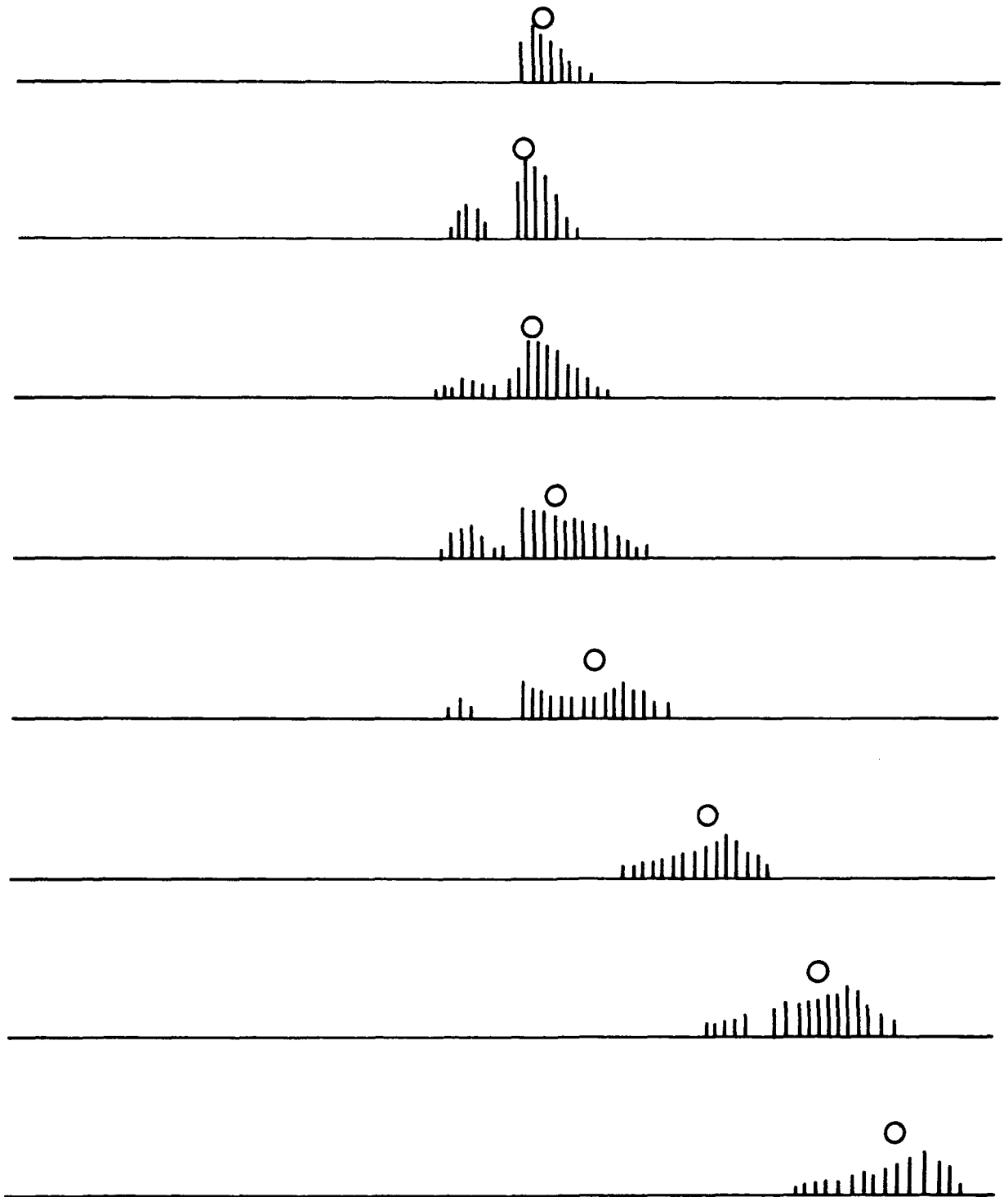


FIGURE 19 - AXIAL DISPERSION DATA. See Table 9.
Run IV

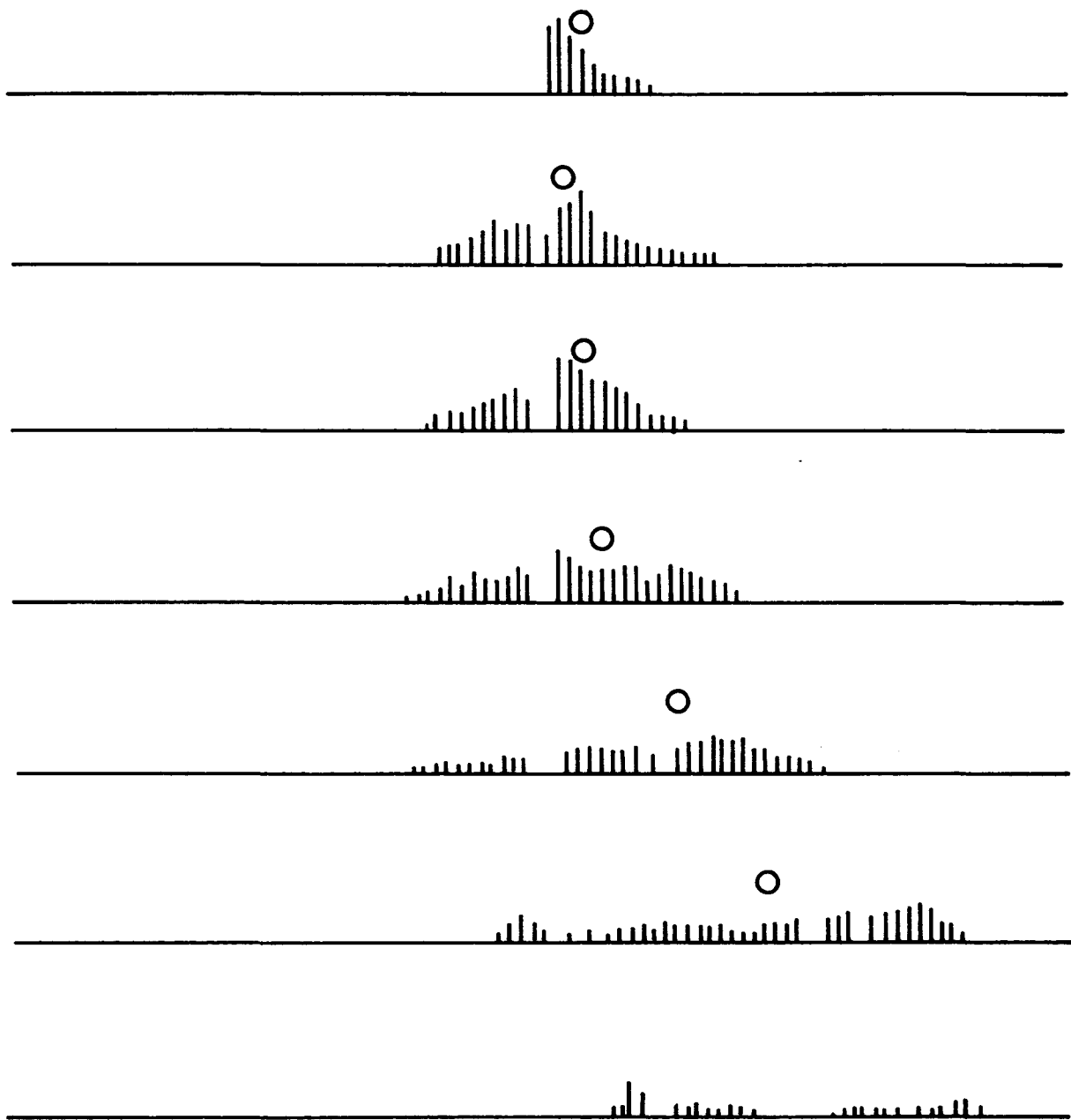


FIGURE 20 - AXIAL DISPERSION DATA. See Table 9.
Run V

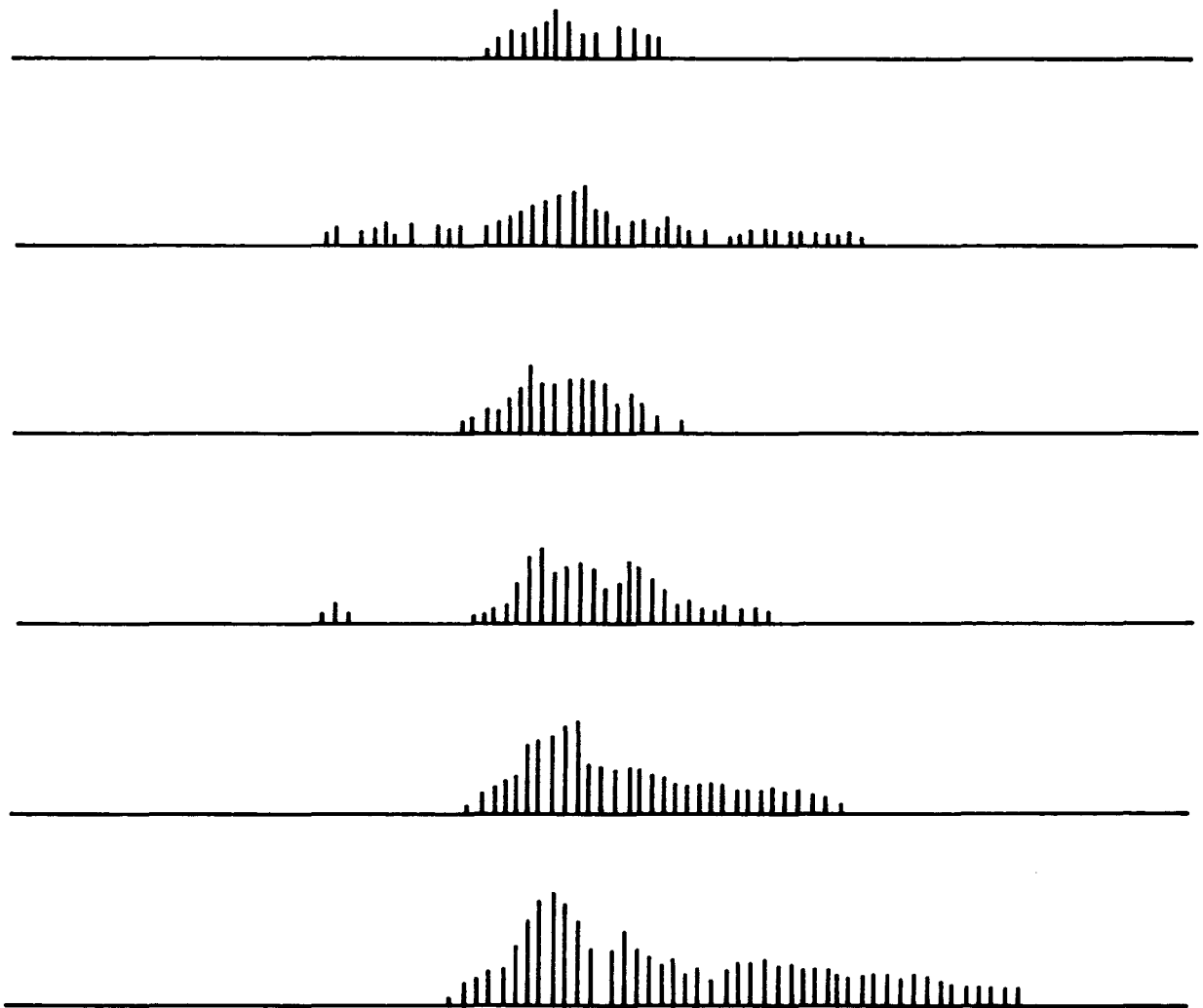


FIGURE 21 - AXIAL DISPERSION DATA. See Table 9.
Run VI

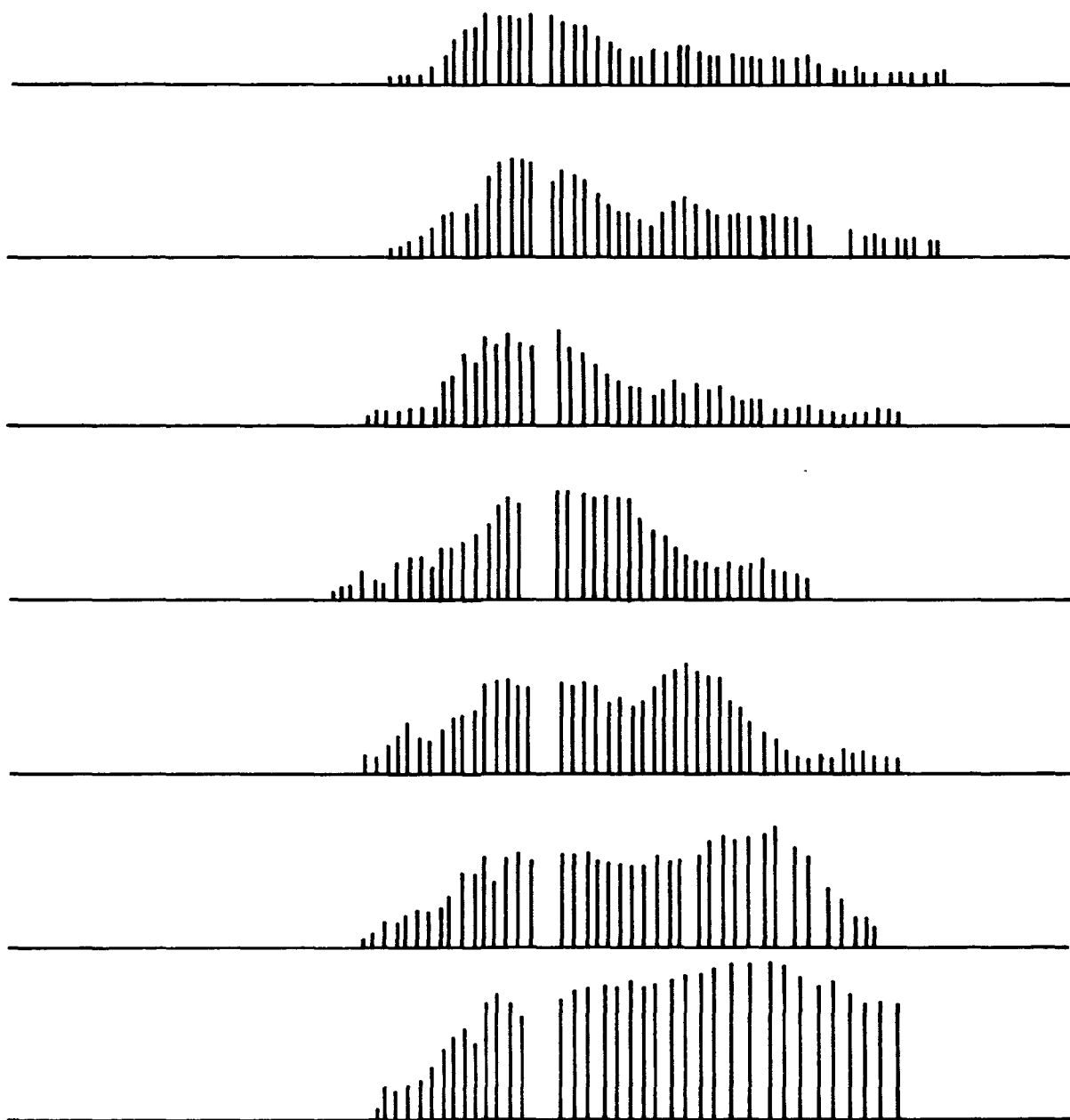


FIGURE 22 - AXIAL DISPERSION DATA. See Table 9.
Run VII

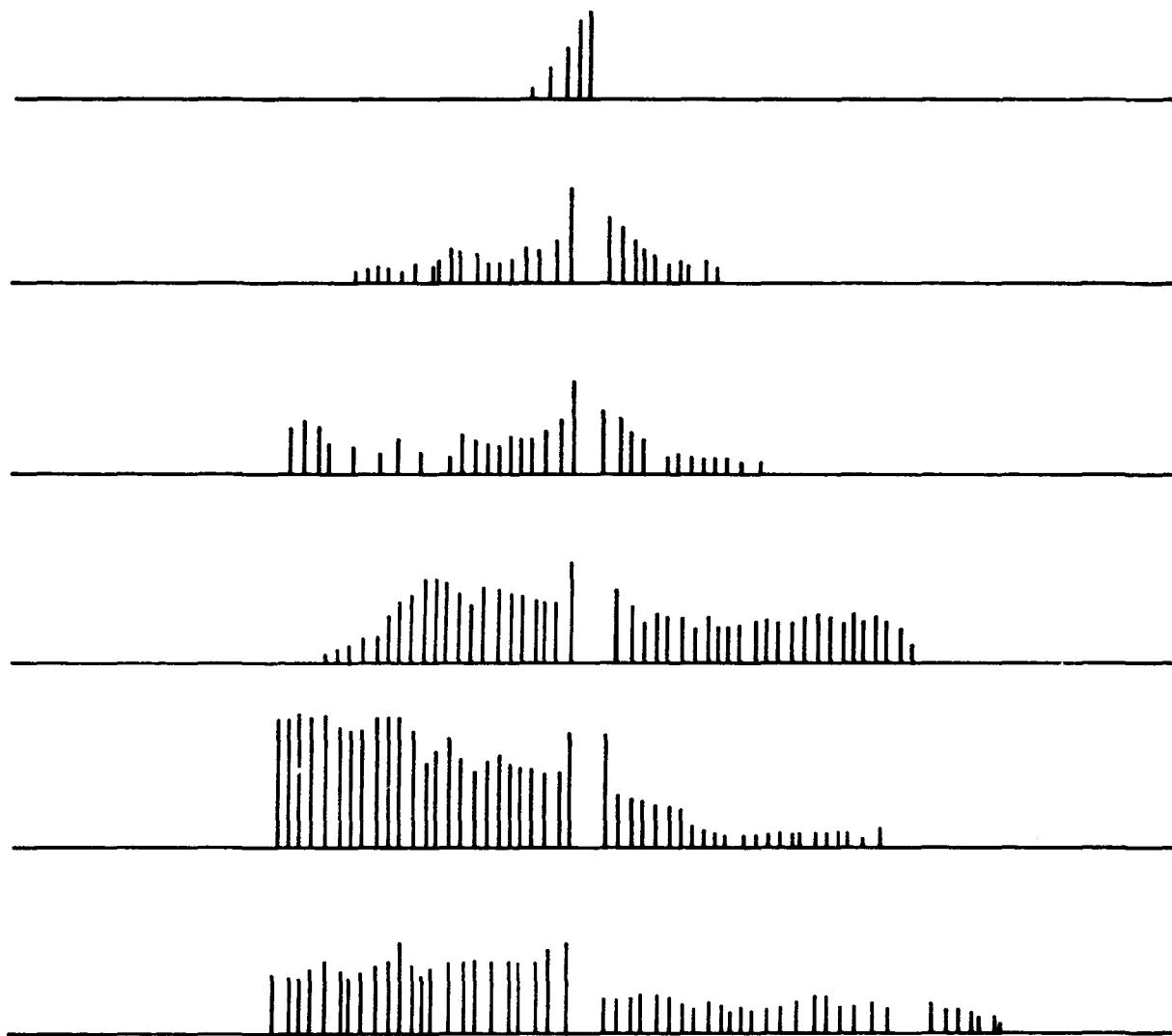


FIGURE 23 - AXIAL DISPERSION DATA. See Table 9.
Run VIII

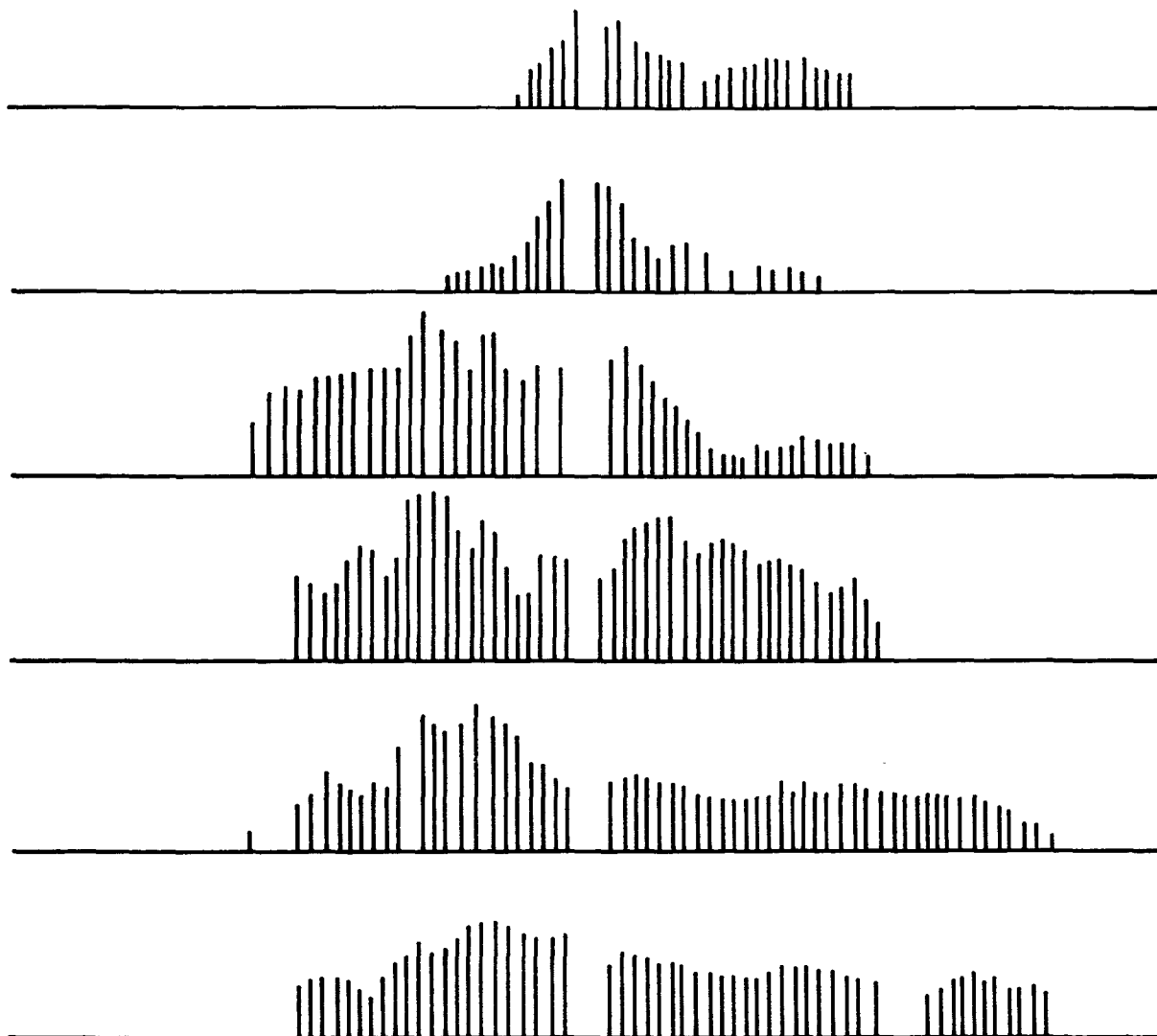


FIGURE 24 - AXIAL DISPERSION DATA. See Table 9.
Run IX

coated with a micellar double layer of surfactant ions, with the outer layer presenting ionic heads (the sulfate groups) to the surrounding water. Floc particles so coated are hydrophilic, air bubbles are unable to attach to them, and flotation does not readily occur. The pulse of ferric hydroxide therefore spreads throughout the column, and only a partial separation is achieved.

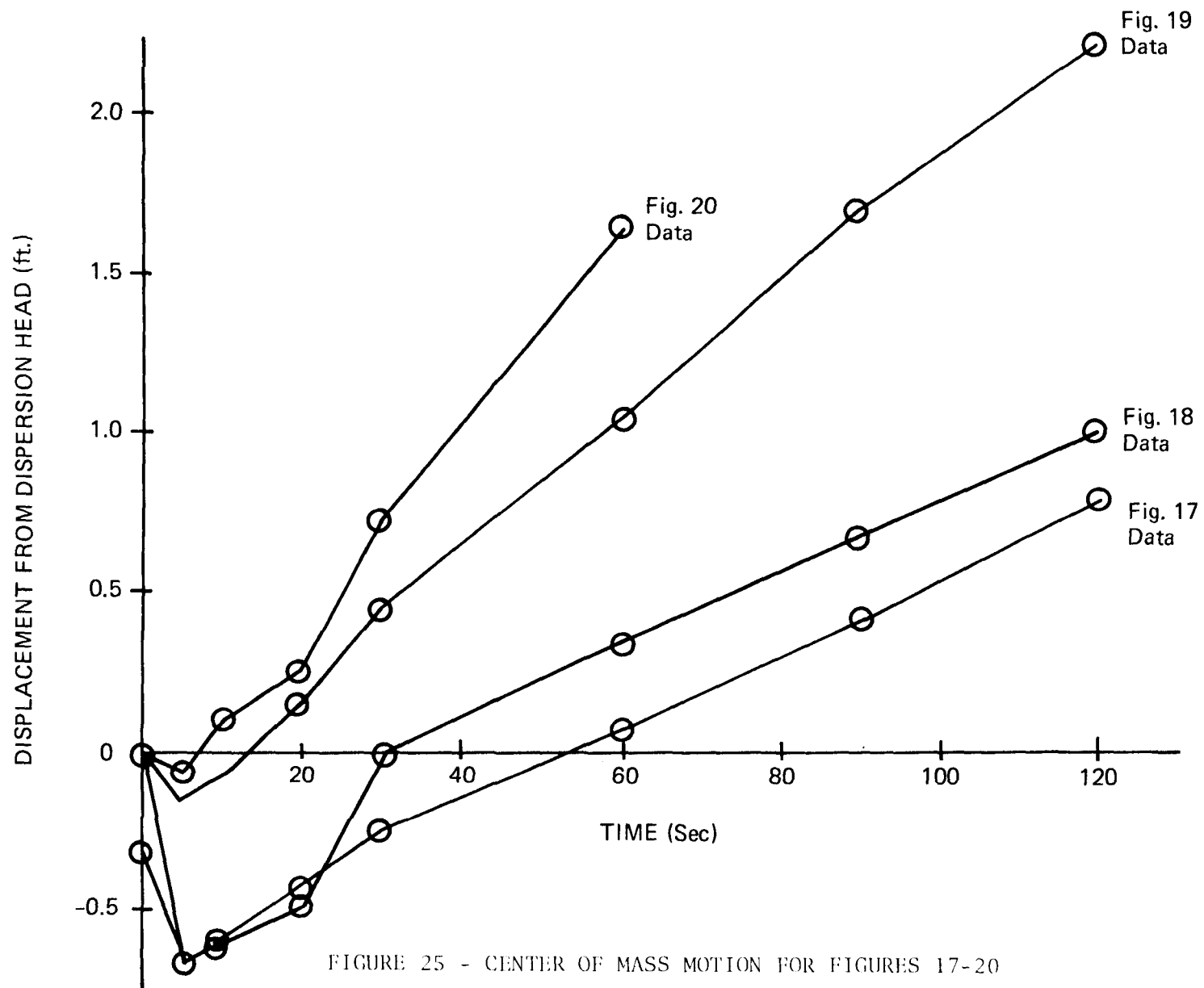
The consequences of having too large a specific air flow rate in an otherwise stable floc removing run are shown in Figure 20. There is so much turbulence in the upper half of the column (above the influent dispersion head) that the pulse is very rapidly spread out. The upper edge of the pulse is rapidly carried out the top of the column, but the pulse is smeared out so badly by turbulence that its lower portion clears the column quite slowly. Actually; the specific air flow rate is quite important to the flow pattern of the foam (ideally plug flow), but seems to be less influential on the effectiveness of separation. Several runs were made at high specific air flow rates at which turbulence occurred in the upper half of the column and nevertheless ferric hydroxide removal was quite effective. Evidently, the deleterious effect of increased axial dispersion is counterbalanced by the increased linear velocity of the rising interfaces. Increased specific air flow rates also resulted in larger bubble sizes and in an increase in the wetness of the foam, due to decreased drainage time.

Step change runs are shown in Figures 21 through 24. Here, column operation was allowed to stabilize at a particular set of parameters, and then either the influent hydraulic loading or the specific air flow rate was changed to a new value. The dynamic response of the system to such changes is seen in these figures.

Figure 21 portrays a change in the influent hydraulic loading from 8.6 to 52 m /day-m . In both cases the system restabilized in approximately 2 min, and the separation was not impaired.

The runs depicted in Figures 23 and 24 exhibit the response of the system to a sudden increase in ionic strength. As was usual for a continuous flow test run, the column was primed with 2 to 4 l of a 200 mg/l NLS-tap water solution and air was bubbled into the column for several minutes to charge it with foam. The influent solution containing ferric hydroxide and NLS (50 mg/l) was then fed to the column until it was apparent that effective separation was taking place. The ionic strength of the feed was then increased. In both cases separation of the floc remained satisfactory initially, but then rapidly deteriorated. After only minutes a new steady state was achieved with most of the floc being discharged in the effluent from the bottom of the column. Interpretation of these two runs was complicated somewhat by a tendency of the floc to adhere to the lucite wall of the column.

Figure 25 plots position of the "center of mass" of the pulse versus time for the runs exhibited in Figures 17 - 20, in which these "centers of mass" are indicated by encircled dots. The specific airflow rate and the mean floc velocity are approximately equal for the three runs which exhibited plug flow. The data presented here plus the results of other runs not shown indicate that in this apparatus the specific airflow rate has a relatively small working range compared to the influent hydraulic loading, which was variable over a much larger percentage change.



We had hoped to estimate axial dispersion constants by plotting pulse spread as a function of time. The root-mean-square width of the pulse and its width at half maximum should, according to diffusion theory, be given by

$$(\Delta x^2)^{1/2} = 4(Dt)^{1/2}$$

$$X_{1/2} = 4(\log_e 2 Dt)^{1/2}$$

where D is the axial dispersion constant. Diffusion theory also predicts that the pulses should be gaussian in shape. It is apparent from Figures 16 through 20 that the pulses deviate from gaussian form substantially; and we see from Figure 26 that pulse width does not appear to increase proportional to $t^{1/2}$. Evidently, the axial dispersion processes taking place are not adequately described by simple diffusion. We speculate that the size scale of the eddies and turbulence contributing to axial dispersion is comparable to the size of the pulse itself, which would invalidate the use of simple diffusion theory except as a very rough approximation.

We conclude from this work on axial dispersion that, under conditions where axial dispersion seriously affects column performance the mechanisms responsible for axial dispersion, which include foam overturn and channelling, are not well modelled by simple diffusion. At present, we can do little more than employ specific air flow rates and influent hydraulic loadings which do not yield excessive visible turbulence, channelling, and overturn. For this apparatus, influent hydraulic loadings must be less than 170m³/day-m², and specific air flow rates should be in the range 0.18-0.3 m³/min-m².

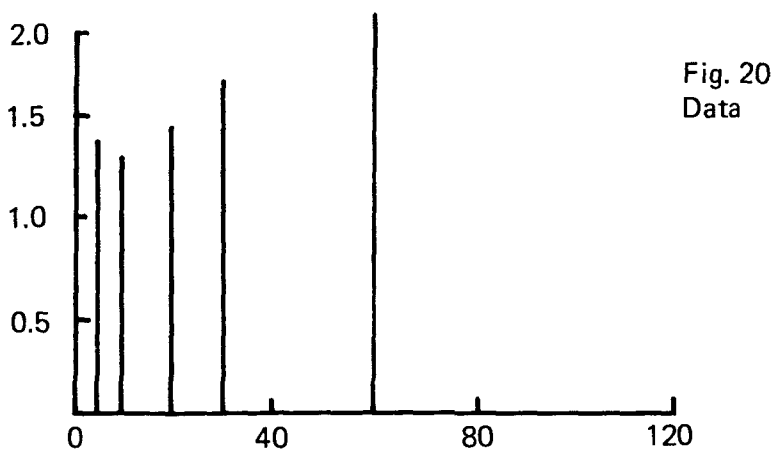
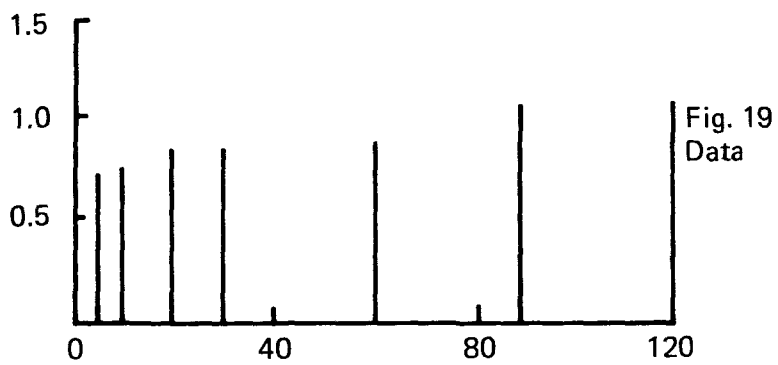
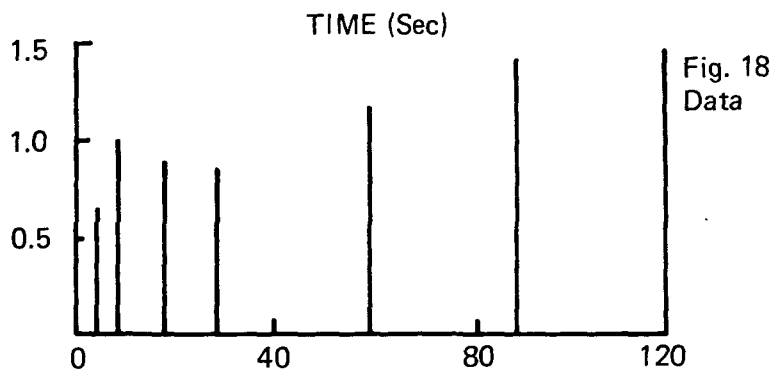
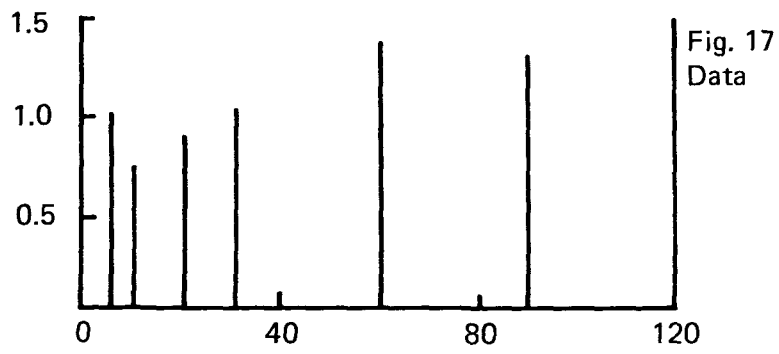


FIGURE 26 - PULSE WIDTH VERSUS TIME FOR FIGURES 17-20.

SECTION 9

BATCH TECHNIQUE LABORATORY STUDIES

BATCH FLOTATION OF ZINC(II)

We report here experimental results on batch floc foam flotation of zinc(II) with aluminum and ferric hydroxides, with sodium lauryl sulfate (NLS) as collector. Dependence of the separations on pH and ionic strength was studied in some detail, and specific ion effects on the separation of zinc(II) with $\text{Al}(\text{OH})_3$ were investigated.

The equipment used was two batch columns essentially identical to the apparatus described by us earlier (1,54,57). House air was passed through ascarite, water (for rehumidification), and glass wool, then through a "fine" glass gas dispersion tube at the bottom of the column. Laboratory grade NLS or HTA (hexadecyltrimethylammonium bromide) was used as the collector; all other chemicals were of reagent grade. Stock solutions (1000 g/l) of the metal ions and surfactant were mixed in the desired amount and diluted with deionized water to nearly 200 ml; ionic strength was adjusted by the addition of sodium nitrate solution, and the pH adjusted by addition of dilute NaOH and HNO_3 . The sample was diluted to 200 ml and added to the column. The air flow rate was measured with a soap film flowmeter. Air flow rates of approximately 65 ml/min were normally used. The pH was monitored during the course of each run, and 7 ml samples were withdrawn from the bottom of the column at 5 min intervals. Zinc analyses were carried out by atomic absorption spectroscopy.

Kim and Zeitlin's studies (59) on the removal of zinc from sea water with dodecylamine and ferric hydroxide at pH 7.6 resulted in 94% recovery from an initial concentration of 3.2 ppb. Our work was carried out at a substantially higher initial concentration of zinc; ferric or aluminum hydroxide was used as floc, NLS was used as the collector, and pH and ionic strength were varied.

Ferric hydroxide is speedily removed by foam flotation with NLS at pH 5.5, but with pH's as high as 7.5 the separation was found to be slow and incomplete. The precipitation point for $\text{Zn}(\text{OH})_2$ is roughly at pH 8 (5), so one could not expect ferric hydroxide and NLS to be an optimum system for zinc removal. Runs made with solutions initially containing 50 ppm NLS and 50 ppm Zn(II) are listed in Table 11, and bear out this surmise; inclusion of 200 ppm Fe(III) appears to interfere with the separation. The air flow rates in all of the work on zinc are 60 to 68 ml/min unless otherwise specified. The samples listed in Table 11 were taken after 5 min of treatment, at which time $\text{Fe}(\text{OH})_3$ removal was essentially complete. There appears to be a competition

TABLE 10. THE EFFECT OF $\text{Fe}(\text{OH})_3$ ON $\text{Zn}(\text{II})$ REMOVAL

Fe(III) concn (ppm)	pH	Final Zn(II) concn (ppm)
0	6.6	20
0	7.1	7.2
200	6.6	25
200	7.1	19

TABLE 11. THE EFFECT OF pH ON $\text{Zn}(\text{II})$ REMOVAL WITH Fe(III) AND NLS

pH	Final Zn(II) concn (ppm)
5.5	42
6.2	37
6.6	25
7.1	25
7.5	8

between the $\text{Zn}(\text{II})$ ions and the ferric hydroxide floc for the collector. The effect of pH on $\text{Zn}(\text{II})$ removal is shown in Table 11. Initial concentrations were 50 ppm $\text{Zn}(\text{II})$, 200 ppm Fe(III), and 50 ppm NLS. At a pH of 7.5 the iron was incompletely removed.

It was found that pulse additions of $\text{Fe}(\text{OH})_3$ floc during the course of the runs did not significantly improve the separations, nor did varying the air flow rate. Increasing the duration of the run and/or the amount of NLS added during the course of the run resulted in some improvement in separation, presumably through an ion flotation mechanism. Our results indicate that this is not an industrially feasible technique for removal of zinc from wastewaters, inasmuch as the use of long time periods and high collector concentrations resulted in final $\text{Zn}(\text{II})$ concentrations of about 3 ppm.

Huang (55) and Clarke (54) have removed $\text{Al}(\text{OH})_3$ with NLS at pH's close to 8, the precipitation point of $\text{Zn}(\text{OH})_2$. We therefore attempted the removal of $\text{Zn}(\text{II})$ with $\text{Al}(\text{OH})_3$ and NLS. The data listed in Table 13 indicate that zinc is effectively flocculated with $\text{Al}(\text{OH})_3$ at pH's at which $\text{Al}(\text{OH})_3$ is removed by foaming with anionic surfactants such as NLS. In these runs the initial $\text{Zn}(\text{II})$ concentration was 50 ppm and the run duration was 15 min. Final $\text{Zn}(\text{II})$ concentrations of less than 0.5 ppm are attained at pH's between 7.7 and 9.2 by adsorbing colloid flotation, and the residual $\text{Zn}(\text{II})$ concentrations are roughly an order of magnitude lower than those obtained by ion flotation alone with a similar quantity of surfactant.

The effect of increasing ionic strength at various pH's is shown in Table 13. All runs lasted 30 min; the initial $\text{Zn}(\text{II})$ concentration was 50 ppm, the initial $\text{Al}(\text{III})$ concentration was 100 ppm; in most of the runs (not starred) the initial NLS concentration was 100 ppm, with 50 ppm added after 15 min. The starred runs (see Table 14) had an initial NLS concentration of 150

TABLE 12. THE EFFECT OF Al(III) ON Zn(II) REMOVAL

pH	Al(III) (ppm)	NLS (ppm)	Final Zn(II) concn (ppm)
6.9	0	150	19.6
	200	150	4.7
7.4	0	150	5.5
	200	150	0.7
7.7	0	150	8.3
	100	100	0.39
	200	150	0.2
8.0	0	100	6.2
	100	100	0.20
8.3	0	100	4.8
	100	100	0.17
	200	100	0.0
8.6	0	100	6.0
	100	100	0.16
8.9	0	100	1.1
	100	100	0.41
9.2	0	100	1.6
	100	100	0.42

TABLE 13. FLOC FLOTATION OF ZINC WITH Al(OH)₃ AND NLS. EFFECT OF IONIC STRENGTH

pH	Added NaNO ₃ (mole/l)						
	0	0.5	0.10	0.15	0.20	0.30	0.40
Residual zinc (ppm)							
9.2	0.06	1.18	4.1	9.2	11.2		
8.9	0.03	0.59	0.33	1.9	2.8		
8.6	0.09	0.11	0.11	0.15	0.60	1.2	4.7*
8.3	0.07	0.13	0.13	0.12	0.9	0.21*	2.3*
8.0	0.10	0.22	0.21	0.42	0.40	0.42*	0.9*
7.7	0.27*	0.32*	0.37*	0.50*	0.56*	0.41*	0.77*
7.4	1.1*				1.3*		1.2*

ppm. We see the usual pattern of decreasing separation efficiency with increasing ionic strength, but good separations can be obtained at ionic strengths below 0.15 mole/l of sodium nitrate.

The effects of different electrolytes on the separation of zinc with NLS and Al(OH)₃ are illustrated in Table 14. In all these runs the initial Al(III), NLS, and Zn(II) concentrations were 100, 150, and 50 ppm, respectively; the pH was adjusted to 8.3, 50 ppm of NLS was added after 15 min; the air flow rate was 60 to 68 ml/min; and samples were taken for analysis after 30 min of treatment. At pH 8.3 equilibrium calculations indicate that ~93% of

the phosphate is present as HPO_4^{2-} , 7% as H_2PO_4^- , as PO_4^{3-} , and as H_3PO_4 . For arsenate at this pH, 96% is present as HAsO_4^{2-} , 4% as H_2AsO_4^- , 0.1% as AsO_4^{3-} , and $10^{-6}\%$ as H_3AsO_4 .

The decreased removal of zinc with sulfate, as opposed to nitrate as the added anion, is probably due to the increased negative charge on the anion, as is indicated by the theoretical results below. The effects of phosphate and arsenate are much too large to be due to merely a change in the charge of the anion. Presumably these effects are due to strong adsorption of these anions onto the floc, which presumably neutralized the charge of the floc.

TABLE 14. FLOC FLOTATION OF ZINC WITH $\text{Al}(\text{OH})_3$ AND NLS:
EFFECT OF ELECTROLYTE IDENTITY

Electrolyte identity	Ionic strength (mole/l)				
	0.05	0.10	0.15	0.20	0.30
	Residual zinc (ppm)				
NaNO_3	0.13	0.13	0.12	0.22	3.4
Na_2SO_4	0.6	2.2		3.6	3.1
Na_2HAsO_4	47	48			
Na_2HPO_4	46	>45			

BATCH FLOTATION OF NICKEL(II), MANGANESE(II), CHROMIUM(III), AND COBALT(II)

Nickel

Essentially the same procedures employed for the flotation of zinc(II) were used to carry out the flotation of nickel(II). One group of runs was made using $\text{Al}(\text{III})$ or $\text{Fe}(\text{III})$ at 50 mg/l, NLS at 50 mg/l, and $\text{Ni}(\text{II})$ at 100 mg/l. Sample volumes were roughly 200 ml, and air flow rates of 60-67 ml/min were used. In the pH range 5.5-8.0 the flocs were rapidly and completely removed, but $\text{Ni}(\text{II})$ removals were very poor; $\text{Ni}(\text{OH})_2$ has a relatively large solubility product (1.6×10^{-16} mole³/l³). Analyses were carried out by atomic absorption spectrophotometry at 231.8 nm. The data for these runs are as follows:

TABLE 15. EFFECT OF pH ON NICKEL(II) FLOC FOAM FLOTATION^a

pH	Runs with $\text{Al}(\text{OH})_3$ Residual Ni (mg/l)	Runs with $\text{Fe}(\text{OH})_3$ Residual Ni (mg/l)
5.5	>50	>50
6.0	>50	>50
6.5	>50	>50
7.0	>50	>50
7.5	17.3	>50
8.0	10.0	38
8.5	5.5	21
9.0	3.8	1.25
9.5	.8	1.25

^aResidual Ni measured after 15 min of treatment.

The effect of ionic strength on flotation of Ni(II) with $\text{Al}(\text{OH})_3$ and NLS is shown in Table 16.

TABLE 16. EFFECT OF IONIC STRENGTH ON NICKEL(II) FLOC FOAM FLOTATION^a

pH	Added NaNO_3 (moles/l)			
	.025	.050	.075	.250
8.5	6.6	1.3	4.2	19
9.0	5.6	1.5	2.5	16
9.5	1.4	1.4	0.6	>50

^aResidual Ni measured after 10 min of treatment.

Another set of runs made under somewhat different conditions. Initial Ni(II) concentrations were 20 mg/l, and 100 mg/l of Fe(III) or Al(III) and 50 mg/l NLS were used, and the air flow rate was about 65 ml/min. The results are tabulated below.

TABLE 17. Ni(II) FLOTATION AT DECREASED Ni(II) CONCENTRATION^a

(added NaNO_3 , m/l)	pH	Residual Ni [$\text{Al}(\text{OH})_3$]	Residual Ni [$\text{Fe}(\text{OH})_3$]
0	6.5	6.5	7.5
	7.0	4.9	5.7
	7.5	3.2	3.4
	8.0	0.43	1.9
.02	6.5	3.3	9.2
	7.0	3.8	6.0
	7.5	0.97	5.3
	8.0	0.68	3.2
.05	6.5	4.5	7.3
	7.0	3.7	8.8
	7.5	2.9	4.8
	8.0	2.4	5.3
.075	6.5	2.9	>10
	7.0	2.0	8.0
	7.5	1.5	9.3
	8.0	1.4	6.6
.10	6.5	4.6	-
	7.0	2.2	-
	7.5	0.75	-
	8.0	0.40	-

^aResidual Ni measured after 10 min of treatment.

In conclusion we have found that residual Ni(II) concentrations below 1 mg/l are achievable at pH's of 8 to 9.5 using $\text{Al}(\text{OH})_3$ and NLS provided the ionic strength is not too great (< .1 m/l).

Manganese

The relatively high solubility product of $\text{Mn}(\text{OH})_2$, 10^{-19} , suggests that the floc flotation of $\text{Mn}(\text{OH})_2$ with ferric or aluminum hydroxides should not yield very high levels of removal. In preliminary runs this was found to be the case. Samples were therefore made alkaline ($\text{pH} \sim 9$) and aerated for various lengths of time. The pH decreased during aeration as oxidation took place, so 0.1 N NaOH was added as needed to bring the pH back to 9. After aeration, flotation runs were made with 100 mg/l of Fe(III), 50 mg/l of NLS, an air flow rate of 60 ml/min, and sample volumes of 200 ml. Duration of treatment was 10 min.

At a flotation pH of 6.0, 1 h of aeration, and an initial Mn concentration of 10 mg/l, removal of the floc was visibly quite incomplete. At a flotation pH of 5.5, 1 hr of aeration, and other conditions as before, removal of the floc was complete after 2 min, and residual Mn concentrations were a fifth to a third of the initial values over a range of initial Mn concentrations from 5 to 50 mg/l. Residual Mn was present as Mn(II), indicating incomplete oxidation to $\text{Mn}(\text{OH})_3$ or MnO_2 . Samples were therefore aerated at pH 9 for 24 hrs and then treated by floc foam flotation at pH 5.5 as described above. Samples initially containing 30 mg/l of Mn yielded residuals of less than 2.0 mg/l; samples initially containing 15 mg/l yielded residuals of less than 1.0 mg/l. Additional work on pH optimization and the effects of ionic strength are being carried out. We conclude that Mn(II) can be effectively removed by floc foam flotation with ferric hydroxide and NLS only if adequate aeration at an alkaline pH is provided.

Chromium

Chromium(III) itself forms a highly insoluble hydroxide floc ($K_{sp} = 7 \times 10^{-31} \text{ m}^4/\text{l}^4$), so we carried out its flotation without the addition of Fe(III) or Al(III). Initial Cr(III) and NLS concentrations of 50 mg/l were used, and the air flow rate was about 67 ml/min. Sample volumes were about 200 ml. Samples were taken for analysis after 10 min of treatment; chromium was determined by atomic adsorption at 357.6 nm. Results were as follows:

TABLE 18. PRECIPITATE FLOTATION OF CHROMIC HYDROXIDE

pH	Added NaNO_3 (m/l)			
	0	.025	.050	.075
5.5	23	>40	>40	>40
6.0	18	11	15	10
6.5	8.6	5.5	4.2	12
7.0	22	16	5.4	13
7.5	>40	-	-	-
8.0	>40	-	-	-

The data indicate that simple precipitate flotation of $\text{Cr}(\text{OH})_3$ is not able to reduce $\text{Cr}(\text{III})$ down to the 1 mg/ℓ range.

We therefore investigated the coprecipitation of $\text{Cr}(\text{III})$ with ferric hydroxide; if this provides effective removal, one would anticipate that adsorbing colloid flotation of $\text{Cr}(\text{III})$ with ferric hydroxide and NLS should also be effective. Solutions were prepared containing the desired concentrations of $\text{Cr}(\text{III})$ and $\text{Fe}(\text{III})$ as nitrates, the pH was adjusted to the desired level (5, 6, or 7) with NaOH and HNO_3 , the solutions slowly stirred for about 5 min, the precipitates allowed to settle, and samples taken for analysis. At pH 5.0 solutions initially containing $\text{Cr}(\text{mg}/\ell)$: $\text{Fe}(\text{mg}/\ell)$ of 50:50, 50:100, 50:150, and 25:100 all contained more than 1 mg/ℓ $\text{Cr}(\text{III})$ after precipitation; a solution of initial composition 20:100 contained 0.5 mg/ℓ of $\text{Cr}(\text{III})$ after precipitation. At pH's 6.0 and 7.0 the supernates of all the solutions contained less than 0.5 mg/ℓ of Cr.

On the basis of these results we carried out adsorbing colloid flotation runs on solutions containing 20 mg/ℓ of $\text{Cr}(\text{III})$ and 100 mg/ℓ of $\text{Fe}(\text{III})$ at pH's in the range 5.5-7.25. The solutions were slowly stirred for 5-10 min after precipitation; they were then made 50 mg/ℓ in NLS and transferred to the flotation column. Air flow rates of about 65 ml/min were used. The solutions became clear within 2 min after the initiation of flotation. The results (after 10 min of foaming) are shown in Table 19.

TABLE 19. EFFECT OF pH ON CHROMIUM(III) FLOC FOAM FLOTATION

pH	Residual Cr(mg/ℓ)
5.5	<.25
6.0	<.25
6.15	<.25
6.5	<.25
7.0	.5
7.25	1.3

The effects of varying the initial $\text{Fe}(\text{III})$ concentration are shown in Table 20.

TABLE 20. EFFECT OF IRON(III) CONCENTRATION ON CHROMIUM(III) FLOC FOAM FLOTATION^a

Initial Fe(III) (mg/ℓ)	pH	Residual Cr (mg/ℓ)
100	6.15	<.25
80	6.1	<.25
40	6.1	<.25
	6.4	<.25
20	6.4	.4

^aInitial $\text{Cr}(\text{III})$ concentration 20 mg/ℓ, air flow rate 65 ml/min, run time 10 min.

The effects of increasing the ionic strength by the addition of NaNO_3 are shown in Table 21.

TABLE 21. EFFECT OF INERT SALT CONCENTRATION ON CHROMIUM(III)
FLOC FOAM FLOTATION^a

Added NaNO_3 (moles/l)	pH	Residual Cr (mg/l)
0	6.15	.25
.05	6.25	.3
	6.50	.3
.10	6.30	2.2, 3.6

^aInitial Cr(III) concentration 20 mg/l, air flow rate 65 ml/min, run time 10 min.

We noticed that if, in the course of adjusting the pH before flotation, one overshot and the pH got up to 9-10 or more (after which it was adjusted back to the desired level with 0.1N HNO_3), flotation did not remove all the precipitate from the column, and the solution contained more than 1 mg/l of chromium after flotation. We explored this by carrying out four runs in which the pH was held at 10 for various periods of time, then reduced to 6.2 for another period of time before flotation was carried out. In all of these runs 20 mg/l of Cr(III), 100 mg/l of Fe(III), and 50 mg/l of NLS were used; the air flow rate was in the range 60-65 ml/min; and the solution volume was 200 ml.

In the first run the pH was held at 10 for 1 min; it was then adjusted to 6.2 and flotation was immediately carried out. After 10 min of flotation the residual Cr(III) level was 0.4 mg/l, somewhat in excess of the values of <.25 mg/l which were routinely obtained in the absence of pH overshoot. After 25 min of flotation the residual Cr(III) level was 0.2 mg/l.

The pH was held at 10 for 4 min for the second run; flotation was carried out immediately after adjustment of the pH of 6.2. After 10 min of flotation the residual Cr(III) concentration was 8.1 mg/l; after 25 min, 6.4.

The pH was held at 10 for 1 hr for the third run; the pH was then reduced to 6.2 and the solution permitted to stand for 2 hr. The pH tended to increase, and was readjusted to 6.2 several times during this period. After 10 min of flotation the residual Cr(III) concentration was 5.0 mg/l; after 25 min, 4.3.

In the fourth run the pH was kept at 10 for 8 min; the pH was then reduced to 6.2 and the solution permitted to stand overnight. The next morning the pH was again adjusted down to 6.2 and flotation carried out. After 10 min of flotation the residual Cr(III) level was 2.8 mg/l; after 25, 2.0.

We interpret these results as indicating the formation of a soluble, relatively non-labile hydroxide complex ion of Cr(III) at pH 10. Chromium(III) complexes generally tend to be rather non-labile. We have not observed this effect with other metals. Its occurrence with chromium dictates the careful

avoidance of high pH's at all times if effective separations by floc foam flotation or by precipitation techniques are to be achieved at reasonably rapid rates.

We conclude that Cr(III) may readily be removed from aqueous solution by adsorbing colloid flotation with ferric hydroxide and NLS, provided that the pH is kept low enough to avoid the formation of soluble, relatively non-labile chromium complexes with hydroxide.

Cobalt

The removal of Co(II) by floc foam flotation is similar to that of Ni(II). The solubility product of Co(OH)_2 is $2.5 \times 10^{-15} \text{ m}^3/\ell^3$, slightly larger than that of Ni(OH)_2 . 200 ml samples were treated; air flow rates of about 67 ml/min were used; and samples were taken for analysis after 15 min of treatment. Data showing the pH dependence of the separations are shown in Table 22.

TABLE 22. FLOC FOAM FLOTATION OF COBALT(II) WITH Al(OH)_3 OR Fe(OH)_3 AND NLS

Al(OH)_3 runs ^a		Fe(OH)_3 runs ^b	
pH	Residual Co(II) (mg/ℓ)	pH	Residual Co(II) (mg/ℓ)
6.5	>8	6.0	>8
7.2	7.6	6.5	>8
7.4	5.4	7.0	7.2
7.8	3.5	7.5	3.0
8.3	1.2	8.0	2.4
8.8	1.4	8.5	1.9
		9.0	6

^aInitial Al(III) concn. = 100 mg/ℓ. ^bInitial Fe(III) = 20 mg/ℓ.
Initial Co^{++} concn. = 50 mg/ℓ.

The effect of ionic strength is shown in Table 23.

TABLE 23. EFFECT OF IONIC STRENGTH ON FLOTATION OF Co(II) WITH Al(OH)_3 AND NLS

pH	Added NaNO_3			
	0	.025	.050	.075
7.2	7.6	5.3	2.7	6.3
7.8	3.5	2.4	2.4	2.5
8.3	1.2	1.5	2.2	2.7
8.8	1.4	3.6	8.2	-
9.3	6.	8.1	-	-

We conclude, that residual Co(II) levels in the range 1-2 mg/l can be achieved at a pH of about 8.5 provided that the ionic strength is less than .05 m/l.

COMPATIBILITY OF FLOC FOAM FLOTATION WITH PRECIPITATION PRETREATMENTS

We noted in our first report that foam flotation techniques appear to be best adapted to the treatment of wastewaters, which are rather dilute in the substance being removed. We also note that precipitation treatment at times does not yield an effluent of adequate quality. These facts motivated our investigation of the compatibility of several precipitation pretreatment procedures for the removal of copper(II) by adsorbing colloid flotation with $\text{Fe}(\text{OH})_3$ as the floc and NLS as the collector. This separation was used because it had previously been shown to be a very effective one, (1) and because the atomic absorption spectrophotometric analysis for copper at 324.8 nm is quite sensitive.

1. Use of Na_2CO_3 (soda ash) as a precipitating agent.

Batch runs were made as follows. A solution of 500 mg/l of Cu(II) as $\text{Cu}(\text{NO}_3)_2$ was prepared, and to this was added sufficient 0.5 M Na_2CO_3 solution to precipitate the copper and achieve the desired pH. (Precipitation was carried out at pH's of 7.0, 8.0, and 9.0.) After the CuCO_3 precipitate settled out, the supernatant liquid was decanted. Foam flotation was carried out on this supernate, using 100 mg/l of Fe(III), 100 mg/l of NLS (50 mg/l initially, 25 mg/l after 6 min, and 25 mg/l after 11 min). Flotation was carried out at pH's of 5.5, 6.0, 6.5 and 7.0.

After the precipitation step the Cu(II) concentration was in the range 5-15 mg/l, depending on the settling pH. (Typically ~15 ml of Na_2CO_3 solution was added to 300 ml of 500 mg/l Cu(II) solution.) The carbonate ion in the supernatant solution severely hindered subsequent Cu(II) removal by foam flotation. Since carbonates form CO_2 at the lower pH's and can then be sparged from solution, the flotation runs made at acidic pH gave much better results, especially if the solution was allowed to sparge in the column for 10 min before flotation was begun. Flotation runs made at pH 7.0 gave poor Cu(II) removal; flotation runs at 6.5 caused a reduction in Cu(II) from 9.0 mg/l to 0.11 mg/l after 20 min. Similar runs in which the flotation pH was 6.0 gave a Cu(II) concentration of 0.20-0.40 mg/l after 25 min, depending on conditions. Similar runs in which the flotation pH was 5.5 gave somewhat poorer results; residual Cu(II) was 1.0-2.0 mg/l after 25 min of foaming. We also found that, if the solution is placed in the column and sparged with air at a very low pH (2.5-3.0) for 5-10 min, foam flotation at pH 6.5 readily produced residual Cu(II) concentrations in the range 0.10-0.20 mg/l after 10 min of foaming.

Data on the effects of settling pH and foaming pH are shown in Table 25. Data on the effects of a preliminary air sparging at low pH are shown in Table 26.

2. Use of $\text{Ca}(\text{OH})_2$ (lime) as a precipitating agent.

TABLE 24. EFFECTS OF SETTLING AND FOAMING pH's ON Cu(II) REMOVAL AFTER PRECIPITATION WITH Na₂CO₃

Settling pH		7.0	8.0	9.0
Flotation pH	Time, min	Cu(II) (mg/ℓ)		
7.0	0	7.9 (10.5) [†]	7.0 (9.3)	4.3 (5.7)
	5	7.8	6.9	4.2
	10	7.8	6.7	4.3
	15	7.8	6.3	4.2
	20	8.0	6.2	4.3
	25	7.8	5.7	4.3
6.5	0	9.1 (12.1)	- (-)	6.3 (8.5)
	5	7.7	6.3	4.7
	10	5.9	5.8	4.2
	15	3.7	4.3	2.4
	20	0.85	2.29	1.67
	25	0.44	1.20	0.89
6.5*	0	9.0 (12.1)	4.6 (6.1)	3.9 (5.2)
	5	2.57	4.6	-
	10	1.47	2.58	-
	15	0.59	0.71	1.46
	20	0.11	0.31	0.53
	25	0.12	0.30	0.24
6.0	0	10.1 (13.5)	5.0 (6.7)	3.15 (4.2)
	5	4.5	3.6	3.3
	10	1.06	1.88	1.03
	15	0.54	0.41	0.36
	20	0.49	0.27	0.34
	25	0.47	0.24	0.31
6.0*	0	11.5 (15.3)	5.4 (7.1)	3.14 (4.2)
	5	1.22	1.08	0.79
	10	0.85	0.35	0.46
	15	0.68	0.37	0.34
	20	0.63	0.35	0.28
	25	0.77	0.37	-
5.5	0	10.8 (14.4)	4.6 (6.1)	3.29 (4.4)
	5	3.33	1.65	1.40
	10	2.79	1.27	1.04
	15	2.64	1.17	0.96
	20	2.42	1.09	1.00
	25	2.41	1.14	0.99
5.5*	0	9.5 (12.6)	7.6 (10.2)	3.4 (4.6)
	5	2.46	2.05	1.03
	10	2.11	2.09	0.99
	15	1.94	1.86	0.95
	20	1.75	1.79	0.95
	25	2.00	1.62	0.94

*Sample sparged with air for 10 min before foaming.

[†]Parenthetic values are Cu(II) concentrations in the decantate before addition of other reagent solutions.

TABLE 25. EFFECTS OF AIR SPARGING AT LOW pH ON Cu(II) REMOVAL AFTER PRECIPITATION WITH Na_2CO_3^*

Sparging time, min	Time, min	Cu(II) concentration (mg/l)
2	0	10.1 (13.5)
	5	5.3
	10	1.71
	15	0.44
	20	0.35
	25	0.26
4	0	8.7 (11.6)
	5	0.96
	10	0.26
	15	0.26
	20	-
	25	0.21
6	0	8.9 (11.8)
	5	1.30
	10	0.21
	15	0.15
	20	0.15
	25	0.15
8	0	10.6 (14.2)
	5	0.52
	10	0.15
	15	0.15
	20	0.15
	25	0.14
10	0	10.1 (13.4)
	5	0.27
	10	0.18
	15	0.10
	20	0.14
	25	0.12

*Solutions were sparged with air at pH 2.5-3.0, pH of precipitation and settling was 7.0 (Na_2CO_3), initial Cu(II) concentration was 500 mg/l. 150 ml of supernate was made 100 mg/l in Fe(III), placed in column, acidified, and sparged for the desired period. The pH was then raised to 6.5 (NaOH), 50 mg/l of NLS added initially, 25 mg/l after 6 min, 25 mg/l after 11 min. Air flow rate were about 60 ml/min.

Batch runs were as follows. Solid $\text{Ca}(\text{OH})_2$ was added with vigorous stirring to 200 ml of a solution containing 500 mg/l of Cu(II) (as the nitrate) until a pH of ~12 was reached. This required approximately 1.2 gm of $\text{Ca}(\text{OH})_2$ per liter of solution. The solution was allowed to settle for 10 min and the supernatant decanted for further treatment by floc foam flotation with Fe(III) and NLS as described previously. We found that the high Ca(II) concentration

prevented foaming by forming a scum with the NLS, and that foam flotation was not possible under these circumstances. The problem was solved by bubbling CO_2 through the solution until the pH drops to about 10.0; this precipitates CaCO_3 but does not leave excessive $\text{CO}_3^{=}$ or HCO_3^- in the solution to interfere with the foam flotation step. The resulting solution is readily treated by floc foam flotation [100 mg/l of Fe(II) ; 50, 25, and 25 mg/l of NLS initially, after 6 min, after 11 min; air flow rate about 60 ml/min]. The results are shown in Table 26. They indicate that Cu(II) levels, already quite low after

TABLE 26. EFFECT OF FOAMING pH ON Cu(II) REMOVAL AFTER PRECIPITATION WITH Ca(OH)_3

Flotation pH time, min	5.5	6.0	6.5	7.0
	Cu(II) (mg/l)			
0	0.23 (.31) [†]	0.23 (.31)	0.19 (.25)	0.25 (.35)
5	0.10	0.05	0.13	0.20
10	0.11	0.03	0.04	0.05
15	0.08	0.01	0.06	0.08
20	0.06	0.00	0.05	0.08
25	0.05	-	0.04	0.05

[†]Parenthetic values are Cu(II) concentrations in the decantate before addition of other reagent solutions.

precipitation with lime, are readily reduced to extremely low values by floc foam flotation with Fe(OH)_3 and NLS, provided that excessive Ca(II) is removed.

3. Use of Al(III) or Fe(III) as coprecipitating agents.

In these runs solutions were prepared containing 500 mg/l of Cu(II) as the nitrate; aluminum nitrate or ferric nitrate and sodium hydroxide were used to generate the coprecipitating Al(OH)_3 or Fe(OH)_3 flocs; coprecipitation was carried out at a pH of 7.0 in all runs. After coprecipitation and settling, supernate was decanted, the pH was adjusted to the desired value with NaOH and HNO_3 ; Fe(III) was added (100 mg/l); and NLS was added (50 mg/l initially, 25 mg/l after 6 min and 25 mg/l after 10 min of flotation). The air flow rate was approximately 60 ml/min.

In the first set of runs 100 mg/l of Al(III) was used in the coprecipitation step. After coprecipitation and settling the supernate contained approximately 1.00 mg/l of Cu(II) . Flotation of the supernate as described above resulted in residual Cu(II) concentrations of 0.05 mg/l (flotation pH 7.0), 0.03 mg/l (6.5), 0.03 mg/l (6.0) and 0.16 mg/l (5.5) after 25 min.

The second set of runs was made using 50 mg/l of Al(III) in the coprecipitation step; after the resulting floc had settled, the supernate contained typically 1.5-2.4 mg/l of Cu(II) . Flotation of the supernate as described above reduced residual Cu(II) levels to 0.05 mg/l (flotation pH - 7.0), 0.03 mg/l (6.0) and 0.15 mg/l (5.5) after 25 min.

Fe(III) at 50 mg/l was used as the coprecipitating agent in the third set of runs. After settling, the supernate contained 3.0-4.0 mg/l of Cu(II). Flotation of this solution as described above produced residual Cu(II) levels of 0.01 mg/l (flotation pH = 7.0), 0.05 mg/l (6.5), 0.03 mg/l (6.0), and 0.23 mg/l (5.5). It was found that the Cu(II) concentrations after coprecipitation with 100 mg/l of Fe(III) were approximately the same as those resulting when 50 mg/l of Fe(III) was used. See Table 27.

TABLE 27. EFFECT OF FOAMING pH ON Cu(II) REMOVAL AFTER COPRECIPITATION WITH Al(OH)_3 or Fe(OH)_3

Precipitating agent and concentration		100 mg/l Al(III)	50 mg/l Al(III)	50 mg/l Fe(III)
Flotation pH	Time, min			
7.0	0	.95 (1.27) [†]	2.40 (3.20)	4.5 (5.9)
	5	.21	.25	.15
	10	.07	.13	.01
	15	.07	.07	.01
	20	.07	.07	.01
	25	.05	.07	.01
6.5	0	.89 (1.19)	2.26 (3.01)	4.0 (5.3)
	5	.20	.13	.30
	10	.03	.04	.06
	15	.03	.03	.06
	20	.03	.03	.05
	25	.03	.03	.05
6.0	0	1.05 (1.40)	1.80 (2.40)	2.70 (3.60)
	5	.16	.07	.08
	10	.03	.03	.05
	15	.03	.03	.03
	20	.03	.03	.03
	25	.03	.03	.03
5.5	0	1.13 (1.51)	1.37 (1.83)	2.82 (3.76)
	5	.20	.17	.34
	10	.19	.15	.26
	15	.17	.15	.24
	20	.17	.15	.23
	25	.16	.15	.23

[†] Parenthetic values are Cu(II) concentrations in the supernate before addition of other reagent solutions.

We conclude that coprecipitation with Al(OH)_3 or Fe(OH)_3 is quite compatible with adsorbing colloid flotation.

INTERFERENCES WITH FLOC FOAM FLOTATION RESULTING FROM FOREIGN IONS

One of the factors which can very markedly affect the efficiency of adsorbing colloid flotation and surfactant recovery from flotation sludges is

the extent to which other ions are adsorbed into the primary layer of the floc. The theory of this effect is discussed in references (42) and (51), and in Appendix D. The very large changes in surface potential and in surface concentration of surfactant result (in the model analyzed) from varying the salt concentration and identity of added salts. Earlier in this section we demonstrated very marked differences in the ability of different anions to interfere with the flotation of zinc(II) with $\text{Al}(\text{OH})_3$ and NLS; in order of increasing interference we found $\text{NO}_3^- < \text{SO}_4^{2-} \ll \text{H}_2\text{PO}_4^- \approx \text{HAsO}_4^{2-}$. [See also (56).] In the present work we examine the effects of various added salts on the batch flotation of ferric hydroxide flocs with sodium lauryl sulfate at pH 5.0. We choose this system and these conditions [100 mg/l of Fe(III), 50 mg/l of sodium lauryl sulfate] because (1) in the absence of added salts flotation is very rapid; (2) the system is quite effective for a number of separations; and (3) the flotation of the strongly colored $\text{Fe}(\text{OH})_3$ is readily observed visually.

Batch runs of about 200 ml were made in an apparatus of the sort previously described (1,54,57). Removal rates were graded as rapid [removal of $\text{Fe}(\text{OH})_3$ visually complete in 5 min], slow [visual evidence of $\text{Fe}(\text{OH})_3$ in the foam, but removal not complete in 5 min], or none [no visual evidence of $\text{Fe}(\text{OH})_3$ in the foam]. A variety of anions were chosen having different charges and coordination affinities for Fe(III) (15). Glycerol, which coordinates readily with Fe(III), was also investigated. The results are shown in Table 29.

We find that phosphate, hexaphosphate, arsenate, EDTA, and oxalate are extremely effective in suppressing the flotation of ferric hydroxide under conditions at which, in the absence of these ions, it floats rapidly and completely. In all the runs a possibly interfering substance was added to the solution after the ferric hydroxide was precipitated to avoid possible loss of the interfering ion by coprecipitation in the bulk of the solid where it would presumably be ineffective. It was somewhat surprising to us that cyanide and thiocyanate, both of which complex readily with Fe(III) in solution, were nowhere nearly as effective in blocking flotation as the ions mentioned above. Neither did we anticipate that ClO_4^- would be somewhat more effective than NO_3^- and Cl^- in blocking flotation, since it is one of the weakest-binding ligands known.

These results suggest a number of potential applications. Addition of interfering anions might be used to make precipitate flotations more selective and could also facilitate the recovery of surfactant from foam flotation sludges. Our findings also introduce a complication into the use of foam flotation techniques for the removal of metals from wastewater which may contain interfering ions. The behavior of the flocs in the presence of interfering ions suggest that these ions may interfere severely with precipitation separations also.

SIMULTANEOUS FLOC FOAM FLOTATION OF Cu(II), Pb(II), AND Zn(II)

Most metal-containing industrial wastes contain several different metal ions, so we carried out some work on the simultaneous removal of copper, lead and zinc from solutions containing these metals. The concentration of each

TABLE 28. EFFECT OF VARIOUS ADDED SALTS AND GLYCEROL ON THE FLOTATION OF FERRIC HYDROXIDE

Substance	Concentration (moles/l) ^a					
	0.0025		0.01	0.03	0.05	
NaClO ₄			R	S	S	N
NaNO ₃			R	R	R	R
NaCl			R	R	R	R
KCN			S-R	S	S	N
KCNS		R	S	S	S	S
NaF	R	S	N			
Glycerol			S	S	S	S
Na ₂ SO ₄	R	S	S	N		
Na ₂ HPO ₄	N	N	N			
Na ₂ HAsO ₄	N	N	N			
Concentration	0.0005	0.005				
Na ₂ EDTA	N	N				
Concentration	2.5 x 10 ⁻⁵	6.25 x 10 ⁻⁵	1.25 x 10 ⁻⁴	3.13 x 10 ⁻⁴	6.25 x 10 ⁻⁴	1.25 x 10 ⁻³
Na ₂ C ₂ O ₄	R	S	S	S	N	N
Concentration	4.2 x 10 ⁻⁴	8.3 x 10 ⁻⁴	1.67 x 10 ⁻³	5 x 10 ⁻³	8.3 x 10 ⁻³	
(NaPO ₃) ₆	N	N	N	N	N	

^aR = rapid removal; S = slow and/or incomplete removal after 5 min; N = no visible removal.
 Operating conditions: pH = 5.0 ± 0.1; 100 ppm Fe(III); 50 ppm NLS; air flow 85 ml/min.

of the metal ions was 20 mg/l, 100 mg/l of NLS was used as the collector, sample volumes were about 200 ml, air flow rates were about 67 ml/min, and flotation was carried out for 20 min. Copper, lead and zinc analyses were carried out by atomic adsorption. Ionic strength was varied by the addition of sodium nitrate.

The results of this work are shown in Table 29, and indicate that simultaneous removal of several metals by floc foam flotation is possible.

TABLE 29. RESULTS OF THE FLOW FOAM FLOTATION OF Cu(II), Pb(II), AND Zn(II) WITH $\text{Fe}(\text{OH})_3$ AND NLS

Added NaNO_3 (m/l)	pH	Fe(III) (m/l)	Residual	Cu(II) (mg/l)	Pb(II) (mg/l)	Zn(II) (mg/l)
.02	6.1	100		.30	.20	3.2
.02	6.5	100		.25	.15	2.1
.02	7.02	100		.20	.20	1.8
.05	6.05	100		.27	.15	2.9
.05	6.55	100		.26	.15	2.9
.05	7.05	100		.30	.30	2.2
.10	6.05	100		.35	.4	3.2
.10	6.56	100		.26	.30	2.8
.10	7.02	100		1.25	1.2	2.9
.075	8.05	100		7.75	>10	3.3
.075	8.05	150		>8.0	>10	3.5
.075	8.05	200		>8.0	>10	3.5

FLOC FOAM FLOTATION OF CYANIDES

Various treatment technologies (physical, chemical and biological) exist for the removal of cyanide from wastewaters. These include: alkaline chlorination; electrolytic decomposition; ozonation; complexation with metals; ion exchange; reverse osmosis; dialysis, irradiation; permanganate oxidation; peroxide oxidation; complexation with polysulfides; the Kastone process; liquid-liquid extraction with primary and secondary amines; copper-catalyzed activated carbon adsorption; and biological oxidation using trickling filters and activated sludge. Many of these processes are well adapted to treating waste streams of low volume and high concentration (e.g. wastewater from an electroplating facility). Some exhibit technical difficulties, while others at present lack full-scale demonstration. The alkaline chlorination process is most commonly employed.

The iron cyanide complexes are so stable (see Table 30) that standard alkaline chlorination does not affect them. Since they exhibit little dissociation, they have acquired "non-toxic" labels. Table 31 lists the solubilities of some complex cyanide salts. Iron complexes are capable of releasing cyanide ion through photo dissociation in strong sunlight. Also, bacterial decomposition of the complex in the receiving water to form CN^- is possible as well as increased solubility under alkaline conditions. Consequently the deliberate complexing of simple cyanides with iron salts as an

TABLE 30. STABILITY CONSTANTS FOR CYANIDE COMPLEXES

Complex	K _s (25°C)
Co(CN) ₆ ⁻⁴	1 x 10 ¹⁹
Cu(CN) ₄ ⁻²	1 x 10 ²⁵
Fe(CN) ₄ ⁻⁴	1 x 10 ²⁴
Fe(CN) ₆ ⁻³	1 x 10 ³¹
Ni(CN) ₄ ⁻²	1 x 10 ²²
Zn(CN) ₄ ⁻²	8.3 x 10 ¹⁷

(from A. J. Bard, Chemical Equilibria, Harper and Row, New York, 1966)

TABLE 31. SOLUBILITIES OF CYANIDE COMPOUNDS

Compound	Solubility, g/l	Temp, °C
Ni(CN) ₂	5.92 x 10 ⁻²	18
Zn(CN) ₂	5.8 x 10 ⁻³	18
Fe ₄ [Fe(CN) ₆] ₃	2.5 x 10 ⁻⁴	22
Zn ₂ Fe(CN) ₆	2.6 x 10 ⁻³	N/A
Zn ₃ [Fe(CN) ₆] ₂	2.2 x 10 ⁻⁵	N/A
Cu(CN) ₂	0.014	20

(from ASTM, 1975 and Linke, 1958, 1965)

economical wastewater treatment should be unacceptable. The insoluble iron cyanide in a solid waste can best be treated by burial or landfill in an area where acid conditions are common. The other metallo-cyanide complexes are susceptible to chlorine oxidation but proceed at different rates.

Grieves, Bhattacharyya, and co-workers studied the removal of iron-complexed cyanide by foaming with a cationic surfactant, ethylhexadecyldimethylammonium bromide (81,82). After treatment the free residual cyanide averaged 7.5 mg/l; residual complexed cyanide, 2.9 mg/l. The reduction in free cyanide ranged from approximately 80 to 90%. Other studies involving metallo-cyanide complexes include: batch foam fractionation experiments concerning the selectivity of several chloride vs cyanide complex ions (81); and a similar determination of the selectivity coefficients for Ag(CN)₂⁻ and Au(CN)₂⁻ vs I⁻ (87).

Here we report on a study of the removal of metallo-cyanide complexes using NLS. We have considered the precipitate and/or adsorbing flotation of cobalt, copper, chromium, iron, nickel and zinc systems, individually and in combination. Their removal is addressed from two aspects: (1) the removal of cyanide ion itself; and (2) the removal of complexes which could be

present or readily formed in the wastewater. Particular interest was paid to iron-iron-cyanide systems because of their low toxicity and low cost.

Experimental

Batch foam separations were carried out in the batch columns described earlier. Metals analyses were performed on acidified aqueous samples by atomic absorption. Cyanide determinations were performed on basic (pH 13) solutions with an Orion specific ion probe electrode, model 96-06. The standard curves were linear in the range studied, 0.05-10.0 mg/l. The average correlation coefficient (for the first order fit of log concentration vs MV) was 0.9970.

A semi-quantitative method was developed for the determination of residual iron-cyanide complex in solution. A solution was prepared as described below, but not foamed. The first metal added was Fe^{+2} (100 mg/l); the second, Fe^{+3} (150 mg/l). The additional pH adjustments to prepare for the cyanide and metals analyses were also performed on the sample. This insured comparable ionic strength of the solutions. The solution was then permitted to stand, covered, to simulate the oxidation experienced in the column. Aliquots were diluted to yield a series of standards representing 0-20% of the initial concentration. Absorbance vs percent of initial concentration were run on a Beckman DB spectrophotometer at a wavelength of 732 m μ . The results were linear in the range studied with a correlation coefficient of 0.9996 for a first order fit.

Stock solutions of cyanide (50 mg/l) from KCN were prepared daily. Two hundred ml were placed in a beaker and the appropriate amount of the "first metal" was added. In all cases 1 ml of stock metal solution resulted in a 50 mg/l concentration. It was presumed that the "first metal" forms the metal-cyanide complex anion. The stock metal solutions were prepared from the corresponding nitrate salts except for the Fe^{+2} solution, for which ferrous ammonium sulfate was used. All metal solutions were kept at acidic pH. The metal cyanide solution was stirred for approximately 5 min, pH was monitored throughout. The "second metal" was added and the solution stirred for approximately 10 min. Longer stirring periods were tested but yielded no increase in CN removal. The pH was adjusted to the desired value by adding NaOH or HNO_3 as necessary. Five ml of 1000 mg/l NLS were added before the test solution was poured into the column. Additional surfactant was added in a series of 5 ml injections throughout the run as required. Air flow rate in the column was approximately 60 ml/min.

Results and Discussions

A series of runs was performed to determine the optimum operating parameters for the foam removal of cyanide. Optimization required the assessment not only of residual cyanide concentrations but also residual levels of cyanide complex and iron. The parameters which were varied were: Fe(II) concentration; Fe(III) concentration; NLS concentration; pH; and duration of foaming. The manner of NLS addition was also studied. Second order effects were also briefly assessed. These included the effect of increased stirring time after iron addition and use of dry weight iron salts additions (instead

of acidified stock solutions). The latter was tried in an effort to maintain ionic strength as low as possible. Both second order effects produced no more than minor variations, well within the experimental precision of the results.

Table 32 shows the results of preliminary tests in which precipitate flotation was employed to remove cyanide. (Earlier runs determined optimum pH for removal.) The precipitation with Fe(III) effected no removal. Ferric hydroxide was formed and an odor of HCN was noticed escaping from the column, so the run was terminated. Precipitation with Fe(II) produced better results. Foaming effected an average of 82.8% free CN reduction and a 91.1% iron reduction.

TABLE 32. PRECIPITATE FLOTATION RUNS

Initial Conc.						
Run	Fe(II), mg/l	Fe(III), mg/l	pH	Foaming Time	Residual CN, mg/l	Residual Fe, mg/l
A	50	0	4.9	40	8.6	4.1
B	50	0	4.9	40	8.6	4.8
C	0	50	4.9→6.5	*	17.1	N/A

* Aborted - see text.

TABLE 33. MOLARITY AND mg/l CONVERSIONS

Species	at	mg/l	yields	Molarity ($\times 10^5$)	Solution
CN		50		19.2	
Fe		50		8.95	
Cu		50		7.87	
Cr		50		9.61	
Co		50		8.48	
Ni		50		8.52	
Zn		50		7.65	

Species	ratio mg/l in moles	ratio Fe/CN in moles
$\text{Fe}(\text{CN})_6^{-3}$.358	0.167
$\text{Fe}(\text{CN})_6^{-4}$.358	0.167
$\text{Fe}[\text{Fe}(\text{CN})_6]$	0.716	0.333
$\text{Fe}_4[\text{Fe}(\text{CN})_6]_3$	0.835	0.389
50 ppm Fe & 50 ppm CN	1.00	0.466

For 50 ppm CN total conversion to $\text{Fe}_4[\text{Fe}(\text{CN})_6]_3$ yields 9.45 mg/l complex salt or 1.1×10^{-5} moles complex salt.

Table 33 presents a summary of required molar ratios and mg/l equivalents for the iron cyanide complexes and precipitated compounds. Similar informa-

tion for the heavy metals studied (and discussed later) is also included. It was assumed that the Fe(II) formed the stable complex $\text{Fe}(\text{CN})_6^{-4}$ and excess iron formed $\text{Fe}_4[\text{Fe}(\text{CN})_6]_3$ - the excess Fe(II) being oxidized to Fe(III) upon stirring and/or foaming.

In an effort to increase the removal of cyanide, a series of runs was made using adsorbing colloid flotation. The precipitate formed was still assumed to be predominantly $\text{Fe}_4[\text{Fe}(\text{CN})_6]_3$. This was then adsorbed onto ferric hydroxide floc and foamed with pulsed NLS additions. For 60 min runs, 50 ml (25 mg/l) additions of NLS were added at time = 0, 10, 25 and 40 min. Table 35 shows the results of these runs which determined the standard operating conditions. A fresh ascarite air filtering system adequately removed CO_2 so

TABLE 34. STANDARD OPERATING CONDITIONS: DETERMINING RUNS

Initial Conc.			Operating Conditions				
Run#	Fe^{+2} mg/l	Fe^{+3} mg/l	pH	foaming duration, min.	Total NLS added, mg/l	Free CN, mg/l	Complex, (% initial conc.)
1	100	200	3.85	45	75	3.9	0.8
2	100	200	4.7	45	100	3.2	0
3	100	200	5.3	60	100	2.8	0.5
4	100	200	5.5	60	100	4.1	0
5	100	200	5.7	120	175	1.9	0.5
6	100	200	6.0	aborted-poor floc removal			
7	100	150	4.2	60	125	6.5	0
8	100	150	4.2	90	125	5.9	0.2
9	100	150	4.2	90	125	6.5	0
10	100	150	4.2	120	150	5.9	0
11	100	150	4.2	120	150	5.1	0.2
12	100	150	5.5	60	100	3.6	0
13	100	150	5.5	60	100	4.1	0
14	100	150	5.5	60	100	4.1	0

that initial and final pH in the columns were essentially the same. Two additional pH considerations were included in this study: (1) ferric hydroxide floc floated best with NLS over a pH range of 5 to 7; and (2) most discharge regulations require the pH of plant effluent to be between 6 and 9.

The first series of runs (1-6) employed 100 mg/l Fe(II) to form the ferrocyanide complex and precipitate and 200 mg/l excess Fe(III) to form the adsorbing floc. Overall best results were obtained in the pH 5.3-5.5 range considering duration of foaming and amount of NLS required.

It should be noted that according to Grieves and Bhattacharyya (88), as suggested by Legros (89,90), complete conversion of "free" cyanide to complexed cyanide is impossible. A "reasonable" percentage of non-complexed cyanide was reported to be 20%. This results from the hydrolysis of the ferrocyanide complex ion to form a ferro aquo penta cyanide complex, $[\text{Fe}(\text{CN})_5\text{H}_2\text{O}]^{-3}$, and free cyanide, CN^- .

The next series of runs (7-14) optimized the iron concentration and foaming time. On the basis of the results of series 1, the pH employed was 5.3-5.5. At pH 4.2 the average CN removal was 88.0%. The average iron removal was 87.7%. There was evidence of trace residual iron complex at this pH. At pH 5.5 the CN removal was 92.2% (3.9 ppm average residual) and the average iron removal was 97.8% (5.4 ppm average residual). There was no evidence of residual iron complex when the samples were analyzed as described above. Extended foaming did not decrease the residual free cyanide concentration but did reduce the iron concentration from 5.0 mg/l at 60 min to 3.0 mg/l after 90 min. The foamate volume at the end of the 60 min runs was 5-6% of the initial sample volume for one system; this quantity was 7-8% in another column.

As mentioned previously, the iron cyanide complex is known to photodecompose. A run was made which was shielded from the laboratory fluorescence lights. No decrease in free cyanide concentration was noted, but there was a slight increase in residual complexed cyanide, 0.76%. (Operating conditions were as in runs 12-14.)

The operating conditions from runs 12-14 were selected as the standard operating conditions. Another series of runs using these conditions investigated the effect of increasing ionic strength on residual concentrations. The results are seen in Table 35. As anticipated, the residual concentrations

TABLE 35. IONIC STRENGTH RUNS^{*}

Run	NaNO ₃ Molarity	CN, mg/l	Fe, mg/l	Complex (% initial conc.)
Ave. of Std. Runs	0	3.9	5.4	0
18	0.01	8.8	11.3	0.2
19	0.01	8.8	19.5	0
20	0.1	7.3	44.3	N/A
21	0.1	6.2	54.8	32
22	0.25	3.4	73.6	100
23	0.25	3.2	145.6	100

^{*}Standard operating conditions; pH 5.3-5.4; 100 mg/l Fe⁺²; 150 mg/l Fe⁺³; duration of foaming 60 min; total NLS added, 100 mg/l.

of iron and complex increased with increasing salt concentration. The concentration of free cyanide at the end of the run was found to decrease with increasing salt concentration.

Next, standard operating conditions were used in a study of cyanide removal in the presence of various heavy metals, singly and in combination. The metals selected for study were cobalt, copper, chromium, nickel and zinc. Cobalt was included since it also forms a very stable cyanide complex (see Table 30). The other metals are commonly used in electroplating facilities

and are found in wastewater. Cyanide can be used as a major anion in the plating baths for zinc, nickel or copper. These plated metals often form the basis surface for subsequent chromium plating. The average results for cyanide removal are given in Table 36.

In a Type A run, one first adds the metal of interest, M, to the free cyanide solution to form the complex and then adds the Fe(III). This is completely analogous to the standard runs. In a Type B run the complex is made with Fe(II) and then the metal, M, is added. The operating pH was selected as optimum from an earlier series of test runs. A Type C run reverses the order of the addition used in Type B runs. It is run at the standard pH. The Type D runs combine the five metals in equal concentrations, 20 mg/l each for a total concentration of 100 mg/l metal. Runs of Type D are then handled identically to Type A runs.

For the cobalt study, Type B was the least effective method, although the residual free cyanide is low. It is assumed that the overall lower free cyanide concentration (cf. standard runs) reflects the absence or reduction of the hydrolysis reaction. Run Types A and C give comparable results in cobalt and cyanide residual concentrations but not iron. This could be attributed to the only partial oxidation of Fe(II) to Fe(III). For cobalt, and the other metals, there is general agreement in the percent residual metal between run Types A and D (see Table 37).

Copper, however, gave generally better results with Type B runs. Nickel and chromium gave generally better results with Type A runs. Studies using zinc gave the worst removals of the five metals. This was expected because of zinc's amphoteric character and the comparatively small stability constant of the zinc cyanide complex (See Table 30). Again the increased residual iron concentrations obtained from the A and C Type runs most likely reflect incomplete conversion of Fe(II) to Fe(III) during the stirring and foaming periods.

The residual concentrations of iron and cyanide in the mixed metal runs are lower than those obtained in the standard runs. The average 0.2 mg/l Fe residual is a 99.9% reduction. The average 1.5 mg/l CN residual is a 97% reduction.

Conclusions

The adsorbing colloid flotation of free cyanide by Fe(II)/Fe(III) results in roughly 92.2% removal of free cyanide, and 100% removal of iron/cyanide complex and 97.8 removal of iron after 60 min at a pH of 5.5. NLS was the surfactant used. Increased ionic strength reduces the percent removal of the complex and iron but decreases the presence of free cyanide after the initial increase. Removal of cyanide in the presence of heavy metals, other than iron, can be effected by the addition of Fe(III) to provide the adsorbing precipitate of Fe(OH)₃. The concentration of heavy metal is also reduced. Optimum removal conditions must be determined for each metal or combination.

TABLE 36. HEAVY METAL RUNS: AVERAGE RESIDUAL CONCENTRATIONS

Metal	Run Type	M, ppm	Fe, ppm	CN, ppm
Cobalt	A	70.2	0.4	0.08
	B	100	39.1	0.13
	C	68.6	30.3	0.07
	D	8.2	0.2	1.5
Copper	A	34.6	1.6	7.6
	B	29.2	0.4	0.06
	C	14.1	5.0	0.69
	D	4.9	0.2	1.5
Chromium	A	0.3	0.3	19.2
	B	100	100	7.4
	C	40.0	40.0	45.4
	D	0.1	0.1	1.5
Nickel	A	41.8	0.4	0.23
	B	38.7	N/A	0.23
	C	99.1	43.1	0.43
	D	8.7	0.2	1.5
Zinc	A	80.0	0.4	43.4
	B	91.0	33.8	10.4
	C	89.0	74.9	40.3
	D	15.0	0.2	1.5

Run Type A: $M + Fe^{+3}$; $[M] = 100$ ppm; $[Fe^{+3}] = 150$ ppm; $[CN] = 50$ ppm; pH 5.4-5.5

B: $Fe^{+2} + M$; $[Fe^{+2}] = 100$ ppm; $[M] = 100$ ppm; $[CN] = 50$ ppm; pH 4.7-4.8

C: $M + Fe^{+2}$; $[M] = 100$ ppm; $[Fe^{+2}] = 100$ ppm; $[CN] = 50$ ppm; pH 5.4-5.5

D: $M1 + M2 + M3 + M4 + M5 + Fe^{+3}$; $[M1]$ etc. = 20 ppm; $[Fe^{+3}] = 150$ ppm; $[CN] = 50$ ppm; pH 5.4-5.5

TABLE 37. PERCENT RESIDUAL METALS, RUN TYPES A & D

Run Type	Co	Cu	Cr	Ni	Zn
A	70.2	34.6	0.3	41.8	80.0
D	41.0	24.5	0.5	43.5	75.0

REFERENCES

1. Wilson, D. J., Foam Flotation Treatment of Heavy Metals and Fluoride-Bearing Wastewaters, Environmental Protection Agency EPA-600/2-77-072, U. S. Government Printing Office, Washington, D.C. (1977).
2. Hallowell, J. B., Shea, J. F., Smithson, G. R., Jr., Tripler, A. B., and Gonser, B. W., Water Pollution Control in the Primary Nonferrous-Metals Industry, Vols. 1 and 2, Environmental Protection Agency EPA-R2-73-247a, b, U. S. Government Printing Office, Washington, D.C. (1973).
3. Olsen, A. E., and Hauf, E. N., In-Process Pollution Abatement: Upgrading Metal Finishing Facilities to Reduce Pollution, EPA Technology Transfer Seminar Publ. No. 1 (1973).
4. Lancy, L. E., and Rice, R. L., Waste Treatment: Upgrading Metal-Finishing Facilities to Reduce Pollution, EPA Technology Transfer Seminar Publ. No. 2 (1973).
5. Clarke, A. N., and Wilson, D. J., Separation by Flotation, *Separ. Purif. Methods*, 7 55 (1978).
6. Lemlich, R., ed. Adsorptive Bubble Separation Techniques, Academic Press, New York (1972).
7. Somasundaran, P., Foam Separation Methods, *Separ. Purif. Methods*, 1 117 (1972).
8. Somasundaran, P., Separation Using Foaming Techniques, *Separat. Sci.*, 10, 93 (1975).
9. Grieves, R. B., Foam Separations: A Review, *Chem. Eng. J.*, 9, 93 (1975).
10. Ahmed, S. I., A Survey of the Laws of Foam Formation and Its Applications in Separation Processes, *Separat. Sci.*, 10, 649 (1975).
11. Bahr, A., and Hense, J., Flotation, *Fortschr. Verfahrenstech., Abt. F*, 14 503 (1976).
12. Panou, O., Flotation, *Rapp. Tech., Cent. Belge Etude Corros.*, 129 (RT. 234), 153 (1976).
13. Richmond, R., Some Fundamental Concepts in Flotation, *Chem. Ind. (London)*, 19, 792 (1977).

14. Balcerzak, W., Foaming Processes-Foam Utilization and Elimination, *Gaz, Woda Tech. Sanit.*, 51 (5), 131 (1977).
15. Ecklund L., and Anderson, C., Wastewater Purification by Flotation, *Ind.-Anz.*, 99 (49), 875 (1977).
16. Hyde, R. A., Miller, D. G., Packham, R. F., and Richards, W. N., Water Clarification by Flotation, *J. Am. Water Works Assoc.*, 69 (7), 369 (1977).
17. Marks, R. H., and Thurston, R. J., Application of Flotation to Industrial Effluent Treatment, *Environ. Pollut. Manage.*, 7 (4), 94 (1977).
18. Somasundaran, P., and Grieves, R. B., eds., "Advances in Interfacial Phenomena of Particulate/Solution/Gas Systems; Applications to Flotation Research," *AIChE Symp. Ser. No. 150, Vol. 71* (1975).
19. Goldberg, M., and Rubin, E., Foam Fractionation in a Stripping Column, *Separat. Sci.*, 7, 51 (1972).
20. Wang, L. K.-P., Granstrom, M. L. and Kown, B. T., Continuous Bubble Fractionation: Part I, Theoretical Considerations, *Environmental Letters*, 3, 251 (1972).
21. Ibid., Continuous Bubble Fractionation: Part II, Effects of Bubble Size and Gas Rate, *Environmental Letters*, 4, 233 (1973).
22. Ibid., Continuous Bubble Fractionation: Part III, Experimental Evaluation of Flow Parameters, *Environmental Letters*, 5, 71 (1973).
23. Goldberg, M., and Rubin, E., Foam Fractionation in a Stripping Column, *Separat. Sci.*, 7, 51 (1972).
24. Cannon, K. D., and Lemlich, R., A Theoretical Study of Bubble Fractionation, *AIChE Symposium Series 68* (124), *Water-1971*, 180 (1972).
25. Lee, S. J., Bubble Tower Performance in Concentrating Dilute Aqueous Surfactant Ph.D. Dissertation. Univ. of Tenn., 1969, *Diss. Abstr. Int. B.*, 31 (4), 1927 (1970).
26. Sastry, K. V. S. and Fuerstenau, D. W., Theoretical Analysis of a Counter-current Flotation Column *Trans. AIME*, 247, 46 (1970).
27. Wilson, J. W., Wilson, D. J., and Clarke, J. H., Electrical Aspects of Adsorbing Colloid Flotation. IV. Stripping Column Operation, *Separat. Sci.*, 11, 223 (1976).
28. Grieves, R. B., Ogbu, I. U., Bhattacharyya, D., and Conger, W. L., Foam Fractionation Rates. *Separat. Sci.*, 5, 583 (1970).
29. Petrakova, A. G., Golovanchikov, A. B., and Mamakov, A., Mechanism of Interaction of Gas Bubbles with Mineral Particles During Flotation and Electroflotation, *Chem. Abstr.*, 85, 16244a (1976).

30. Abramov, A. A., and Avdokhin, V. M., Physicochemical Modeling of Flotation Systems, Chem. Abstr., 87, 204644a (1977).
~~
31. Reay, D., and Ratcliff, G. A., Removal of Fine Particles from Water by Dispersed Air Flotation: Effects of Bubble Size and Particle Size on Collection Efficiency, Can. J. Chem. Eng., 51, 178 (1973).
~~
32. Scheludko, A., Toshev, B. V., and Bojadjev, D. T., Attachment of Particles to a Liquid Surface (Capillary Theory of Flotation), J. Chem. Soc., Faraday Trans. I, 72 (12), 2815 (1976).
~~
33. Deryagin, B. V., Rulev, N. N., and Dukhin, S. S., Effect of Particle Size on Heterocoagulation in an Elemental Flotation Act, Kolloidn. Zh., 39 (4), 680 (1977).
~~
34. Bleier, A., Goddard, E. D., and Kulkarni, R. D., Adsorption and Critical Flotation Conditions, J. Colloid Interface Sci., 59 (3), 490 (1977).
~~
35. Lai, R. W. M. and Fuerstenau, D. W., Model for the Surface Charge of Oxides and Flotation Response, Soc. of Min. Eng.-AIME, Trans., 260, 104 (1976).
~~~
36. Wilson, J. W., and Wilson, D. J., Electrical Aspects of Adsorbing Colloid Flotation, Separat. Sci., 9, 381 (1974).  
~
37. Huang, S.-D., and Wilson, D. J., Electrical Aspects of Adsorbing Colloid Flotation. II. Theory of Rate Effects, Separat. Sci., 10, 405 (1975).  
~~
38. Wilson, J. W., and Wilson, D. J., Electrical Aspects of Adsorbing Colloid Flotation. III. Excluded Volume Effects, Separat. Sci., 11, 89 (1976).  
~~
39. Wilson, D. J., Electrical Aspects of Adsorbing Colloid Flotation, V. Non-ideal Floes and Salts, Separat. Sci., 11, 391 (1976).  
~~
40. Wilson, D. J., Electrical Aspects of Adsorbing Colloid Flotation. VI. Electrical Repulsion between Floe Particles, Separat. Sci., 12, 231 (1977).  
~~
41. Wilson, D. J., Electrical Aspects of Adsorbing Flotation. VII. Cooperative Phenomena, Separat. Sci., 12, 447 (1977).  
~~
42. Clarke, A. N., Wilson, D. J., and Clarke, J. H., Electrical Aspects of Adsorbing Colloid Flotation. VIII. Specific Adsorption of Ions by Floes, Separat. Sci. Technol., 13, 573 (1978).  
~~
43. Fuerstenau, D. W., Healy, T. W., and Somasundaran, P., The Role of the Hydrocarbon Chain of Alkyl Collectors in Flotation, Trans. AIME, 229, 321 (1964).  
~~~
44. Gaudin, A. M., and Fuerstenau, D. W., Quartz Flotation with Cationic Collectors, Trans. AIME, 202, 958 (1955).
~~~
45. Somasundaran, P., and Fuerstenau, D. W., Mechanism of Alkyl Sulfonate Adsorption at the Alumina-Water Interface, J. Phys. Chem., 70, 90 (1966).  
~~

46. Wakamatsu, T., and Fuerstenau, E. W., Effect of Hydrocarbon Chain Length on the Adsorption of Sulfonates at the Solid-Water Interface, *Adv. Chem. Ser.*, 79, 161 (1968).  
~~
47. Somasundaran, P., and Fuerstenau, D. W., On Incipient Flotation Conditions *Trans. AIME*, 241, 102 (1968).  
~~~~
48. Somasundaran, P., The Relationship between Adsorption at Different Interfaces and Flotation Behavior, *Trans. AIME*, 241, 105 (1968).
~~~~
49. Somasundaran, P., Healy, T. W., and Fuerstenau, D. W., Surfactant Adsorption at the Solid-Liquid Interface-Dependence of Mechanism on Chain length *J. Phys. Chem.*, 68, 3562 (1964).  
~~
50. Fuerstenau, D. W., and Healy, T. W., Principles of Mineral Flotation, in *ref. 6*, p. 92.
51. Currin, B. L., Potter, F. J., Wilson, D. J., and French, R.H., Surfactant Recovery in Adsorbing Colloid Flotation, *Separat. Sci. Technol.*, 13, 285 (1978).  
~~
52. Wilson, D. J., A Non-Coulombic Model for Adsorbing Colloid Flotation, *Separat. Sci. Technol.*, 13, 107 (1978).  
~~
53. Ferguson, B., Hinkle, C., and Wilson, D. J., Foam Flotation of Lead and Cadmium in Industrial Wastes, *Separat. Sci.*, 9, 125 (1974).
54. Clarke, A. N., and Wilson, D. J., The Adsorbing Colloid Flotation of Fluoride Ion by Aluminum Hydroxide in Aqueous Media, *Separat. Sci.*, 10, 417 (1975).
55. Huang, S.-D., and Wilson, D. J., Foam Separation of Mercury (II) and Cadmium (II) from Aqueous Systems, *Separat. Sci.*, 11, 215, (1976).  
~~
56. Robertson, R. P., Wilson, D. J., and Wilson, C. S., The Adsorbing Colloid Flotation of Lead (II) and Zinc (II) by Hydroxides, *Separat. Sci.*, 11, 569, (1976).  
~~
57. Chatman, T. E., Huang, S.-D., and Wilson, D. J., Constant Surface Charge Model in Floc Foam Flotation. The Flotation of Copper (II), *Separat. Sci.*, 12, 461 (1977).  
~~
58. Zeitlin, H., and Kim, Y. S., Separation of Trace-Metal Ions from Seawater by Adsorptive Colloid Flotation, *J. Chem. Soc.D.(Chem. Comm.)*, 13, 672 (1971).  
~~
59. Kim, Y. S., and Zeitlin, H. The Separation of Zinc and Copper from Seawater by Adsorbing Colloid Flotation, *Separat. Sci.*, 7, 1 (1972).  
~~
60. Kim, Y. S., and Zeitlin, H. Thorium Hydroxide as a Collector for Molybdenum from Seawater, *Anal. Chim. Acta*, 51, 516 (1970).  
~~
61. Kim, Y. W., and Zeitlin, H., A Rapid Adsorbing Colloid Method for the Separation of Molybdenum from Seawater, *Separat. Sci.*, 6, 505 (1971).

62. Kim, Y. S., and Zeitlin, H., Separation of Uranium from Seawater by Adsorbing Colloid Flotation, *Anal. Chem.*, 43, 1390 (1971).
63. Leung, G., Kim, Y. S., and Zeitlin, H., An Improved Separation and Determination of Uranium in Seawater, *Anal. Chim. Acta*, 60, 229 (1972).
64. Voyce, D. and Zeitlin, H., The Separation of Mercury from Seawater by Adsorption Colloid Flotation and Analysis by Flameless Atomic Absorption, *Anal. Chim. Acta*, 69, 27 (1974).
65. Chaine, F. E., and Zeitlin, H., The Separation of Phosphate and Arsenate from Seawater by adsorption Colloid Flotation, *Separat. Sci.*, 9, 1 (1974).
66. Rothstein, N., and Zeitlin, H., The Separation of Silver from Seawater by Adsorption Colloid Flotation, *Anal. Lett.*, 9, (5), 461 (1976).
67. Hagadone, M., and Zeitlin, H., The Separation of Vanadium from Seawater by Adsorption Colloid Flotation, *Anal. Chim. Acta*, 86, 289 (1976).
68. Matsuzaki, C., and Zeitlin, H., The Separation of Collectors Used as Co-precipitants of Trace Elements in Seawater by Adsorbing Colloid Flotation, *Separat. Sci.*, 8, 185 (1973).
69. Zhorov, V. A., Barannik, V. P., Lyashenko, S. V., Kirchanova, A. I., and Kobylanskaya, A. G., Use of Adsorption Colloid Flotation for Separating Trace Elements from Seawater, *Chem. Abstr.*, 86, 143432d (1976).
70. Grigor'ev, Yu. O., Tyurin, N. G., Pushkarev, V. V., Pustovalov, N. N., and Perederii, O. G., Sorption of Arsenic Ions by Ferrous Sulfide, *Zh. Fiz. Khim.*, 50, 1004 (1976).
71. Bhattacharyya, D., Carlton, J. A., and Grieves, R. B., Precipitate Flotation of Chromium, *AIChEJ*, 17, 419 (1971).
72. Grieves, R. B., Schwartz, R. M., and Bhattacharyya, D., Precipitate Co-flotation of Calcium Sulfite and Calcium Carbonate: Application to Solids Removal from SO<sub>2</sub> Wet-Scrubbing Slurries *Separat. Sci.*, 10, 777 (1975).
73. Goldberg, M., and Rubin, E., Mechanical Foam Breaking, *Ind. Eng. Chem., Process Des. Develop.*, 6, 195 (1967).
74. Rubin, E., and Goly, M., Foam Breaking with a High Speed Rotating Disk, *Ind. Eng. Chem., Process Des. Develop.*, 9, 341 (1970).
75. Fuerstenau, M. C., ed., Flotation, A. M. Gaudin Memorial Volume, AIME, New York, 1976.
76. Fowler, R., and Guggenheim, E. A., Statistical Thermodynamics, Cambridge University Press, 1952, pp. 429-443.
77. Macdonald, J. R., and Brachman, M. K., Exact Solution of the Debye-Hückel Equations for a Polarized Electrode, *J. Chem. Phys.*, 22, 1314 (1954).

78. Patterson, J. W., Technical Inequities in Effluent Limitation Guidelines, JWPCF, 49 (7), 1586 (1977).  
~~
79. Patterson, J. W., Wastewater Treatment Technology, Ann Arbor Science Publishers Inc., Mich., 1975, ch. 9.
80. Bard, A. J., Chemical Equilibria, Harper and Row, New York, 1966.
81. Grieves, R. B., Ghosal, J. K., and Bhattacharyya, D., Foam Separation of Complexed Cyanide: Studies of Rate and Pulsed Addition of Surfactants, J. Appl. Chem. (London), 19, 115 (1969).  
~~
82. Grieves, R. B., Ghosal, J. K., and Bhattacharyya, D., Ion Flotation of Dichromate and of Complexed Cyanide: Surfactants for Qualitative Analysis, J. Amer. Oil Chem. Soc., 45, 591 (1968).  
~~
83. Grieves, R. B., and Bhattacharyya, D., "Ion, Colloid and Precipitate Flotation of Inorganic Anions," in ref. 6, p. 187.
84. Walkowiak, W., and Grieves, R. R., "Foam Fractionation of Cyanide Complex Anions of Zn(II), Cd(II), Hg(II), and Au(III), " J. Inorg. Nucl. Chem., 38, 1351 (1976).  
~~
85. Hill, T. L., Introduction to Statistical Thermodynamics, Addison-Wesley, Reading, Mass., 1960, pp. 130-132.
86. Adamson, A. W., A Textbook of Physical Chemistry, Academic Press, New York 1973, p. 25.
87. Walkowiak, W., and Rudnik, Z., "Selectivity Coefficients for  $\text{Ag}(\text{CN})_2^-$  and  $\text{Au}(\text{CN})_2^-$  from Continuous Foam Fractionation with a Quaternary Ammonium Surfactant," Separat. Sci. Technol., 13, 127 (1978).  
~~
88. Grieves, R. B., and Bhattacharyya, D., "Foam Separation of Cyanide Complexed by Iron," Separat. Sci., 3, 185 (1968).  
~
89. Emschwiller, G., and Legros, J., "Cinétique et Equilibre de Dissociation des Ferrocyanures en Solution Aqueuse," Compt. Rend., 241, 44 (1955).  
~~~
90. Legros, J., "Etudes Cinétiques sur l'Hydrolyse de quelques Complexes Cyanes du Fer Bivalent," J. Chim. Phys., 61, 909 (1964).
~~

APPENDIX A

DATA ON LEAD REMOVAL FROM WASTES AND SIMULATED
WASTES WITH THE 10-CM AND 30-CM COLUMNS

TABLE A-1. DATA ON LEAD REMOVAL FROM WASTES AND SIMULATED WASTES WITH THE 10-CM AND 30-CM COLUMNS

| Run No. | pH | Fe(III)
mg/ℓ | NLS
mg/ℓ | Air Flow
ℓ/min ^a | Influent Flow
Rate (gal/hr) ^b | Hydraulic
Loading
gal/min-ft ² | Effl.
Pb(II)
mg/ℓ | Comments |
|---------|-----|-----------------|-------------|--------------------------------|---|---|-------------------------|---------------|
| 93 | 5.9 | 150 | 40 | 4 | 10 | 1.9 | .05 | Foam very |
| | | | | | 15 | 2.9 | .10 | stable, but |
| | | | | | 12 | 2.3 | .10 | wet. Foamate |
| | | | | | 12 | 2.3 | .05 | volume ~6% of |
| | | | | | 12 | 2.3 | .05 | influent vol- |
| | | | | | 12 | 2.3 | <.05 | ume. |
| | | | | | 12 | 2.3 | .12 | |
| | | | | | 11 | 2.1 | .05 | |
| | | | | | 12.5 | 2.4 | .08 | |
| | | | | | 12.5 | 2.4 | .31 | Foam over- |
| | | | | | | | | turning |
| | | | | | 12.5 | 2.4 | .31 | Foam over- |
| | | | | | | | | turning |
| | 6.0 | 200 | 40 | 4 | 8 | 1.5 | .20 | Overturning |
| | | | | | 11 | 2.1 | .37 | occurred |
| | | | | | 11 | 2.1 | .24 | throughout |
| | | | | | 10.5 | 2.0 | .44 | most of the |
| | | | | 5 | 10 | 1.9 | .57 | run. One of |
| | | | | | 10 | 1.9 | .37 | the screen |
| | | | | | 10 | 1.9 | .47 | baffles was |
| | | | | | 10 | 1.9 | .47 | tilted |
| | | | | | | | | slightly |

(continued)

TABLE A-1. (continued)

| Run No. | pH | Fe(III)
mg/ℓ | NLS
mg/ℓ | Air Flow
ℓ/min ^a | Influent Flow
Rate (gal/hr) ^b | Hydraulic
Loading
gal/min-ft ² | Effl.
Pb(II)
mg/ℓ | Comments |
|-------------|-----|-----------------|-------------|--------------------------------|---|---|-------------------------|-----------------------------------|
| 3 | 6.1 | 150 | 35 | 3 | 8 | 1.5 | .10 | Some overturning in foam |
| | | | | 2 | 9 | 1.7 | .14 | |
| | | | | | 12 | 2.3 | .30 | |
| | | | | | 12 | 2.3 | .64 | |
| | | | | | 15 | 2.9 | .57 | |
| | | | | | 15 | 2.9 | 1.3 | |
| | | | | | 13 | 2.5 | 1.0 | |
| | | | | | 13 | 2.5 | .44 | |
| | | | | | 13 | 2.5 | .61 | |
| | | | | | 13 | 2.5 | .47 | |
| 4 | 6.0 | 150 | 35 | 1 | 7.5 | 1.4 | .10 | Severe over turning
Recovering |
| | | | | 1 | 9 | 1.7 | .13 | |
| | | | | 1.5 | 12.5 | 2.4 | 1.5 | |
| | | | | 1.5 | 12.5 | 2.4 | .96 | |
| | | | | | | | | |
| 5 | 6.4 | 150 | 35 | 2 | 5.5 | 1.0 | .05 | Beginning to turn |
| | | | | | 5.5 | 1.0 | .06 | |
| | | | | | 8 | 1.5 | .10 | |
| | | | | | 10 | 1.9 | .36 | |
| | | | | | 10 | 1.9 | .68 | |
| | | | | | 12 | 2.3 | .84 | |
| | | | | | 12 | 2.3 | 1.0 | |
| | | | | | | | | |
| 6 | 7.1 | 150 | 35 | 2 | 8.5 | 1.6 | .84 | No overturning evident |
| | | | | | 10.0 | 1.9 | 2.3 | |
| | | | | | 12.5 | 2.4 | 3.2 | |
| 7 | 5.8 | 150 | 35 | 2 | 5.5 | 1.0 | .08 | Slight over-
turning |
| | | | | | 10.5 | 2.0 | .17 | |
| | | | | | 12.5 | 2.4 | .32 | |
| | | | | | | | | |
| (continued) | | | | | 14.5 | 2.8 | .49 | |

TABLE A-1. (continued)

| Run No. | pH | Fe(III)
mg/l | NLS
mg/l | Air Flow
l/min ^a | Influent Flow
Rate (gal/hr) ^b | Hydraulic
Loading
gal/min-ft ² | Effl.
Pb(II)
mg/l | Comments |
|---------|----|-----------------|-------------|--------------------------------|---|---|-------------------------|--|
| 95 | 8 | 5.0 | 150 | 2 | 5.5 | 1.0 | .38 | Some overturning
Recovering |
| | | | | | 10.5 | 2.0 | .28 | |
| | | | | | 10.5 | 2.0 | .11 | |
| | | | | | 12.5 | 2.4 | .10 | |
| | | | | | 12.5 | 2.4 | .07 | |
| | | | | | 15 | 2.9 | .05 | |
| | | | | | 15 | 2.9 | .13 | |
| | 9 | 4.9 | 150 | 2 | 4 | 0.8 | .11 | Overturning
beginning |
| | | | | | 8 | 1.5 | .72 | |
| | | | | | 10.5 | 2.0 | .87 | |
| | | | | | 10.5 | 2.0 | 1.4 | |
| | | | | | 10.5 | 2.0 | 1.7 | |
| | 10 | 4.3 | 150 | 2 | 8 | 1.5 | 1.8 | Severe over-
turning
throughout
run |
| | | | | | 10.5 | 2.0 | 2.8 | |
| | | | | | 10.5 | 2.0 | 2.9 | |
| | | | | | 12.5 | 2.4 | 2.3 | |
| | | | | | 15 | 2.9 | 2.2 | |
| | | | | | 16.5 | 3.2 | 3.0 | |
| | | | | | 16 | 3.1 | 1.6 | |
| | | | | | 16 | 3.1 | 2.2 | |
| | 11 | 5.2 | 100 | 2 | 3 | 0.6 | .64 | Little or no
overturning
present |
| | | | | | 8.5 | 1.6 | .51 | |
| | | | | | 10.5 | 2.0 | .37 | |
| | | | | | 12.5 | 2.4 | .41 | |
| | | | | | 15 | 2.9 | .42 | |
| | | | | | 15 | 2.9 | .40 | |

(continued)

TABLE A-1. (continued)

| Run No. | pH | Fe(III)
mg/l | NLS
mg/l | Air Flow
l/min ^a | Influent Flow
Rate (gal/hr) ^b | Hydraulic
Loading
gal/min-ft ² | Effl.
Pb(II)
mg/l | Comments |
|---------|-----|-----------------|-------------|--------------------------------|---|---|-------------------------|---|
| 12 | 5.4 | 200 | 30 | 2 | 8.5 | 1.6 | .30 | Some overturning present |
| | | | | | 10.5 | 2.0 | .55 | |
| | | | | | 10.5 | 2.0 | .69 | |
| | | | | | 12.5 | 2.4 | .95 | |
| | | | | | 12.5 | 2.4 | .90 | |
| | | | | | 12.5 | 2.4 | .77 | |
| 13 | 5.8 | 100 | 35 | 2 | 8.5 | 1.6 | .45 | Very little overturning evident |
| | | | | | 10.5 | 2.0 | .15 | |
| | | | | | 10.5 | 2.0 | .34 | |
| | | | | | 12.5 | 2.4 | .45 | |
| | | | | | 12.5 | 2.4 | .56 | |
| | | | | | 16.5 | 3.2 | .81 | |
| 96 14 | 5.7 | 200 | 35 | 2 | 8.5 | 1.6 | .05 | Slight overturning |
| | | | | | 10 | 1.9 | .10 | |
| | | | | | 12.5 | 2.4 | .36 | |
| | | | | | 12.5 | 2.4 | .39 | |
| | | | | | 12.5 | 2.4 | .45 | |
| | | | | | | | | |
| 15 | 5.7 | 150 | 35 | 2 | 5 | .96 | .68 | 0.1 moles/l
NaNO ₃ added.
Very little overturning. |
| | | | | | 7 | 1.3 | .44 | |
| | | | | | 7 | 1.3 | .44 | |
| | | | | | 8.5 | 1.6 | .53 | |
| | | | | | 8.5 | 1.6 | .53 | |
| | | | | | 10.5 | 2.0 | .38 | |
| | | | | | 10.5 | 2.0 | .35 | |
| 16 | 5.8 | 150 | 35 | 3 | 5.5 | 1.0 | 1.1 | 0.2 moles/l
NaNO ₃ added. |
| | | | | | 7 | 1.3 | 1.8 | |
| | | | | | 8.5 | 1.6 | 2.1 | |
| | | | | | 8.5 | 1.6 | 3.2 | |
| | | | | | 8.5 | 1.6 | 2.9 | |

(continued)

TABLE A-1. (continued)

| Run No. | pH | Fe(III)
mg/l | NLS
mg/l | Air Flow
l/min ^a | Influent Flow
Rate (gal/hr) ^b | Hydraulic
Loading
gal/min-ft ² | Effl.
Pb(II)
mg/l | Comments |
|---------|-----|-----------------|-------------|--------------------------------|---|---|-------------------------|--------------------------|
| 17 | 5.8 | 150 | 35 | 2 | 7 | 1.3 | 1.0 | 0.3 moles/l |
| | | | | | 6.5 | 1.2 | 2.8 | NaNO ₃ added. |
| | | | | | 8.5 | 1.6 | 3.8 | |
| | | | | | 8.5 | 1.6 | 3.9 | |

^a2 l/min = 0.24 m³/min-m².

^b10 gal/hr = 1.9 gal/min-ft² = 112 m³/day-m².

TABLE A-2. DATA ON LEAD REMOVAL (SYNTHETIC WASTE) WITH THE 30-cm COLUMN

EXPERIMENTAL DATA FOR RUN 1

| Sample Number | pH | Fe(III)
(mg/l) | NLS
(mg/l) | Air Flow
Rate
(SCFH) | Hydraulic
Loading Rate
(gal/min-ft ²) | Influent
Flow Rate
(gal/min) | Ionic
Strength
(moles) | Waste
Pb(II)
Sample
(mg/l) | Effluent
Pb(II)
Sample
(mg/l) |
|---------------|-----|-------------------|---------------|----------------------------|---|------------------------------------|------------------------------|-------------------------------------|--|
| 1 | | | | | | | | 16.8 | |
| 2 | 4.4 | 70 | 70 | 50 | 3.47 | 2.5 | 0 | | 8.7 |
| 3 | 4.5 | 70 | 70 | 50 | 3.47 | 2.5 | 0 | | 7.6 |
| 4 | 5.0 | 70 | 70 | 50 | 3.47 | 2.5 | 0 | | 2.1 |
| 5 | 4.2 | 70 | 70 | 50 | 3.47 | 2.5 | 0 | | 7.1 |
| 6 | 4.0 | 70 | 70 | 50 | 3.47 | 2.5 | 0 | | 13.0 |
| 7 | 4.5 | 70 | 70 | 50 | 3.47 | 2.5 | 0 | | 6.3 |
| 8 | | | | | | | | 11.5 | |

EXPERIMENTAL DATA FOR RUN 2

| | | | | | | | | | |
|---|-----|----|----|----|------|-----|---|------|-----|
| 1 | | | | | | | | 16.9 | |
| 2 | 4.7 | 70 | 70 | 50 | 3.47 | 2.5 | 0 | | 5.2 |
| 3 | 5.0 | 70 | 70 | 50 | 3.47 | 2.5 | 0 | | 3.3 |
| 4 | 4.5 | 70 | 70 | 50 | 3.47 | 2.5 | 0 | | 8.5 |
| 5 | 4.4 | 70 | 70 | 50 | 3.47 | 2.5 | 0 | | 4.1 |
| 6 | 4.2 | 70 | 70 | 50 | 3.47 | 2.5 | 0 | | 7.2 |
| 7 | | | | | | | | 15.1 | |

(continued)

TABLE A-2. (continued)

EXPERIMENTAL DATA FOR RUN 3

| Sample
Number | pH | Fe(III)
(mg/l) | NLS
(mg/l) | Air Flow
Rate
(SCFH) | Hydraulic
Loading Rate
(gal/min-ft ²) | Influent
Flow Rate
(gal/min) | Ionic
Strength
(moles) | Waste
Pb(II)
Sample
(mg/l) | Effluent
Pb(II)
Sample
(mg/l) |
|------------------|-----|-------------------|---------------|----------------------------|---|------------------------------------|------------------------------|-------------------------------------|--|
| 1 | | | | | | | | 19.8 | |
| 2 | 5.9 | 70 | 70 | 60 | 2.77 | 2 | 0 | | 1.7 |
| 3 | 6.3 | 70 | 70 | 60 | 2.77 | 2 | 0 | | 1.7 |
| 4 | 6.2 | 70 | 70 | 60 | 2.77 | 2 | 0 | | 3.1 |
| 5 | 5.6 | 70 | 70 | 60 | 2.77 | 2 | 0 | | 3.7 |
| 6 | 5.0 | 70 | 70 | 60 | 2.77 | 2 | 0 | | 5.3 |
| 7 | 5.5 | 70 | 70 | 60 | 2.77 | 2 | 0 | | 3.6 |
| 8 | 5.8 | 70 | 70 | 60 | 2.77 | 2 | 0 | | 3.6 |
| 9 | | | | | | | | 16.9 | |

EXPERIMENTAL DATA FOR RUN 4

| | | | | | | | | | |
|---|-----|-----|----|----|------|---|---|------|-----|
| 1 | | | | | | | | 15.8 | |
| 2 | 7.0 | 100 | 40 | 60 | 2.77 | 2 | 0 | | 0.9 |
| 3 | 6.7 | 100 | 40 | 60 | 2.77 | 2 | 0 | | 1.1 |
| 4 | 6.6 | 100 | 40 | 60 | 2.77 | 2 | 0 | | 1.1 |
| 5 | 7.1 | 100 | 40 | 60 | 2.77 | 2 | 0 | | 0.7 |
| 6 | | | | | | | | 14.1 | |

(continued)

TABLE A-2. (continued)

EXPERIMENTAL DATA FOR RUN 5

| Sample Number | pH | Fe(III)
(mg/) | NLS
(mg/) | Air Flow
Rate
(SCFH) | Hydraulic
Loading Rate
(gal/min-ft ²) | Influent
Flow Rate
(gal/min) | Ionic
Strength
(moles) | Waste
Pb(II)
Sample
(mg/) | Effluent
Pb(II)
Sample
(mg/) |
|---------------|-----|-------------------|---------------|----------------------------|---|------------------------------------|------------------------------|-------------------------------------|--|
| 1 | | | | | | | | 18.5 | |
| 2 | 6.5 | 100 | 40 | 60 | 2.77 | 2 | 0 | | 0.6 |
| 3 | 6.9 | 100 | 40 | 60 | 2.77 | 2 | 0 | | 0.6 |
| 4 | 6.9 | 100 | 40 | 60 | 2.77 | 2 | 0 | | 0.6 |
| 5 | 7.0 | 100 | 40 | 60 | 2.77 | 2 | 0 | | 0.9 |
| 6 | 7.0 | 100 | 40 | 60 | 2.77 | 2 | 0 | | 0.8 |
| 7 | 7.2 | 100 | 40 | 60 | 2.77 | 2 | 0 | | 0.9 |
| 8 | | | | | | | | 15.4 | |

EXPERIMENTAL DATA FOR RUN 6

| | | | | | | | | | |
|---|-----|-----|----|----|------|---|---|----------------------|-----|
| 1 | | | | | | | | 19.7 | |
| 2 | 6.5 | 150 | 40 | 60 | 2.77 | 2 | 0 | | 1.5 |
| 3 | 6.5 | 150 | 40 | 60 | 2.77 | 2 | 0 | 19.7(mixing chamber) | |
| 4 | 6.7 | 150 | 40 | 60 | 2.77 | 2 | 0 | | 1.5 |
| 5 | 6.9 | 150 | 40 | 60 | 2.77 | 2 | 0 | | 1.6 |
| 6 | 5.6 | 150 | 40 | 60 | 2.77 | 2 | 0 | | 7.0 |
| 7 | | | | | | | | 19.2 | |

EXPERIMENTAL DATA FOR RUN 7

| | | | | | | | | | |
|---|-----|-----|----|-------|------|---|------|------|-----|
| 1 | | | | | | | | 19.0 | |
| 2 | 6.7 | 100 | 50 | 50-60 | 2.77 | 2 | 0.01 | | 0.5 |
| 3 | 7.3 | 100 | 50 | 50-60 | 2.77 | 2 | 0.01 | | 0.4 |

(continued)

TABLE A-2. (continued)

EXPERIMENTAL DATA FOR RUN 8

| Sample Number | pH | Fe(III)
(mg/l) | NLS
(mg/l) | Air Flow
Rate
(SCFH) | Hydraulic
Loading Rate
(gal/min-ft ²) | Influent
Flow Rate
(gal/min) | Ionic
Strength
(moles) | Waste
Pb(II)
Sample
(mg/l) | Effluent
Pb(II)
Sample
(mg/l) |
|---------------|-----|-------------------|---------------|----------------------------|---|------------------------------------|------------------------------|-------------------------------------|--|
| 1 | 7.2 | 100 | 50 | 40-50 | 2.77 | 2 | 0.05 | 20* | 2.6 |
| 2 | 6.7 | 100 | 50 | 40-50 | 2.77 | 2 | 0.05 | 20 | 2.4 |
| 3 | 6.4 | 100 | 50 | 40-50 | 2.77 | 2 | 0.10 | 20 | 6.1 |
| 4 | 6.2 | 100 | 50 | 40-50 | 2.77 | 2 | 0.10 | 20 | 12.8 |
| 5 | 7.2 | 100 | 50 | 40-50 | 2.77 | 2 | 0.10 | 20 | 11.0 |

EXPERIMENTAL DATA FOR RUN 9

| | | | | | | | | | |
|---|-----|-----|----|----|------|---|---|----|------|
| 1 | 6.5 | 100 | 50 | 40 | 2.77 | 2 | 0 | 20 | 1.14 |
| 2 | | | | | | | 0 | | |
| 3 | 6.8 | 100 | 50 | 40 | 2.77 | 2 | 0 | | 1.14 |
| 4 | 6.5 | 100 | 50 | 40 | 2.77 | 2 | 0 | | 1.14 |
| 5 | 6.3 | 100 | 50 | 40 | 2.77 | 2 | 0 | | 1.85 |
| 6 | 6.3 | 100 | 50 | 40 | 2.77 | 2 | 0 | | 3.00 |
| 7 | 6.5 | 100 | 50 | 40 | 2.77 | 2 | 0 | | 3.14 |

(continued)

TABLE A-2. (continued)

EXPERIMENTAL DATA FOR RUN 10

| Sample
Number | pH | Fe(III)
(mg/ℓ) | NLS
(mg/ℓ) | Air Flow
Rate
(SCFH) | Hydraulic
Loading Rate
(gal/min-ft ²) | Influent
Flow Rate
(gal/min) | Ionic
Strength
(moles) | Waste
Pb(II)
Sample
(mg/ℓ) | Effluent
Pb(II)
Sample
(mg/ℓ) |
|------------------|-----|-------------------|---------------|----------------------------|---|------------------------------------|------------------------------|-------------------------------------|--|
| 1 | | | | | | | 0.01 | 10 | |
| 2 | 6.6 | 100 | 50 | 40 | 2.77 | 2 | 0.01 | | 0.86 |
| 3 | 6.4 | 100 | 50 | 40 | 2.77 | 2.5 | 0.01 | | 1.57 |
| 4 | 6.5 | 100 | 50 | 40 | 2.77 | 2 | 0.05 | | 2.29 |
| 5 | 6.3 | 100 | 50 | 40 | 2.77 | 2.5 | 0.05 | | 1.86 |
| 6 | 6.4 | 100 | 50 | 40 | 2.77 | 2 | 0.05 | | 2.43 |
| 7 | 6.5 | 100 | 50 | 40 | 2.77 | 2 | 0.07 | | 2.57 |
| 8 | 6.7 | 100 | 50 | 40 | 2.77 | 2 | 0.07 | | 3.14 |
| 9 | 6.7 | 100 | 50 | 40 | 2.77 | 2 | 0.07 | | 3.29 |

TABLE A-3. DATA ON ZINC REMOVAL (PLATING WASTE) WITH THE 30-cm COLUMN

EXPERIMENTAL DATA FOR RUNS 1, 2 and 3

| Description
of sample | pH | Influent Flow
Rate, GPM | Air Flow Rate
(SCFH) | NLS
(mg/l) | Fe(III)
(mg/l) | Zn
(mg/l) | Cu
(mg/l) |
|--------------------------|------|----------------------------|-------------------------|---------------|-------------------|--------------|--------------|
| Raw waste, run 1 | 8.8 | - | - | - | - | 114 | 1.2 |
| After liming | 11.4 | - | - | - | - | 6 | 0(<.01) |
| Column effluent | 11.3 | 2.5 | 40 | 0 | 80 | .7 | 0 |
| " | 11.3 | 2.5 | 40 | 0 | 80 | .7 | 0 |
| " | 11.3 | 2.5 | 40 | 0 | 80 | 2 | 0 |
| Raw waste, run 2 | 1.9 | - | - | - | - | 420 | 32 |
| After liming | 11.4 | - | - | - | - | 7.4 | 0 |
| Column effluent | 11.3 | 2.0 | 40 | 33 | 67 | 7.4 | 0 |
| " | 11.2 | 2.0 | 40 | 33 | 67 | 5.6 | 0 |
| Raw waste, run 3 | 10.3 | - | - | - | - | 134 | 3.3 |
| After liming | 11.3 | - | - | - | - | 15 | .10 |
| Column effluent | 11.3 | 2.5 | 40 | 0 | 100 | 7 | 0 |
| " | 11.3 | 2.5 | 40 | 0 | 100 | 8 | 0 |
| " | 11.3 | 2.5 | 40 | 0 | 100 | 5 | 0 |
| " | 11.3 | 2.5 | 40 | 0 | 100 | 6 | 0 |
| " | 11.3 | 2.5 | 40 | 0 | 100 | 8 | 0 |
| " | 11.3 | 2.5 | 40 | 0 | 100 | 9 | 0 |

(continued)

TABLE A-3. (continued)

EXPERIMENTAL DATA FOR RUNS 4, 5, AND 6

| Description of sample | pH | Influent Flow Rate, GPM | Air Flow Rate (SCFH) | NLS (mg/ℓ) | Fe(III) (mg/ℓ) | Zn (mg/ℓ) | Cu (mg/ℓ) |
|--|------|-------------------------|----------------------|------------|----------------|-----------|-----------|
| Raw waste, run 4 | 2.7 | - | - | - | - | 320 | 14 |
| After liming | 11.4 | - | - | - | - | 14 | .3 |
| " | 11.4 | - | - | - | - | 18 | .2 |
| Column effluent | 11.3 | 2.0 | 40 | 33 | 67 | 11 | 0 |
| " | 11.3 | 2.0 | 40 | 33 | 67 | 6 | 0 |
| " | 11.3 | 2.0 | 40 | 0 | 80 | 10 | 0 |
| " | 11.3 | 2.0 | 40 | 0 | 80 | 11 | 0 |
| Raw waste, run 5 | 6.5 | - | - | - | - | 214 | .4 |
| After liming | 11.2 | - | - | - | - | 19 | 0 |
| Column effluent | 11.2 | 2.5 | 40 | 0 | 80 | 13 | 0 |
| " | 11.2 | 1.5 | decreasing | 0 | 110 | 12 | 0 |
| " | 11.2 | 2.0 | to | 0 | 100 | 12 | 0 |
| " | 11.2 | 2.0 | | 0 | 100 | 14 | - |
| " | 11.2 | 2.0 | 18 | 0 | 100 | 14 | - |
| Raw waste, run 6 | 9.4 | - | - | - | - | .8 | 0 |
| After liming | 11.4 | - | - | - | - | <.2 | 0 |
| Column effluent (poor floc separation) | 11.3 | 1.5 | 25 | 33 | 67 | <.2 | 0 |

(continued)

TABLE A-3. (continued)

EXPERIMENTAL DATA FOR RUNS 7 AND 8

| Description of sample | pH | Influent Flow Rate, GPM | Air Flow Rate (SCFH) | NLS (mg/l) | Fe(III) (mg/l) | Zn (mg/l) | Cu (mg/l) |
|-----------------------|------|-------------------------|----------------------|------------|----------------|-----------|-----------|
| Raw waste, run 7 | 8.8 | - | - | - | - | 15 | .8 |
| After liming | 11.3 | - | - | - | - | 4.3 | 0 |
| Column effluent | 11.3 | 2.0 | 45 | 50 | 100 | .3 | 0 |
| " | 11.3 | 2.0 | 45 | 0 | 100 | .3 | 0 |
| " | 11.2 | 2.0 | 45 | 0 | 66 | .3 | 0 |
| Raw waste, run 8 | 9.0 | - | - | - | - | 21 | .8 |
| After liming | 11.2 | - | - | - | - | 3.2 | 0 |
| Column effluent | 11.2 | 2.0 | 54 | 0 | 80 | .2 | 0 |
| " | 11.2 | 2.0 | 54 | 0 | 80 | .2 | 0 |
| " | 11.2 | 2.0 | 54 | 0 | 80 | .2 | 0 |
| " | 11.2 | 2.0 | 54 | 0 | 80 | .2 | 0 |
| " | 11.2 | 2.0 | 54 | 0 | 80 | .2 | 0 |
| " | 11.2 | 2.0 | 54 | 0 | 80 | .2 | 0 |
| " | 11.2 | 2.0 | 54 | 0 | 80 | .2 | 0 |
| " | 11.2 | 2.0 | 54 | 0 | 80 | .2 | 0 |

APPENDIX B

ADSORPTION ISOTHERMS

In our previous report (1) and other papers, (27,36-40,42) we examined a Gouy-Chapman type model for the binding of a floc particle to an air-water interface. Fuerstenau, Somasundaran, and others have used an alternate model to describe ore flotation (43-50), and it adequately describes quite a number of observed effects. In their model the ionic heads of the surfactant ions adsorb into the primary layer of the solid particle; the hydrocarbon chains of the surfactant ion then present a hydrophobic surface to the solution. This results in changes in the surface free energies; if these result in non-zero bubble contact angles on the solid, bubbles attach and flotation occurs.

We here examine first, the adsorption isotherms of particles to air-water interfaces resulting from finite contact angles (52), and second, the adsorption isotherms of surfactant on the surfaces of the solid particles (41).

1. Particle Adsorption Isotherms

Let the binding energy between a floc particle and the air-water interface be due only to differences in the surface free energies γ_{aw} (air-water), γ_{as} (air-solid) and γ_{sw} (solid-water). We approximate our floc particles as spheres, and assume that floc particle-bubble attachment is as shown in Figure 27. We assume that the air bubble is much larger than the floc particle.

Let θ be the contact angle of the air-water, air-solid, and solid-water interfaces (see Figure 27), and r be the floc particle radius. As the particle attaches, the loss in air-water interface is given by

$$L_{aw} = \pi r^2 \sin^2 \theta \quad (B-1)$$

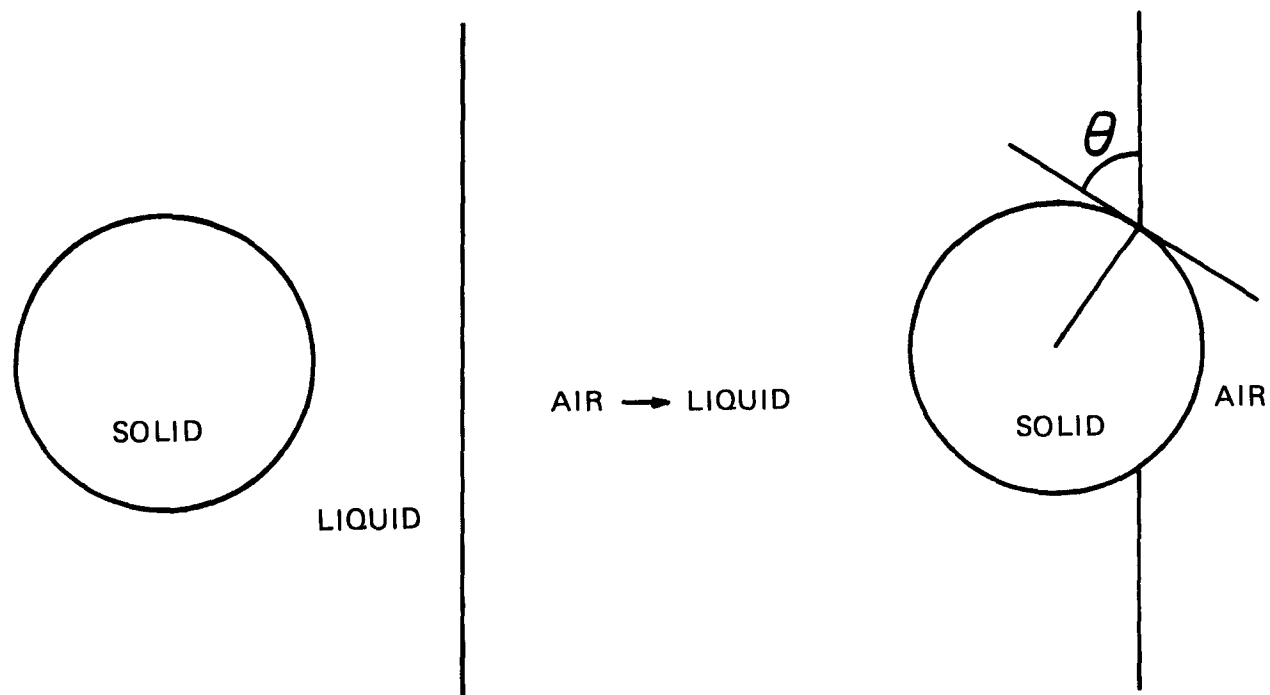


FIGURE B-1 - MODEL OF FLOC-BUBBLE ATTACHMENT

The loss in solid-water interface (and the gain in air-solid interface) is given by

$$L_{sw} = 2\pi r^2(1 - \cos\theta) \quad (B-2)$$

The free energy of attachment is therefore

$$\Delta G = -\gamma_{aw}\pi r^2 \sin^2\theta + (\gamma_{as} - \gamma_{sw})2\pi r^2(1 - \cos\theta) \quad (B-3)$$

The contact angle is given by

$$\cos\theta = (\gamma_{as} - \gamma_{sw})/\gamma_{aw} \quad (B-4)$$

at equilibrium, so that Eq. (B-3) can be written as

$$\Delta G = -\gamma_{aw}\pi r^2(1 - \cos\theta)^2 \quad (B-5)$$

We next determine the adsorption isotherm of the floc particles on the air-water surface by use of the grand partition function; we follow Hill (85). Consider an area of the air-water interface capable of accommodating one particle, $6r^2/\sqrt{3}$, and a column of liquid based on this area and capable of containing a maximum of m floc particles. This constitutes a site, which contains m cells; we take the sites to be independent of each other.

The grand partition function for a site is then given by

$$\xi = \prod_{i=1}^m \{1 + q\lambda \exp[-\beta V_i]\} \quad (B-6)$$

where q = partition function for the internal degrees of freedom of a floc particle, assumed independent of the cell in which the particle is located

λ = absolute activity of the floc particles, $\exp(\mu/kT)$, where μ is the chemical potential of a floc particle

$\beta = 1/kT$

V_i = potential energy of a floc particle in cell i .

$V_1 = \Delta G$, given by Eq. (B-5);

$V_i = 0$, $i > 1$.

The average number of floc particles per site is then given by

$$\bar{s} = \frac{\sum_{i=1}^m \lambda q \exp(\beta V_i)}{\sum_{i=1}^m 1 + \lambda q \exp(-\beta V_i)} \quad (B-7)$$

$$= \frac{\lambda q \exp(-\beta \Delta G)}{1 + \lambda q \exp(-\beta \Delta G)} + \frac{(m-1)\lambda q}{1 + \lambda q} \quad (B-8)$$

In the absence of the interface,

$$\bar{s} = m\sigma = \frac{m\lambda q}{1 + \lambda q} \quad (B-9)$$

which we obtain from Eq. (B-8) by setting $\Delta G = 0$. Here σ is the average number of floc particles per cell in the bulk solution. Eq. (B-9) yields

$$\lambda q = \sigma / (1 - \sigma) \quad (B-10)$$

and using this in Eq. (B-8) yields

$$\bar{s} = \frac{1}{1 + \frac{1-\sigma}{\sigma} \exp(\beta \Delta G)} + (m-1)\sigma \quad (B-11)$$

The surface excess of floc particles in the site is given by

$$\bar{s}_{\text{excess}} = \bar{s} - m\sigma \quad (B-12)$$

which is given by

$$\bar{s}_{\text{excess}} = \frac{\sigma(1-\sigma)[1 - \exp(\beta \Delta G)]}{\sigma + (1-\sigma)\exp(\beta \Delta G)} \quad (B-13)$$

Generally, as we shall see, $\exp(\beta \Delta G) \ll 1$, so Eq. (B-13) can be well approximated by

$$\bar{s}_{\text{excess}} = \frac{1}{1 + \exp(\beta \Delta G)/\sigma} \quad (B-14)$$

The basal area of a site is $2\sqrt{3}r^2$ (on assuming hexagonal close-packing in the planer, and the volume of a cell is given by

$$V = 4\sqrt{3}r^3 \quad (B-15)$$

The concentration of floc particles in the bulk solution, c_b , is therefore related to σ by

$$4\sqrt{3}r^3 c_b = \sigma \quad (B-16)$$

and the excess surface concentration in particles/cm², c_s , is related to \bar{s}_{excess} by

$$c_s = \bar{s}_{\text{excess}} / (2\sqrt{3}r^2) \quad (B-17)$$

From Eqs. (B-13) and (B-16) we may readily show that the bulk floc particle concentration at which the surface is half saturated ($\bar{s}_{\text{excess}} = \frac{1}{2}$) is given by

$$\begin{aligned} c_b' &= [1 - (1 - \frac{8\exp(\beta \Delta G)}{1 - \exp(\beta \Delta G)})^{\frac{1}{2}}] / 16\sqrt{3}r^3 \\ &\approx \exp(\beta \Delta G) / (4\sqrt{3}r^3) \end{aligned} \quad (B-18)$$

We next examine the sizes of the floc particle-bubble energies for representative values of the parameters. We set $\lambda_{aw} = 40$ dynes/cm, corresponding to the surface tension of NLS solutions at roughly the critical micelle concentration. We assume floc particles 200 nm in diameter. The floc-bubble binding energy as a function of contact angle is then given in Table B-1.

TABLE B-1. FLOC-BUBBLE BINDING ENERGY AS A FUNCTION OF CONTACT ANGLE^a

| $\cos\theta$ | $-\Delta G(\text{erg}) \times 10^{10}$ |
|--------------|--|
| 1.0 | 0 |
| 0.9 | 1.257 |
| 0.8 | 5.027 |
| 0.6 | 20.11 |
| 0.4 | 45.24 |
| 0.2 | 80.42 |
| 0 | 125.66 |
| -1.0 | 502.64 |

$$^a kT = 4.14 \times 10^{-14} \text{erg at } 25^\circ\text{C}$$

Even for these rather small particles the floc-bubble binding energy is roughly a thousand times larger than kT ; $|\Delta G|$ remains much larger than kT for contact angles of any appreciable size for particles of 20 nm diameter. Floc-bubble attachment is evidently an interaction which overwhelms the effects of random thermal motions unless the contact angle is essentially zero, so floc foam flotation should be an extremely efficient process as long as the floc is hydrophobic. This requires that the surfactant concentration and the floc surface potential be such that the surfactant can form a condensed surface phase (hemimicelle) with the hydrophobic hydrocarbon chains of the surfactant presented to the liquid phase; conditions for this to occur are explored later in this Appendix.

Estimation of contact angles in this model is likely to be difficult. The flocs of interest are often hydrous oxides, extensively and probably irreproducibly hydrated, and their characteristics are surely changing with time. Contact angle measurements on well-characterized crystalline materials can be no more than a rough guide in estimating contact angles on these fresh, unaged flocs.

We have also examined in detail an alternative model, in which small bubbles interact with plane solid surfaces (corresponding to large particles). The analysis, presented elsewhere (52) is slightly more tedious, and yields conclusions basically similar to those of the model treated above. The particle-bubble binding energy is orders of magnitude larger than kT for bubbles of diameter 20 nm or greater. Thus, with either of the two models, the binding energy is ample to produce efficient separations, despite random thermal forces.

In stripping columns there is a countercurrent flow of liquid downward between rising air-water interfaces. We will next demonstrate that the

viscous drag forces resulting from this countercurrent flow are insufficient to tear loose floc particles bound to the air-water interface (52).

We equate the gravitational pull down on an element of liquid $l \text{ cm} \times l \text{ cm} \times$ thickness dx to the viscous drag in the opposite direction to obtain

$$\rho g = -\eta d^2 v / dx^2 \quad (\text{B-19})$$

where ρ = liquid density

g = gravitational constant

η = viscosity

$v(x)$ = velocity of the liquid in the downward direction a distance x from one side of a vertically oriented lamella.

Integration of Eq. (B-19) and use of the boundary conditions $v(0) = v(l) = 0$ yields

$$v = \frac{\rho g}{2\eta} (\ell x - x^2) \quad (\text{B-20})$$

where ℓ is the thickness of the lamella.

We estimate the viscous drag force on the floc particle by assuming that the spherical particle is attached to the air-water interface and is moving with it, and that the relative velocity of the liquid streaming past it is given by $v(x)$. We let the particle radius be r and estimate an upper limit to the viscous drag on the particle

$$v(x = 2r) = \frac{\rho g}{2\eta} (2\ell r - 4r^2) \quad (\text{B-21})$$

$$\text{Viscous force} = f_v = 6\pi\eta r v \quad (\text{B-22})$$

$$f_v = 6\pi\rho g r^2 (\ell - 2r) \quad (\text{B-23})$$

If the diameter of our particle is 200 nm and the film thickness is 10^{-2} cm, the viscous force is 1.84×10^{-8} dynes. We roughly estimate the binding force of the floc particle to the air-water interface as

$$f_b = \frac{\Delta G}{r} \approx \frac{10^{-10} \text{ erg}}{10^{-5} \text{ cm}} > 10^{-5} \text{ dynes} \quad (\text{B-24})$$

at least three order of magnitude greater than the viscous drag. The binding force increases proportional to r , while the viscous force increases roughly proportional to r^2 , so viscous drag may impede floc foam flotation when particle radii are of the order of 10^{-2} cm or larger, or if the foams are extremely wet (large ℓ).

We have presented elsewhere (51) a discussion of the viscous drag forces on floc particles attached to spherical bubbles rising in liquid in batch foam flotation work.

2. Surfactant Adsorption Isotherms

We here examine a model for the formation of hydrophobic surfaces on floc particles by adsorption of the surfactant ionic heads directly into the primary layer on the surface of the floc (41). The hydrocarbon chain tails of these surfactant ions then, at sufficiently high surface concentration, form a hydrophobic surface. Surface free energies are thereby changed such that non-zero contact angles of air bubbles on the solid surface occur, and flotation takes place.

Of particular interest is the formation of a condensed surface phase of surfactant (a hemimicelle) on the floc particle surface at sufficiently high surfactant concentrations in the bulk solution. This cooperative phenomenon results from the Van der Waals stabilization energy of the surfactant hydrocarbon chains when they are able to pack closely together; and Fuerstenau, et al. (50) have showed experimentally that, as one would expect, it occurs at lower surfactant concentrations as surfactant chain length increases. This cooperative phenomenon accounts for the abrupt and large increase of flotation efficiency which is observed with increasing surfactant concentration at intermediate surfactant concentrations. The competition of non-surfactant ions with surfactant ions for space in the primary layer accounts for the effects of varying ion identities and ionic strength, as discussed in Appendix C.

We calculate the adsorption isotherm of surfactant on the solid by means of an approximate method described by Fowler and Guggenheim (76); exact treatments of even quite simple two-dimensional cooperative phenomena are extremely complex and difficult. The binding energy of an isolated surfactant ion to the solid is calculated by calculating the electric potential in the vicinity of the solid surface by means of a modified Poisson-Boltzmann equation. Fuerstenau and Healy (50) estimate the free energy of removal of hydrocarbon chains from water as approximately -0.6 kcal/mole of CH₂ groups; this information is needed in connection with the surface condensation phenomenon.

We take as our starting point the following adsorption isotherm, the derivation of which is given in Fowler and Guggenheim's book (76).

$$c(\theta) = \frac{c^0 \theta}{1 - \theta} \left(\frac{2 - 2\theta}{\beta + 1 - 2\theta} \right)^z \quad (\text{B-25})$$

$$\beta = [1 - 4\theta(1 - \theta) \{1 - \exp(-2w/zkT)\}]^{1/2} \quad (\text{B-26})$$

$$c^0 = \left(\frac{2\pi mkT}{h^2} \right)^{3/2} kT \frac{j^S(T)}{j^A(T)} \exp(-\chi_0/kT) \quad (\text{B-27})$$

Here

θ = fraction of surface sites on the solid which are occupied by surfactant ions
 $c(\theta)$ = concentration of surfactant in bulk solution in equilibrium

with solid surface having a fraction θ of its sites occupied by surfactant

z = maximum number of nearest neighbors of a surfactant ion on the surface, taken here as six

$2w/z$ = increase in energy when a new pair of nearest neighbors is formed

χ_0 = increase in energy when a surfactant ion is adsorbed on an isolated site on the solid surface

m = mass of surfactant ion

k = Boltzmann's constant

h = Planck's constant

T = absolute temperature

$j^S(T)$ = partition function for the internal degrees of freedom of a surfactant ion in solution

$j^A(T)$ = partition function for the internal degrees of freedom of an adsorbed surfactant ion

Assume that j^S/j^A is essentially independent of the inert salt concentration, and that χ_0 can be calculated by multiplying the charge on an adsorbed surfactant ion by the electric potential at that point. We write $c^0 = c' \exp(-\chi_0/kT)$, where c' is assumed to be independent of ionic strength and no more than weakly temperature-dependent. For dodecyl sulfate at room temperature, $c' \approx 2.85 \times 10^{-4}$ mole/l. We define a reduced concentration, σ , as

$$\sigma(\theta) = \frac{c(\theta)}{c'} = \exp(-\chi_0/kT) \frac{\theta}{1-\theta} \left(\frac{2-2\theta}{\beta+1-2\theta} \right)^z \quad (B-28)$$

As noted above, the free energy for the removal of hydrocarbon chains from water has been estimated as -0.6 kcal/mole of CH_2 groups. This yields Eq. (B-29) for w , where n is the number of CH_2 groups in the surfactant tail plus 1. We note that roughly six new pairs of nearest neighbors are formed when a surfactant ion goes into the condensed surface phase.

$$w = -n \times 2.070 \times 10^{-14} \text{ ergs} \quad (B-29)$$

We previously showed (39) how the method of Macdonald and Brachman (77) could be used to calculate electric potentials in the electric double layer for solutions in which the finite volume of the electrolyte ions was taken into account. The Poisson-Boltzmann equation for the case of planar geometry is

$$\frac{d^2\psi(x)}{dx^2} = \frac{A \sinh(z'e\psi/kT)}{1 + \beta \cosh(z'e\psi/kT)} \quad (B-30)$$

where $\psi(x)$ = electric potential a distance x from the solid-liquid interface
 $|z'e|$ = magnitude of the charge of the ions of $z'-z'$ electrolyte

$$A = \frac{8\pi z'e c_\infty}{(1 - 2 c_\infty/c_{\max}) D}$$

$$B = 2 c_\infty / (c_{\max} - 2 c_\infty)$$

c_{∞} = anion (or cation) concentration in bulk solution, ions per cm^3
 c_{max} = maximum possible concentration of ions in solution, ions per cm^3
 D = dielectric constant

The solution to Eq. (B-30) is given by

$$x = \frac{-\psi_0}{\psi_0} \int_{\psi_0}^{\psi(x)} \frac{d\psi}{\left\{ \frac{2AkT}{Bz'e} \log \left[\frac{1 + B \cosh z'e\psi/kT}{1 + B} \right] \right\}^{1/2}} \quad (\text{B-31})$$

where ψ_0 is the potential at the solid-liquid interface. We assume that the center of charge of the surfactant ion is at a distance ℓ from the charged floc surface; $\psi(\ell)$ is then obtained from Eq. (B-31). The binding energy of an isolated surfactant ion on the solid surface is given by

$$\chi_0 = z_s e \psi(\ell), \quad (\text{B-32})$$

where $z_s e$ is the charge of the surfactant ion. (This estimate neglects the contribution of the ionic atmosphere of the surfactant ions.)

The isotherms obtained from Eq. (B-25) exhibit a critical temperature given by (76)

$$T_c = -w/kz \log(z/z-2) \quad (\text{B-33})$$

Below this temperature, values of θ in the vicinity of one-half are unstable, and the system breaks up into two stable phases. It has been shown (76) that the values of θ for the phases are the two roots of the equation

$$o(\frac{1}{2}) \equiv \exp[(w-\chi_0)/kT] = \exp(-\chi_0/kT) \cdot \frac{\theta}{1-\theta} \cdot \left(\frac{2-2\theta}{\beta(\theta) + 1-2\theta} \right)^z \quad (\text{B-34})$$

other than $\theta = \frac{1}{2}$. Thus, if on calculating $\sigma(\theta)$ we find $\sigma(\theta) > \sigma(\frac{1}{2})$ for $\theta < \frac{1}{2}$, we set $\sigma(\theta) = \sigma(\frac{1}{2})$; if $\sigma(\theta) < \sigma(\frac{1}{2})$, $\theta > \frac{1}{2}$, we set $\sigma(\theta) = \sigma(\frac{1}{2})$. The situation is essentially identical to that arising with Van der Waals isotherms for nonideal gases below the critical temperature (86).

Results

Some representative adsorption isotherms are shown in Fig. B-2 which exhibits the effects of varying w , the surfactant-surfactant interaction energy. The values of w used here are somewhat smaller than would be used, say, for sodium lauryl sulfate (2.48×10^{-14} erg) in order to make the features of the plots clearer. The reduced concentration at which hemimicelle formation occurs, σ_{crit} , is seen to decrease rather rapidly with increasing values of w (and of the hydrocarbon chain length), as noted by Fuerstenau and co-workers (50), and the critical temperature increases, as indicated by Eq. (B-33).

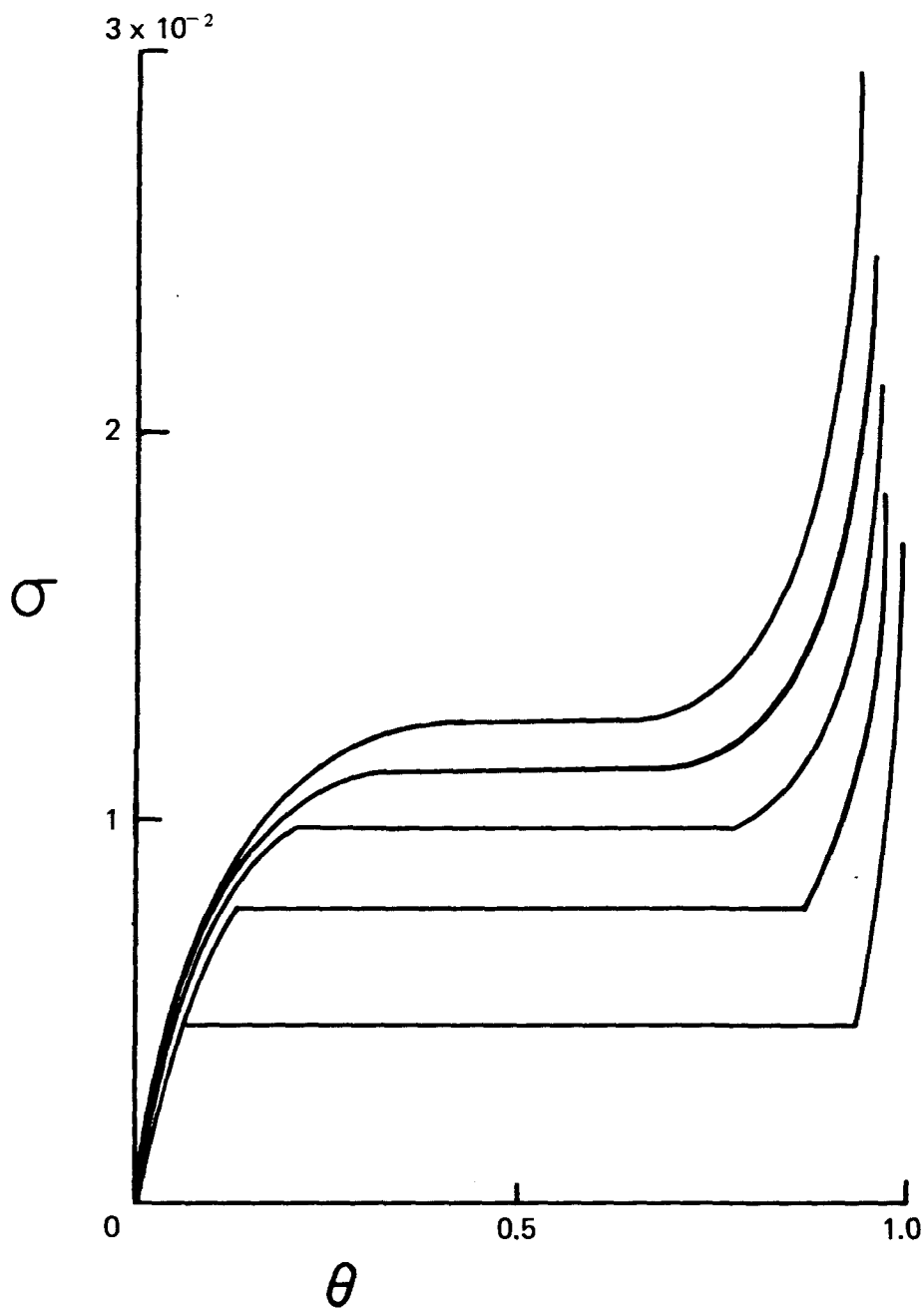


FIGURE B-2 - ADSORPTION ISOTHERMS OF SURFACTANT ON FLOC WITH CONDENSATION. FOR ALL PLOTS $T = 298^{\circ}\text{K}$, $\chi_0 = 8.0 \times 10^{-14}$ erg. FROM THE TOP DOWN: - $w = 1.0, 1.04, 1.1, 1.2,$ and 1.4×10^{-13} erg.

The dependence of σ_{crit} on w is indicated over a much wider range of w in Fig. -3. On noting that $\sigma_{\text{crit}} = \sigma(\frac{1}{2})$ and using Eqs. (B-29) and (B-34), we obtain

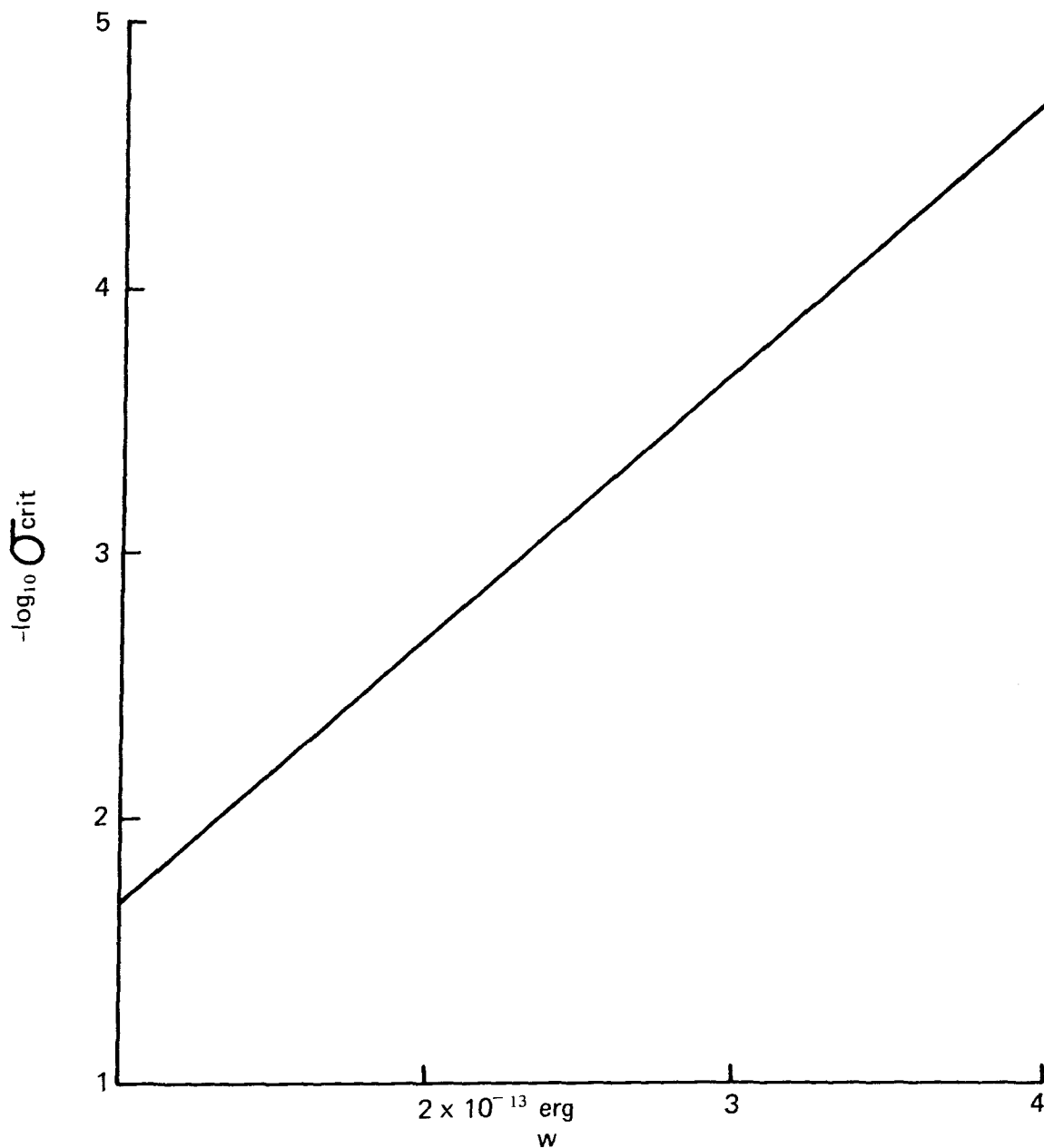


FIGURE B-3 - DEPENDENCE OF σ_{crit} on w . $\psi_0 = 50 \text{ mV}$, $T = 320^\circ\text{K}$,
 $l = 10^{-7} \text{ cm}$, $c_\infty = 10^{-3} \text{ mole/l}$, $z_s = -1$, $c_{\text{max}} = 1.0 \text{ mole/l}$.

$$\frac{-\partial \log \sigma_{\text{crit}}}{\partial n} = \frac{1}{kT} \times 2.070 \times 10^{-14}$$

$$\frac{-\partial \log_{10} \sigma_{\text{crit}}}{\partial n} = 65.2/T = 0.2919 \quad (\text{B-35})$$

at 298°K. The value of this derivative, which we obtain from the results of Fuerstenau, Somasundaran, and his co-workers (50), is approximately 0.32. Increasing the magnitude of the interaction energy of the hydrocarbon chains from 0.6 to 0.88 kcal/mole of CH₂ groups eliminates the discrepancy; in view of uncertainty in the figure of 0.6 and the approximations inherent in the theory, the agreement is better than one might expect.

The effects of surface potential ψ_0 on the value of σ_{crit} are shown in Fig. B-4, and the dramatic decrease in σ_{crit} with increasing surface potential is what one would intuitively anticipate. Ionic strength also exhibits a marked effect upon σ_{crit} as shown in Fig. B-5, as is well established experimentally. We note that our analysis here is predicated upon the assumption that the concentration of surfactant in the bulk solution is at all times sufficiently low that the surfactant is an ideal solute; in particular, we have ignored the possibility of micelle formation in the bulk solution. This surely leads to spurious results at the upper end of the curve in Fig. B-4, where one would expect σ_{crit} to be a very rapidly increasing function of $\log_{10} c_\infty$. The binding energy of the surfactant to the solid, χ_0 , is reduced to values less than kT with increasing c_∞ , and the formation of micelles then should become competitive with the formation of hemimicelles on the solid surface. At this point, between roughly $c_\infty = 0.1$ and 1.0 in Fig. B-5, foam flotation should cease.

Experimentally, we did observe that foam flotation is less efficient at higher salt concentrations and that increasing the surfactant concentration above the levels which are effective at lower ionic strengths is of little or no help. The ionic strength at which failure occurs depends somewhat on pH, and therefore upon ψ_0 , as one would anticipate (56).

TABLE B-2. EFFECT OF TEMPERATURE ON σ_{crit} ^a

| T | σ_{crit} |
|-----|------------------------|
| 298 | 1.33×10^{-3} |
| 320 | 2.08×10^{-3} |
| 340 | 2.99×10^{-3} |

^aIn these runs, $\ell = 10^{-7}$ cm, $c_\infty = 10^{-3}$ mole/l, $\psi_0 = 50$ mV, $z_s = -1$, and $z' = 1$.

The effect of temperature on σ_{crit} is shown in Table B-2. We note that σ_{crit} increases with increasing temperature rather rapidly; as long as σ_{crit} does not approach the reduced critical micelle concentration and as long as the reduced surfactant concentration exceeds σ_{crit} , flotation should take place. However, these results indicate that the high-temperature cut-off of

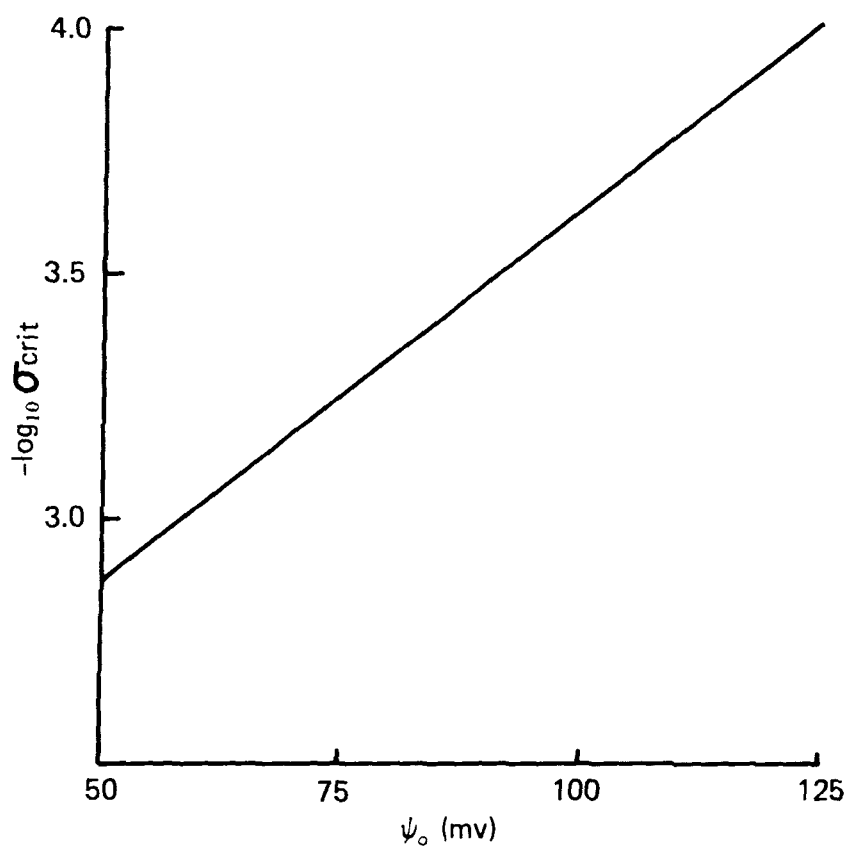


FIGURE B-4 - DEPENDENCE OF σ_{crit} ON ψ_o
 $T = 298^\circ K$, $\ell = 10^{-7}$ cm, $c_\infty = 10^{-3}$ m/l,
 $c_{max} = 1.0$ mole/l, $\omega = -2 \times 10^{-13}$ erg.

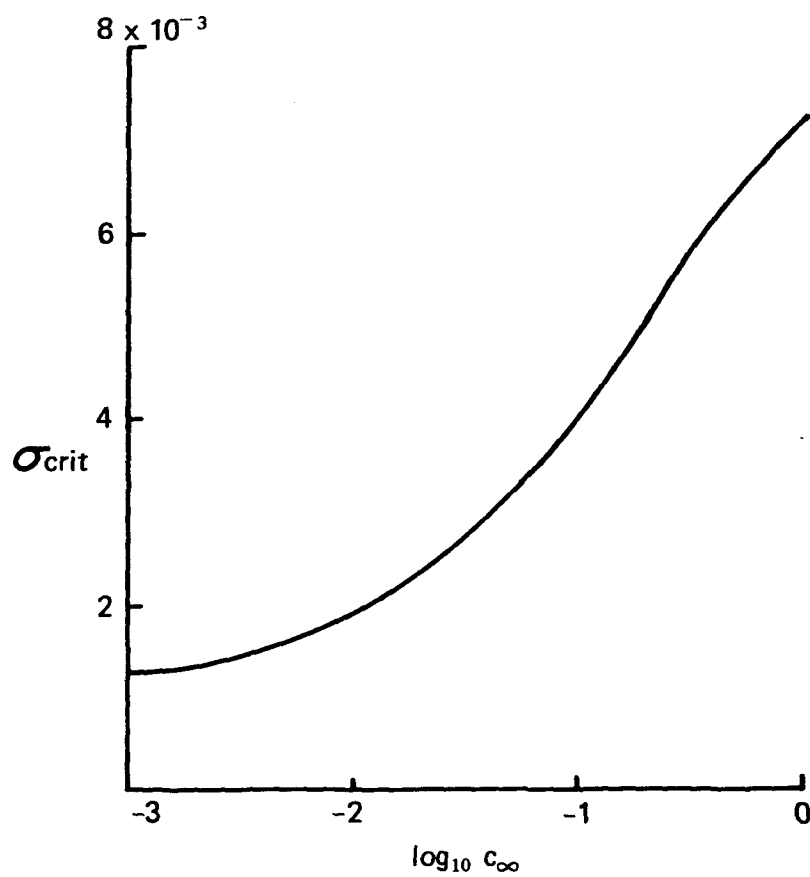


FIGURE B-5 - DEPENDENCE OF σ_{crit} ON c_{∞} . $T = 298^{\circ}\text{K}$, $l = 10^{-7}$ cm, $c_{\text{max}} = 10$ moles/l, $\psi_0 = 50$ mV, $w = -2 \times 10^{-13}$ erg.

foam flotation should depend markedly on surfactant concentration. This type of temperature dependence does not appear in our earlier approach (35-40), and an experimental study of the interaction of temperature and surfactant concentration at relatively low surfactant levels may provide a means of distinguishing between the two models. This result also suggest the importance of investigating the temperature dependence of the air-water surface potential within the framework of our other model. We have discussed this elsewhere (41).

APPENDIX C

THEORY OF SURFACTANT DISPLACEMENT BY SALTS

A matter of considerable impact on the economics of foam flotation is the extent of which surfactant can be recovered for recycling. Within the framework of the Fuerstenau-Somasundaran-Healy model (43-50), one expects that a very substantial fraction of the surfactant in the collapsed foamate from floc foam flotation will be absorbed on the floc sludge, interfering with the settling of the sludge and the recovery of the surfactant. An analysis of the adsorption isotherms of the surfactant on the floc and the effect on these of varying ionic strength is given in Appendix B, in which the adsorption of nonsurfactant ions into the primary layer on the floc, and the competition of surfactant and nonsurfactant ions for sites in the primary layer, is neglected. We here present an analysis which takes these effects into account. Our results indicate the feasibility of displacing surfactant ions from the floc sludge by the addition of nonsurface-active salts.

ANALYSIS

We shall first look at the simple case in which the surfactant ions do not interact with each other; this is readily seen to yield Langmuir-type adsorption isotherms for the surfactant ion and the nonsurface-active competing ion.

N_S = number of surface sites/cm²

θ_A = fraction of sites occupied by surfactant ions A

θ_B = fraction of sites occupied by non-surface-active ions B

c_A = bulk concentration of A

c_B = bulk concentration of B

At equilibrium the rates of adsorption and desorption of A (and also of B) are equal, yielding

$$k_{Af} N_S \theta_A = k_{Ar} c_A N_S (1 - \theta_A - \theta_B) \quad (C-1)$$

$$k_{Bf} N_S \theta_B = k_{Br} c_B N_S (1 - \theta_A - \theta_B) \quad (C-2)$$

Solution of these equations leads in the usual way to

$$\theta_A = \frac{b_A c_A}{(1 + b_A c_A + b_B c_B)} \quad (C-3)$$

$$\theta_B = \frac{b_A c_A}{(1 + b_A c_A + b_B c_B)} \quad (C-4)$$

where $b_A = k_{Ar}/k_{Af}$ and $b_B = k_{Br}/k_{Bf}$. We see, as expected, that increasing c_B results in decreasing θ_A , displacing surfactant from the floc particle surface. The model, however, is rather unrealistic, in that it neglects the Van der Waals interactions of the hydrocarbon chains of the surfactant ions which, as Fuerstenau and his co-workers have observed experimentally (43-50), have a profound effect on the shapes of the adsorption isotherms. Surface condensation may occur, resulting in a sudden increase in θ_A from slightly greater than zero to slightly less than one, with a slight decrease in temperature or a slight increase in surfactant concentration.

We shall next attack the problem of competition for surface sites when interactions between the surfactant ions are significant. We use a generalization of an approximate method described by Fowler and Guggenheim (76).

We let

z = number of nearest neighbors of a site

N_A = number of sites occupied by A

N_B = number of sites occupied by B

N_{XY} = average number of pairs of sites occupied by X and Y; X, Y = A, B or O (empty)

We take into account the A-A pair interaction energy, $2w/z$, as follows:

$$4N_{AA}N_{OO} = N_{AO}^2 \exp(-2w/zkT) \quad (C-5)$$

$$4N_{BB}N_{OO} = N_{BO}^2 \quad (C-6)$$

$$2N_{OO}N_{AB} = N_{AO}N_{BO} \quad (C-7)$$

$$2N_{AA} + N_{AO} + N_{AB} = zN_A \quad (C-8)$$

$$2N_{OO} + N_{AO} + N_{BO} = z(NS - N_A - N_B) \quad (C-9)$$

$$2N_{BB} + N_{BO} + N_{AB} = zN_B \quad (C-10)$$

(This is a straightforward extension of the approach used for a single adsorbed species in Ref. 76.) A lengthy series of successive eliminations finally yields a remarkably simple equation for N_{AA} :

$$4(D-1)N_{AA}^2 - [4(D-1)N_A + 2N_S]zN_{AA} + Dz^2N_A^2 = 0 \quad (C-11)$$

where $D = \exp(-2w/zkT)$. This is identical to Fowler and Guggenheim's Eq. (1010,1). We follow these authors to obtain

$$N_{AA} = zN_S \left\{ \frac{\theta_A}{2} - \frac{\theta_A(1-\theta_A)}{\beta+1} \right\}, \quad (C-12)$$

$$\beta = [1 - 4\theta_A(1-\theta_A)(1-D)]^{1/2} \quad (C-13)$$

The expression for the chemical potential of A is given by (76)

$$\begin{aligned} \frac{\mu_A}{kT} = \log \lambda_A = \log \frac{\theta_A}{1-\theta_A-\theta_B} - \log a_A^\circ(T) + \frac{w}{kT} + \\ \frac{1}{2} z \log \frac{(\beta-1+2\theta_A)(1-\theta_A)}{\theta_A(\beta+1-2\theta_A)}, \end{aligned} \quad (C-14)$$

where $a_A^\circ(T)$ is the partition function for the internal degrees of freedom of the surfactant ion. We note that

$$a_A^\circ(T) = \exp(\chi_A/kT) j_A(T), \quad (C-15)$$

where $j_A(T)$ is the partition function for the internal motions of a surfactant ion in bulk solution and χ_A is the binding energy of an isolated surfactant ion to the floc-water interface.

In solution we assume the chemical potential of a surfactant ion to be given by

$$\frac{\mu_A}{kT} = \text{const.} - \frac{5}{2} \log T + \log c_A - \log j_A(T) \quad (C-16)$$

Equating Eqs. (C-14) and (C-16) then yields

$$\begin{aligned} \log \frac{\theta_A}{1-\theta_A-\theta_B} - \frac{\chi_A}{kT} + \frac{w}{kT} + \frac{z}{2} \log \frac{(\beta-1+2\theta_A)(1-\theta_A)}{\theta_A(\beta+1-2\theta_A)} + \frac{5}{2} \log T = \\ = \log \frac{c_A}{c_A^\circ} = \log c_A', \end{aligned} \quad (C-17)$$

where c_A° is determined by the constant in Eq. (C-16).

In similar but simpler fashion,

$$\log \frac{\theta_B}{1-\theta_A-\theta_B} - \frac{\chi_B}{kT} + \frac{5}{2} \log T = \log \frac{c_B}{c_B^\circ} = \log c_B' \quad (C-18)$$

We can calculate adsorption isotherms from Eqs. (C-17) and (C-18) calculating c_A' and c_B' as functions of θ_A and θ_B ; it is more convenient to calculate c_A' and θ_B as functions of θ_A and c_B' . We solve Eq. (C-18) for θ_B , obtaining

$$\theta_B = bc_B' \frac{(1-\theta_A)}{(1+bc_B')} , \quad b = T^{-5/2} \exp \frac{\chi_B}{kT} \quad (C-19)$$

Some typical isotherms are plotted in Fig. C-1. We see that unstable phases may occur [where $(\partial \mu_A / \partial \theta_A)_{c_B} = kT(\partial \log c_A' / \partial \theta_A')_{c_B}$ is negative], so that the system splits into two stable phases. We next determine the values of θ_A for these stable phases; again we follow Fowler and Guggenheim. If θ_{X1} and θ_{X2} represent the values of θ_X for the two surface phases in equilibrium with each other ($X = A, B$), then we must have

$$\lambda_{A1} \equiv \lambda_A(\theta_{A1}, \theta_{B1}) = \lambda_A(\theta_{A2}, \theta_{B2}) \quad (C-20)$$

$$\lambda_{B1} \equiv \lambda_B(\theta_{A1}, \theta_{B1}) = \lambda_B(\theta_{A2}, \theta_{B2}) \quad (C-21)$$

$$\text{and } \phi(\theta_{A1}, \theta_{B1}) = \phi(\theta_{A2}, \theta_{B2}) , \quad (C-22)$$

where ϕ is the spreading pressure of the surface phase.

We generalize Fowler and Guggenheim's Formula (1008,5) for $d\phi$ (76) to get

$$d\phi = \frac{N_S kT}{\text{Area}} (\theta_A d\log \lambda_A + \theta_B d\log \lambda_B) , \quad (C-23)$$

and note that Eq. (C-22) can be written as

$$\int_1^2 d\phi = 0 \quad (C-24)$$

We regard c_B' as fixed, θ_B as a function of c_B' and θ_A (through Eq. (C-19), and θ_A as the independent variable in Eq. (C-23); $\log \lambda_A$ is given by Eq. (C-14), and $\log \lambda_B$ is given by

$$\frac{\mu_B}{kT} \equiv \log \lambda_B = \log \frac{\theta_B}{1-\theta_A-\theta_B} - \log a_B^\circ(T) \quad (C-25)$$

Then Eq. (C-24) becomes

$$\begin{aligned} 0 = \int_{\theta_{A1}}^{\theta_{A2}} \{ \theta_A \left[\frac{\partial \log \lambda_A}{\partial \theta_A} + \frac{\theta \log \lambda_A}{\partial \theta_B} \frac{\partial \theta_B}{\partial \theta_A} \right] \\ + \theta_B \left[\frac{\partial \log \lambda_B}{\partial \theta_A} + \frac{\partial \log \lambda_A}{\partial \theta_B} \frac{\partial \theta_B}{\partial \theta_A} \right] \} d\theta_A \end{aligned} \quad (C-26)$$

From Eq. (D-19) we find that

$$\frac{\partial \theta_B}{\partial \theta_A} = \frac{bc_B'}{1+bc_B'} \quad (C-27)$$

From Eq. (C-25) we have

$$\frac{\partial \log \lambda_B}{\partial \theta_A} = \frac{1}{1 - \theta_A - \theta_B} \quad (C-28)$$

$$\text{and } \frac{\partial \log \lambda_B}{\partial \theta_B} = \frac{1 - \theta_A}{\theta_B (1 - \theta_A - \theta_B)} \quad (C-29)$$

From Eq. (C-14) we have

$$\frac{\partial \log \lambda_A}{\partial \theta_B} = \frac{1}{1 - \theta_A - \theta_B} \quad (C-30)$$

and

$$\frac{\partial \log \lambda_A}{\partial \theta_A} = \frac{1 - \theta_B}{\theta_A (1 - \theta_A - \theta_B)} + \frac{2 + \frac{\partial \beta}{\partial \theta_A}}{2[\beta - 1 + 2\theta_A]} + \frac{2 - \frac{\partial \beta}{\partial \theta_A}}{\beta + 1 - 2\theta_A} - \frac{1}{\theta_A (1 - \theta_A)} \quad (C-31)$$

$$\frac{\partial \beta}{\partial \theta_A} = \frac{2(1-D)(2\theta_A - 1)}{\beta} \quad (C-32)$$

where β is defined by Eq. (C-13).

We now wish to find values θ_{A1} and θ_{A2} such that Eqs. (C-20) and (C-26) are satisfied. [Use of Eq. (C-19) in Eq. (C-25) guarantees that Eq. (C-21) is satisfied.] We proceed as follows. For fixed c_B' we calculate a table of $\log \lambda_A$ as a function of $\theta_A = n\Delta\theta$, $n = 1, 2, \dots, N$ [θ_B is determined by Eq. (C-19)]. Then we find those values of $n\Delta\theta$ for which $\log \lambda_A[(n+1)\Delta\theta] - \log \lambda_A[n\Delta\theta]$ change sign. If there are none, our table and Eq. (C-16) give us the adsorption isotherm, $\log c_A'$ as a function of θ_A . If there are two, we have a loop in our isotherm, and a phase transition occurs. In this case let the two values of n be n_ℓ and n_r , and calculate $\log \lambda_A[(n_\ell + n_r)/2](\Delta\theta)$. Then increment n above $(n_\ell + n_r)/2$ until $\log \lambda_A(n\Delta\theta) - \log \lambda_A[(n_\ell + n_r)/2](\Delta\theta)$ changes sign; call the value of $n\Delta\theta$ for which this occurs θ_2 . Similarly, decrement n below $(n_\ell + n_r)/2$ until $\log \lambda_A(n\Delta\theta) - \log \lambda_A[(n_\ell + n_r)/2](\Delta\theta)$ changes sign; call this value of $n\Delta\theta$ θ_1 .

We use θ_1 and θ_2 as trial limits for the integral Eq. (C-26), which we evaluate numerically with the aid of Eqs. (C-27) to (C-32). If the integral is greater than (less than) zero, we replace θ_1 by $\theta_1 + \Delta\theta(\theta_1 - \Delta\theta)$, determine the new value of $\log \lambda_A(\theta_1)$ from the table, and we then increase (decrease) θ_A from θ_2 until $\log \lambda_A(\theta_A) - \log \lambda_A(\theta_1)$ changes sign; this value of θ_A is our new upper limit. We use the new values of θ_1 and θ_2 as trial limits for the integral, Eq. (C-26), and continue this process until the integral changes sign. The values of θ_1 and θ_2 for which this occurs are our desired θ_{A1} and θ_{A2} , which specify the fractions of surface coverage by surfactant in the two phases in equilibrium with each other.

RESULTS

Adsorption isotherms were calculated by the procedure outlined above on an XDS Sigma 7 computer; about 3 sec of machine time was required per isotherm. The results are plotted as $\log_e \lambda_A$ vs θ_A for various values of the parameters.

In Fig. C-1 we see the effect of increasing the reduced concentration of salt, c_B' . As the salt concentration increases, the activity of surfactant required to bring about condensation of the surfactant on the floc surface (λ_A^{con}) increases, too, although the shape of the isotherm is unaffected. The dependence of $\log_e \lambda_A^{\text{con}}$ on c_B' is shown in Fig. C-2. The larger the binding energy of the salt ion to the floc, χ_B , the more effective it is in preventing condensation of the surfactant on the floc, or (equivalently) in displacing sorbed surfactant from the floc; this is shown in Figs. C-2 and C-3.

Thus, with positively charged ferric hydroxide flocs, one would expect that univalent anions would be fairly effective in displacing anionic surfactants such as the alkyl sulfates, but that divalent anions would be comparably effective at substantially lower concentrations. One would also anticipate that complexing or chelating ions would be especially effective in displacing surfactant.

The effect of the magnitude of w , the energy of interaction between the surfactant ions, is shown in Fig. C-4, and is in agreement with our earlier calculations on a similar but simpler model [Appendix B (41)]. The effect of the binding energy holding an isolated surfactant ion to the floc surface, χ_A , is shown in Fig. C-5, and is also similar to our earlier results (41). The results of varying temperature are shown in Fig. C-6; the bulk concentration of surfactant required to produce a condensed surface phase increases with temperature, as one would expect.

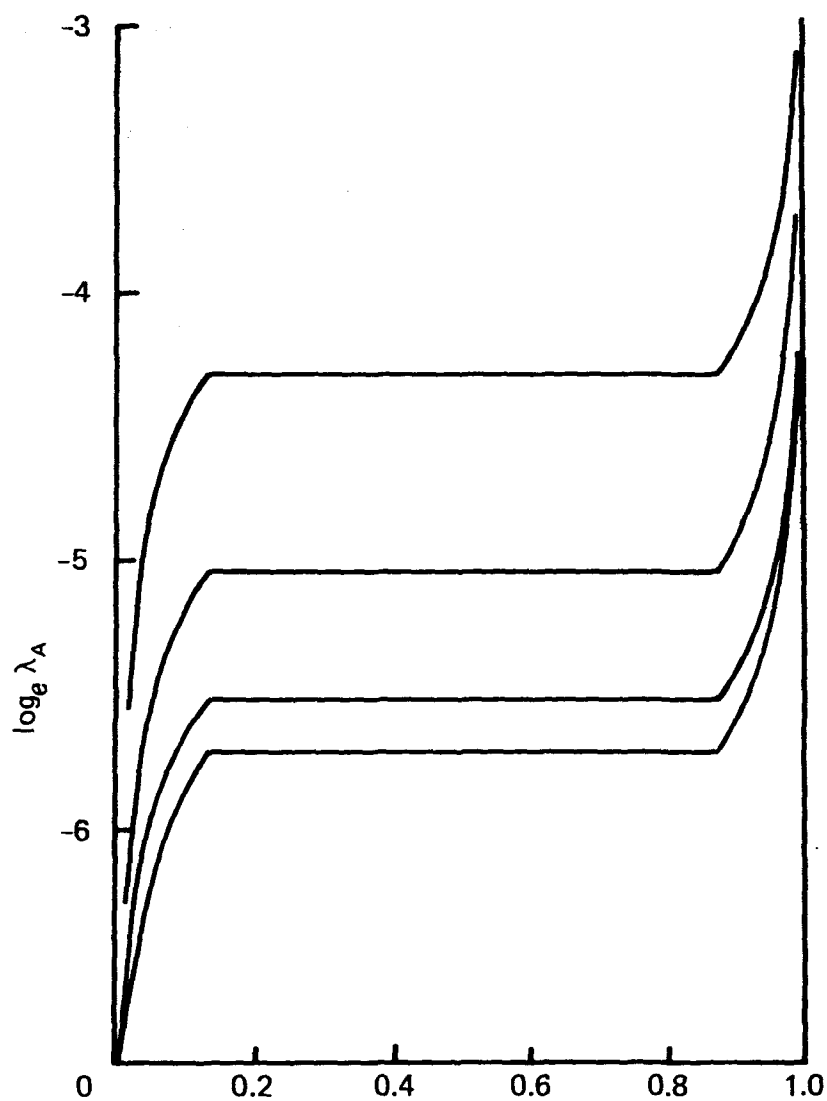


FIGURE C-1 - EFFECT OF COMPETING SALT CONCENTRATION (c_a') ON THE ADSORPTION ISOTHERM. $T = 298^\circ\text{K}$, $\chi_A = 1.2 \times 10^{-13}$, $\chi_B = 1.2 \times 10^{-13}$, $w = -1.234 \times 10^{-13}$ erg, $z = 6$, $c_B' = 30, 10, 3$, and 1×10^5 (TOP TO BOTTOM).

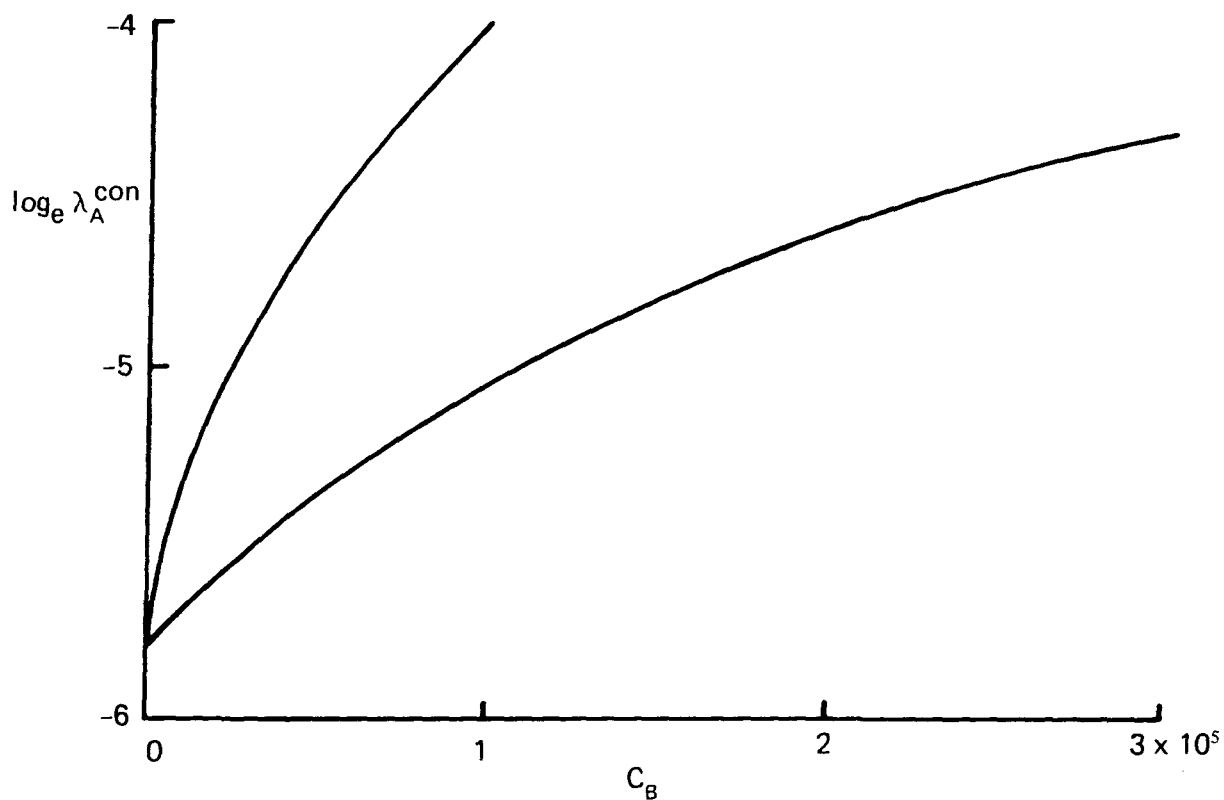


FIGURE C-2 - EFFECT OF c_B ON SURFACTANT CONDENSATION CONCENTRATION. $T = 298^\circ\text{K}$, $\chi_A = 1.2 \times 10^{-13}$, $w = -1.2 \times 10^{-13}$ ERG, $z = 6$. $\chi_B = 1.2 \times 10^{-13}$ (LOWER) and 1.8×10^{-13} (UPPER) ERG.

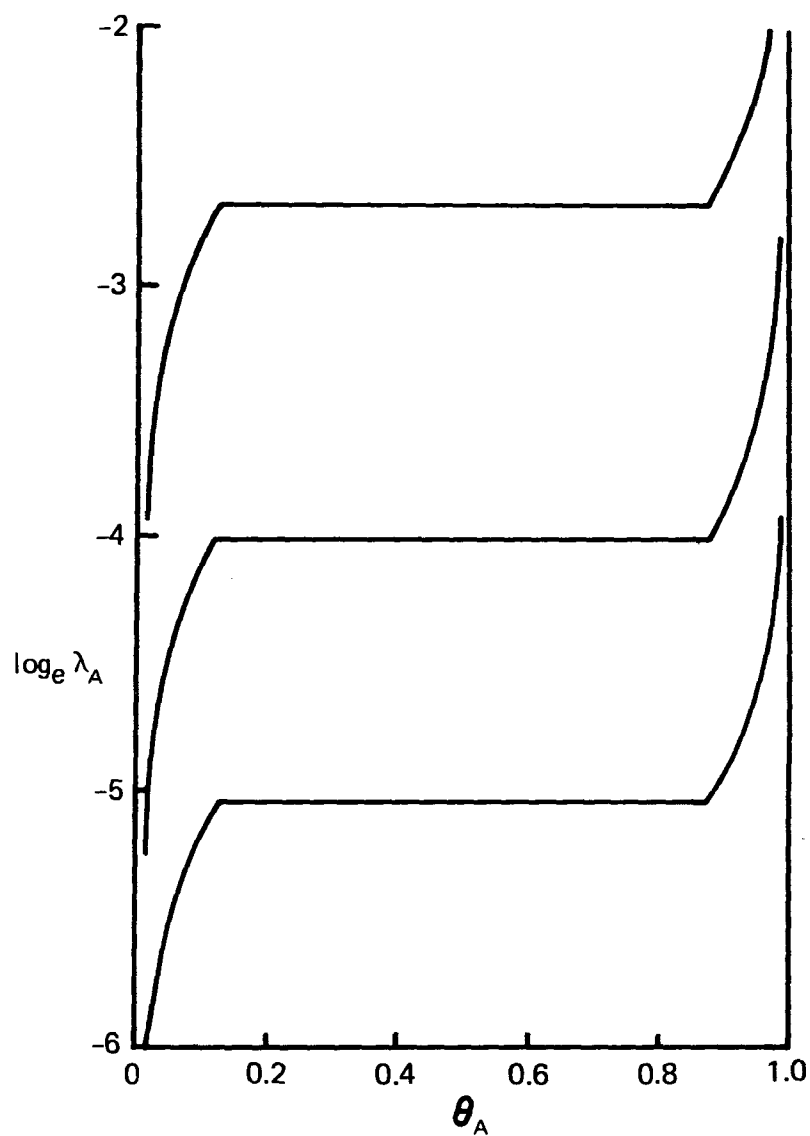


FIGURE C-3 - EFFECT OF χ_B ON THE ADSORPTION ISOTHERM.
 $c_B = 10^5$; $\chi_B = 2.4, 1.8,$ and 1.2×10^{-13} erg (top to bottom);
 other parameters as in Fig. 1.

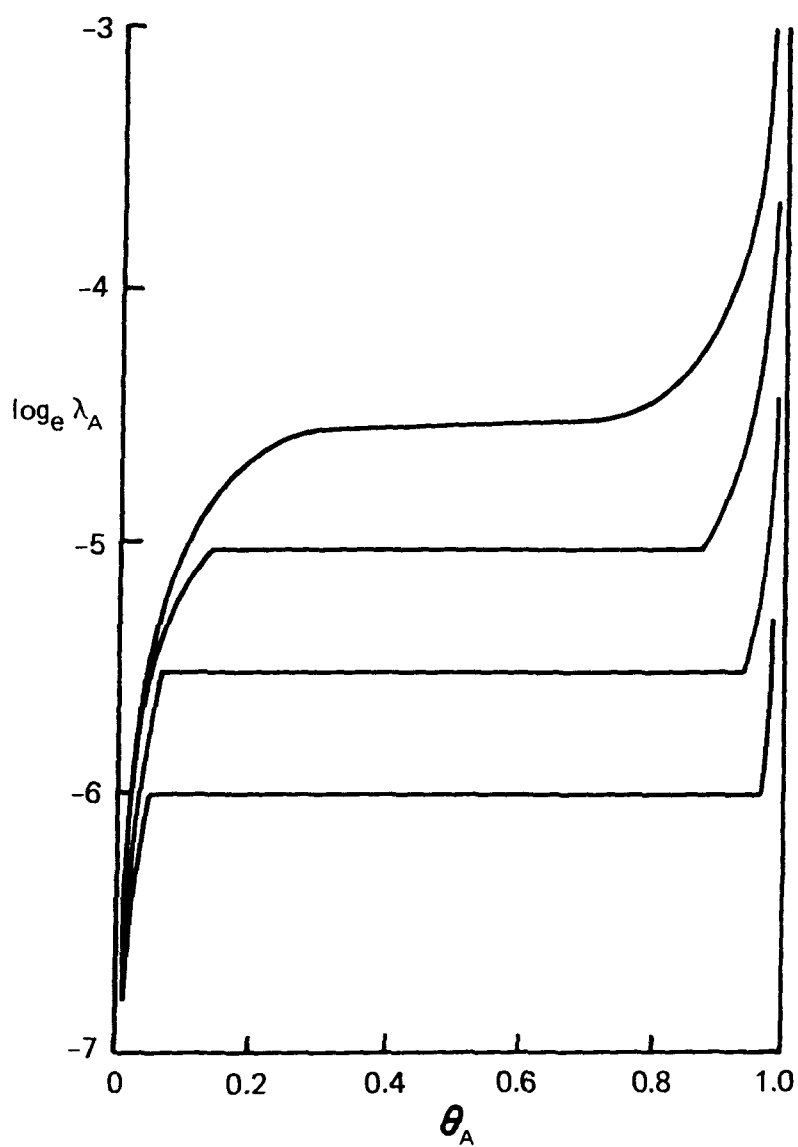


FIGURE C-4 - EFFECT OF w ON THE ADSORPTION ISOTHERM. $w = -1.0, -1.2, -1.4$, and -1.6×10^{-13} ERG (TOP TO BOTTOM); $c_B' \approx 10^5$; OTHER PARAMETERS AS IN FIG. 1.

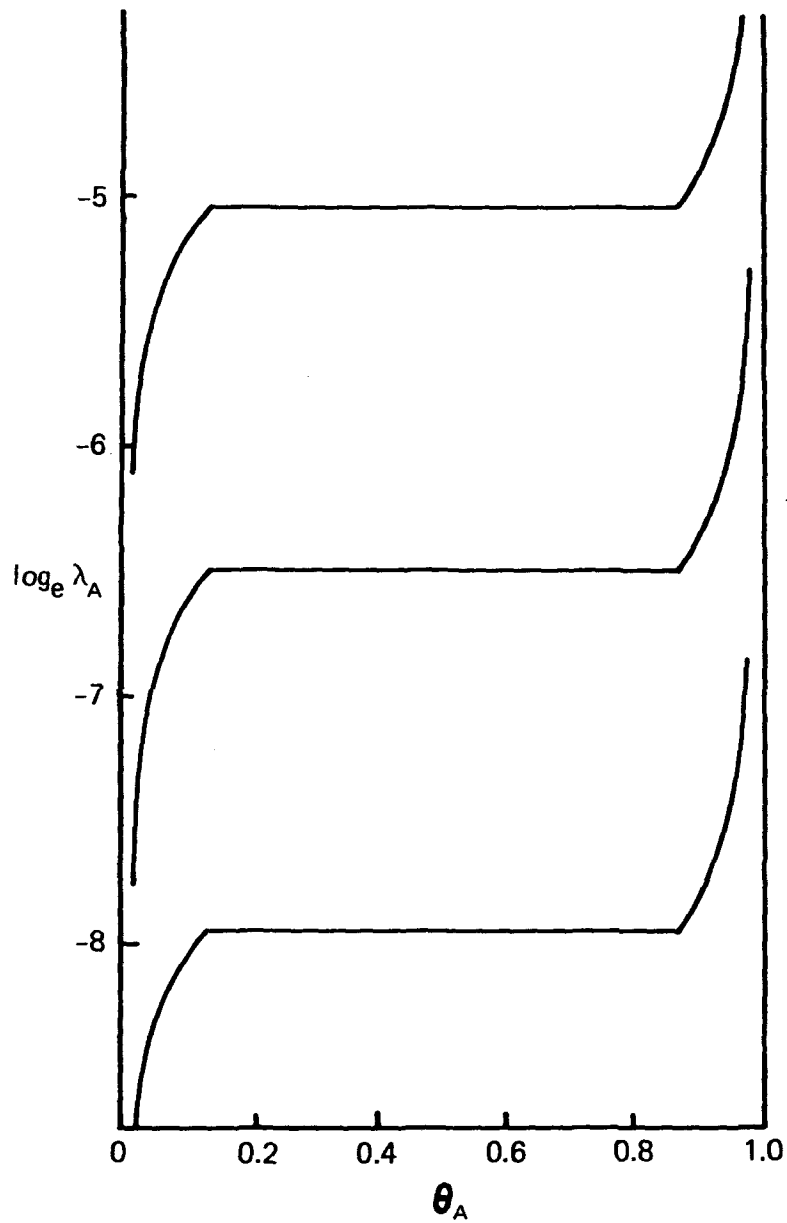


FIGURE C-5 - EFFECT OF χ_A ON THE ADSORPTION ISOTHERM. $c_B' = 10^5$; $\chi_A =$ 1.2, 1.8, and 2.4×10^{-13} ERG (TOP TO BOTTOM); OTHER PARAMETERS AS IN FIG. 1.

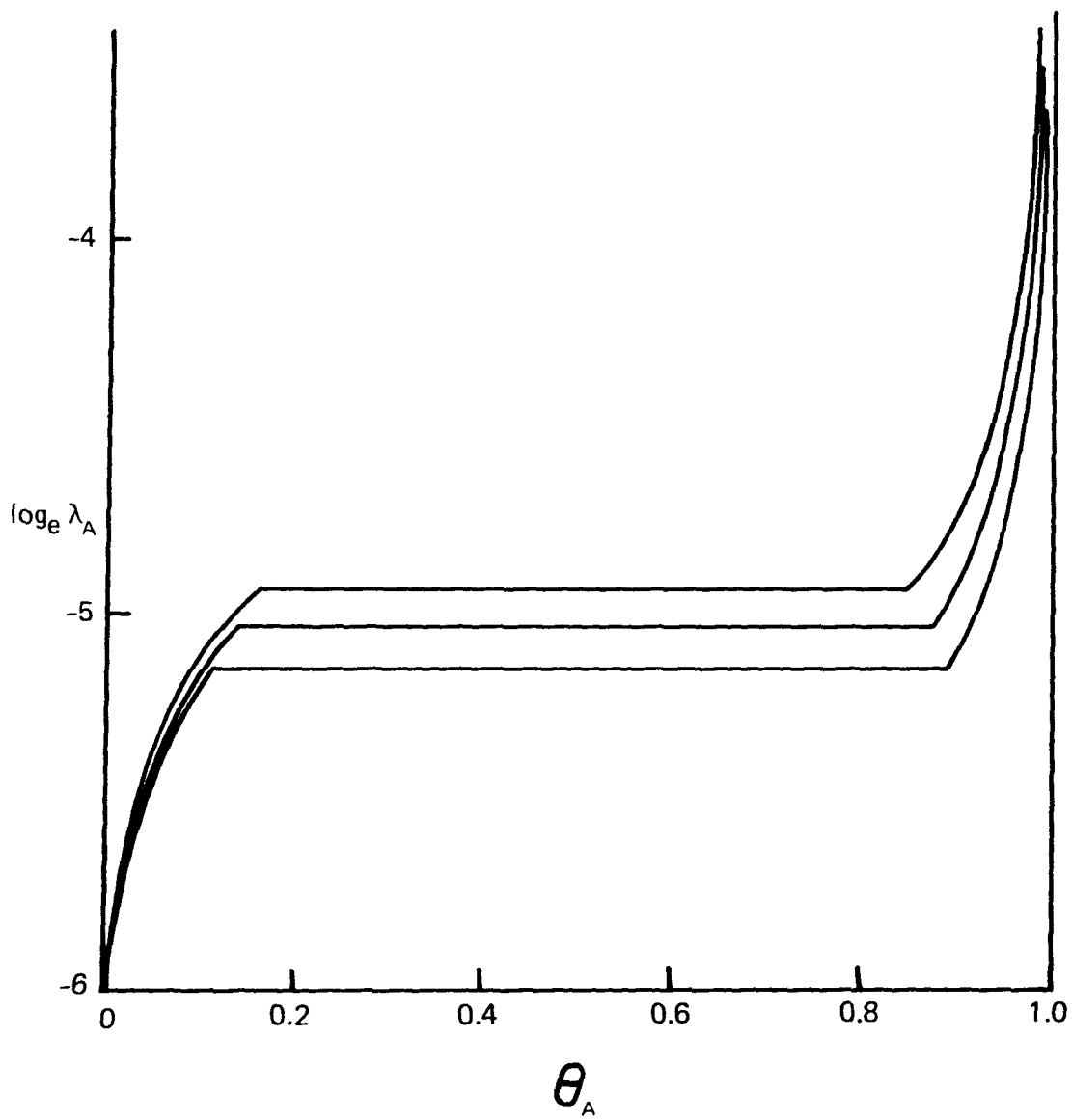


FIGURE C-6 - EFFECT OF TEMPERATURE ON THE ADSORPTION ISOTHERM, $c_B' = 10^5$, $T = 308, 298, \text{ AND } 288 \text{ K}$ (TOP TO BOTTOM); OTHER PARAMETERS AS IN FIG. D-1.

TECHNICAL REPORT DATA

(Please read instructions on the reverse before completing)

| | | | |
|---|--|---|--|
| 1. REPORT NO.
EPA-600/2-80-138 | | 3. RECIPIENT'S ACCESSION NO. | |
| 4. TITLE AND SUBTITLE
FOAM FLOTATION TREATMENT OF INDUSTRIAL WASTEWATERS: LABORATORY AND PILOT SCALE | | 5. REPORT DATE
June 1980 issuing date. | |
| 7. AUTHOR(S)
David J. Wilson, Edward L. Thackston | | 6. PERFORMING ORGANIZATION CODE | |
| 9. PERFORMING ORGANIZATION NAME AND ADDRESS
Vanderbilt University
Nashville, TN 37235 | | 8. PERFORMING ORGANIZATION REPORT NO. | |
| 12. SPONSORING AGENCY NAME AND ADDRESS
Industrial Environmental Research Lab-Cincinnati, OH
Office of Research & Development
U.S. Environmental Protection Agency
Cincinnati, OH 45268 | | 10. PROGRAM ELEMENT NO.
IBB610 | |
| | | 11. CONTRACT/GRANT NO.
R-804438 | |
| | | 13. TYPE OF REPORT AND PERIOD COVERED | |
| | | 14. SPONSORING AGENCY CODE
EPA/600/12 | |
| 15. SUPPLEMENTARY NOTES | | | |
| 16. ABSTRACT
A floc foam flotation pilot plant reduced lead and zinc in dilute solution to very low concentrations. The results suggest a number of design improvements. A simple diffusion model does not adequately describe axial dispersion at high column loadings. The floc foam flotation of zinc, cobalt, nickel, chromium (III), and simple and complexed cyanides was carried out. Modified procedures make floc foam flotation of copper compatible with several precipitation pretreatments. The flotation of ferric hydroxide flocs is profoundly affected by polyvalent anions such as silicates and phosphates. The flotation of mixtures of copper, lead and zinc was successfully carried out. A surface adsorption model for floc foam flotation was analyzed and found to account for the effects of ionic strength, specifically adsorbed ions, surfactant concentration, and surfactant hydrocarbon chain length. | | | |
| 17. KEY WORDS AND DOCUMENT ANALYSIS | | | |
| a. DESCRIPTORS | b. IDENTIFIERS/OPEN ENDED TERMS | c. COSATI Field/Group | |
| Flotation
Wastewaters
Metals
Surfactants | Floc foam flotation
Flotation column
Pilot plant
Continuous flotation | 13B | |
| 18. DISTRIBUTION STATEMENT
Release to Public | 19. SECURITY CLASS (This Report)
Unclassified | 21. NO. OF PAGES
143 | |
| | 20. SECURITY CLASS (This page)
Unclassified | 22. PRICE | |